Performance Analysis of Physical Layer Network Coding

by

Jinho Kim

A dissertation submitted in partial fulfillment
of the requirements for the degree of
Doctor of Philosophy
(Electrical Engineering: Systems)
in The University of Michigan
2009

Doctoral Committee:

Professor Wayne E. Stark, Chair
Professor Kim A. Winick
Associate Professor Achilleas Anastasopoulos
Associate Professor Harm Derksen

ABSTRACT

Performance Analysis of Physical Layer Network Coding

by

Jinho Kim

Chair: Wayne E. Stark

Network coding has emerged as an innovative approach to network operation that can significantly enhance network throughput. The key goal of this thesis is to understand fundamental aspects of physical layer network coding, where network coding is performed at the physical layer.

As a simple but typical example of network coding, we consider a network scenario where two users transmit messages through a common channel and the receiver reconstructs the exclusive-or of the two messages. For this channel, we investigate the error exponent which can provide guidelines for the design of efficient communication systems using network coding. From a practical point of view, we examine the performance of channel codes for this problem. Assuming that each user transmits data using the same low-density parity-check (LDPC) code and each link is an additive white Gaussian noise channel, we evaluate the noise thresholds of LDPC codes via density evolution methods.

Other important issues considered in this thesis are related to transmission over fading channels. First, we study the performance of LDPC codes over non-ergodic fading channels. In non-ergodic channels, reliable communication at a constant rate is impossible. Assuming that the fading coefficient is randomly chosen but fixed during transmission of an LDPC codeword, we derive the outage probability of LDPC-coded systems. We also propose an accurate frequency domain channel estimator based on the

Slepian basis expansion. The proposed scheme operates with high accuracy requiring only the knowledge of the maximum delay spread of the channel. Finally, we investigate the capacity achieving input of non-coherent Rayleigh fading channels taking into account power constraints imposed by a non-linear power amplifier. We show that the optimal input is discrete with finite support which indicates that capacity can be computed using finite dimensional optimization.

To my parents.

ACKNOWLEDGEMENTS

TABLE OF CONTENTS

LIST OF TABLES

LIST OF FIGURES

LIST OF APPENDICES

APPENDIX

CHAPTER 1

Introduction

For decades, the demand in network capacity has continued to increase to support high data rate services such as high speed internet and multimedia applications. The future wireless communication systems are required to meet such growing demands with high spectral efficiency, low energy consumption and high mobility. Consider a network consisting of source nodes, destination nodes and intermediate nodes. Each source node wants to distribute its own message to a set of destination nodes with help of intermediate nodes. Given limited resources such as bandwidth and energy, questions of what is the best performance that the network can support and how it can be achieved efficiently are central problems in wireless network design.

In traditional communication networks, information to be sent from a source node to a destination node is conveyed through a series of intermediate nodes in the network by store-and-forward switching. This method has been a dominant technique for sending data over a network, in which relay nodes decode the received data and merely forward these to the next node without modifying the contents of the original data.

Recently, network coding has emerged as a new paradigm for communication in networks which provides the potential to increase network capacity significantly [1]-[3]. Due to its broad range of potential applications, network coding has received increasing research interest in information theory, networking and many other fields. In contrast to store-and-forward approaches where the function at an intermediate node is restricted

(a) store and forward   (b) network coding
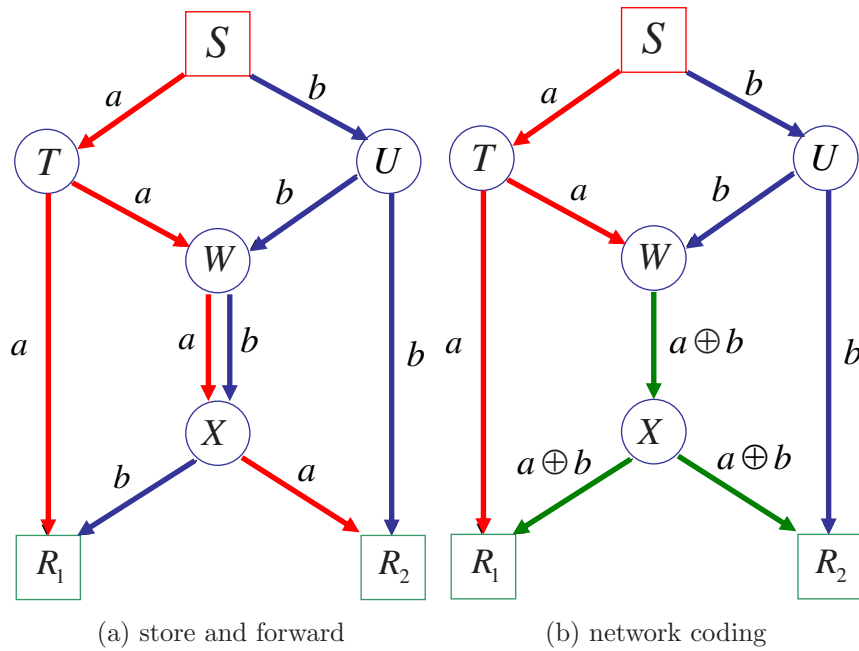
Figure 1.1: Example for network coding (butterfly network)

to that of a switch, the key idea of network coding is to allow an intermediate node to mix and process information from multiple links. In this way, the amount of information transmitted through the network can be reduced and hence the network throughput can be increased. This is well illustrated by the butterfly network example in Fig. 1.1 in [1]. In Fig. 1.1, a source node S wants to transfer two bits a and b to both receivers R_1 and R_2 through the network. Each link in the network is assumed to be error free with unit capacity. When store-and-forward is used, each intermediate node replicates what it receives and then forward it to neighborhood nodes. With store-and-forward switching, the network throughput of the butterfly network is dictated by the bottleneck node W. Since the capacity of the link between W and X is one, the node W transmits one bit at a time. In this way, 10 transmissions are required to complete data transfer. However, when network coding is applied, the bottleneck node W can mix incoming data a and b and compute the exclusive-or (XOR) of the two. Since $R_1(R_2)$ knows both $a(b)$ and $a \oplus b$ it can also figure out $b(a)$ by taking the XOR of $a(b)$ and $a \oplus b$. With network

coding, only 9 transmissions are needed hence we can save bandwidth and energy. For multicast problems in lossless wired networks, it has been shown that the max-flow min-cut upper bound can be achieved with network coding while it is not possible with traditional store-and-forward technique [1].

Network coding was first introduced in wired networks. Recently there have been efforts to apply network coding to wireless networks. In [4], by utilizing broadcasting nature of wireless medium, physical layer network coding (PNC) was proposed which can further improve the network performance. In PNC, the relay computes the desired function from simultaneously transmitted signals by suitable modulation and demodulation. In [6], Nazer *et al.* studied the problem of recovering a function of data simultaneously transmitted from multiple number of sources through a common channel and found an achievable rate for this channel.

For this type of channel, the capacity is unknown in general. Therefore, it is important to study other meaningful performance measures such as an error exponent so that the system behavior can be understood and used for efficient system design. This is the motivation of a major part of this thesis. Another important issue in this problem is the performance of practical channel codes combined with network coding. We analyze the performance of PNC with each user using low-density parity-check (LDPC) codes. The rest of research topics discussed in this thesis are related to communication over fading channels. First, we consider LDPC-coded systems operating in slow fading channels and derive a closed form of the outage probability. Such analysis is required to evaluate the performance of communication systems in slow fading channels. Next, we propose an effective frequency domain channel estimation scheme for orthogonal frequency division multiplexing (OFDM) systems. This channel estimator is based on the Slepian basis expansion and can operate with less complexity and without much prior information about the channel. Finally, we investigate the capacity-achieving input of non-coherent Rayleigh fading channels subject to practical power constraints.

To reflect practical power constraints, we consider the effect of the characteristic of the non-linear power amplifier on the channel input.

1.1 Research Topics and Contributions

In this section, we present research topics covered in this thesis and contributions in each topic.

1.1.1 Error Exponent of Exclusive-Or Multiple Access Channels

Since the seminal work of Ahlswede *et al.* [1], there has been considerable interest in understanding fundamental aspects of network coding due to its potential to improve the efficiency of wireless networks. In [1], it was demonstrated that network coding has advantages over conventional store-and-forward for multicast problems where one source node distributes data to multiple destination nodes through the network. Furthermore, it was proved that the max-flow min-cut upper bound on the capacity can be achieved with network coding for multicast networks. In [2], this problem was formulated in an algebraic framework and linear network coding, in which relay nodes compute and forward linear combinations of incoming data they receive, was shown to be good enough to achieve the capacity of multicast networks. Similar results were also given in [3].

In the work of [1]-[3], each node in the network transmits information at a rate below the channel capacity so that each link is assumed to be error-free. Then network coding is employed at the network layer for subsequent transmission. Recently several studies suggested that network coding can be performed at the physical layer for further performance improvement [4]-[6]. In [4], physical layer network coding (PNC) was first introduced, in which network coding is performed by suitable modulation and demodulation at the relay. The main idea is to recognize that the relay does not

need to determine each message but to compute the desired function of transmitted messages. In [5], analog network coding (ANC) was considered where the relay does not compute the desired function but simply amplifies and forwards incoming signals from multiple links so that the destination node can compute the desired function of messages. However with these approaches, error control coding is not possible at the relay. From an information theoretic point of view, Nazer *et al.* considered the problem of recovering a function of sources over a multiple-access channel (MAC) [6]. In [6], an achievable rate was provided and furthermore the usage of structured codes for this channel was investigated.

A typical example of network coding scenarios is a three-node network in which the receiver wants to compute the XOR of two users' information bits transmitted through a MAC. We call this type of channel the exclusive-or multiple access channel (XMAC). In our study, we address a fundamental problem of understanding the performance of network coding over the XMAC. The capacity of the XMAC is still unknown in general except for special cases. In [6], the capacity for a specific class of MAC, called the *symmetric linear* MAC was found. In this study, we are interested in finding other meaningful performance measures such as the error exponent and the cutoff rate of the XMAC.

We consider two possible network strategies. First, given the channel output, the receiver recovers transmitted messages from two user nodes separately and then computes the XOR of the two messages. We call this approach a multiple-access channel (MAC) strategy and this strategy converts the original problem into a standard MAC problem. In the MAC strategy, we allow time-sharing of the channel among two users so that the interference from the other user can be avoided. Another strategy considered is one where the receiver obtains the XOR directly from the channel output. We call this approach a physical layer network coding (PNC) strategy. Since the error exponent of the MAC has been well studied in the literature [10]-[15], we focus on the PNC strategy in

our work. For both random codes and linear codes, we derive the error exponent of the XMAC when the PNC strategy is applied. For random codes, an upper bound on the error probability is obtained using Gallager's random coding technique [16]. For linear codes, we extend the Shulman-Feder bound [17] to the XMAC. Moreover, we introduce the cutoff rate of the XMAC and evaluate it for the Gaussian XMAC. Analytical and numerical results indicate that in terms of cutoff rate, the PNC strategy shows better performance than the MAC strategy in the high rate region while the MAC strategy performs better in the low rate region.

1.1.2 Performance of LDPC Codes over Exclusive-Or Multiple Access Channels

Most studies of physical network coding have focused on finding the maximal achievable rate for various operations at the relay node including decode-and-forward and amplify-and-forward. However, the problem of how to achieve reliable communication with practical channel codes has not attracted much attention in the literature. This motivates us to investigate the use of error correcting codes over the XMAC. If the same linear codes are applied to both user nodes, the XOR of the two users' message can also be protected by error correcting codes since the mod 2 sum of two codewords, in this case, is also a valid codeword.

In point-to-point communication systems, low-density parity-check (LDPC) codes are one of the most promising error correcting codes and show reliable performance close to channel capacity. In this study, we analyze the performance of LDPC codes over the XMAC. We consider a Gaussian XMAC in which the output at the relay is the sum of transmitted signals plus Gaussian noise. In this work, we only consider the PNC strategy such that two user nodes transmit signals simultaneously and the relay node computes the XOR of the two users' data directly from the channel output.

In [29], density evolution was proposed to analyze the asymptotic performance of

LDPC codes under message passing decoding algorithm. This tool is based on the assumption that the density of messages to be exchanged does not depend on codewords. However, in the Gaussian XMAC, we may have different likelihoods of the two users transmitting different information (0 and 1 or 1 and 0) than we do about them transmitting the same data (both 0 or both 1). In this case, the density of messages can depend on the codeword. For such asymmetric cases, Wang *et al.* proposed a modified density evolution technique which keeps track of the density of messages averaged over all valid codewords [25]. Using this technique, we calculate the noise thresholds of LDPC codes over the XMAC. Our numerical results show that LDPC codes have reliable performance at rates close to the achievable rate which can be obtained from error exponent results. In the Gaussian XMAC, transmitted signals from two user nodes may arrive with different phases. In this work, we also evaluated the effect of phase difference on the performance of LDPC codes via density evolution techniques.

1.1.3   Outage Probability of LDPC-coded Systems

Due to the growing interest in mobile wireless communications, it is important to determine the performance limit over the time-varying channel. Ergodic capacity, which is concerned with maximizing transmission rate averaged over all channel states, is a good performance measure in a fading environment. Depending on the assumptions on the availability of channel side information (CSI), there have been many studies on the capacity of fading channels [26]-[28]. In [26], Goldsmith *et al.* obtained the capacity of fading channels with CSI at both transmitter and receiver and at the receiver alone. They showed that when CSI is available at both transmitter and receiver, the capacity can be achieved by adapting resources such as transmission power and rate based on the channel state. In [27], Caire *et al.* presented capacity results for some fading channels (with or without memory) under various assumptions on CSI. The effect of imperfect CSI on the capacity was evaluated in [28]. To achieve ergodic capacity, an infinite

codeword length is required so that the codeword can experience all possible channel states. However, for non-ergodic channels, a codeword may face deep fading during its transmission and the number of errors may be beyond the error-correcting capability of the channel code employed. For such cases, outage capacity, the maximal achievable rate with an acceptable outage probability, can be a more useful performance measure than ergodic capacity.

In this work, we study the outage probability of LDPC-coded systems over slow fading channels. We assume that channel state is randomly chosen but fixed during transmission of an LDPC codeword. We also assume that the transmitter knows the statistics of fading process while the receiver has perfect or imperfect CSI. The outage occurs when the signal-to-noise ratio (SNR) falls below an acceptable threshold hence the successful decoding under message passing algorithm is not possible. Under these assumptions, the outage probability is derived for both Rayleigh and Rician fading channels in a closed form. The effect of imperfect CSI at the receiver on the outage probability is also investigated. Then a similar method is applied to LDPC-coded code-division multiple-access (CDMA) systems to determine the outage probability.

1.1.4 Frequency Domain Channel Estimation Based on the Slepian Basis Expansion

The presence of multipath between the transmitter and the receiver causes severe performance degradation. Orthogonal frequency division multiplexing (OFDM) has been widely used in wireless communication systems due to its robustness against frequency selective fading and inter-symbol interference (ISI). Although OFDM can convert the frequency selective fading channel into a set of flat fading subchannels, data conveyed on each subchannel still suffer from fading. Therefore accurate channel estimation is required to achieve the maximum transmission rate or the minimum energy consumption.

Many channel estimators for OFDM systems have been proposed in the literature. For some channel estimation schemes such as minimum mean square error (MMSE) channel estimator, it is required for a receiver to know the channel statistics. However, it may be difficult or unavailable to obtain in many practical systems. Furthermore, it is known that a mismatch in channel modeling imposes limitations on the performance of such channel estimators. In a situation where channel statistics are not available at the receiver, the basis expansion model (BEM) can be useful since it requires limited information about the channel such as Doppler frequency and the maximum delay spread. In this model, the wireless channel is approximated with a limited number of basis functions. In [40], an accurate and efficient channel estimation scheme was proposed in which the doubly selective channel (both time and frequency) is expressed as a linear combination of a finite number of complex exponentials. In [39], observing that the channel impulse response is both time- and frequency-concentrated, Zemen *et al.* proposed a time domain channel estimator by approximating the channel with a set of Slepian sequences. They also demonstrated that Slepian sequences are more effective than complex exponentials in the modeling of time-varying channels.

Although wireless channels can be accurately represented with Slepian sequences, when the Doppler frequency is small, the length of required Slepian sequences should be very long for accurate channel estimation. In other words, both decoding delay and complexity are increased. This is because any sequence peaky in the frequency domain is spread widely in the time domain. In this case, it is better to exploit channel correlation in the frequency domain. This motivates us to design a new frequency domain channel estimator based on the Slepian basis expansion. In our channel estimation scheme, the channel frequency response is approximated with a finite number of Slepian sequences. Then the channel is estimated via least square estimation. Simulation results show that the proposed scheme outperforms the channel estimator using the exponential basis expansion.

9

1.1.5 Capacity of Non-coherent Rayleigh Fading Channels under Practical Power Constraints

For a fading channel, when the channel condition varies slowly, the transmitter can send known pilot symbols to help the receiver to estimate fading coefficients. However, when the channel coherence time is very short, it may be difficult to obtain accurate channel estimation. Furthermore, in such a case, it is required to send more pilot symbols for accurate channel estimation which results in low spectral efficiency. Therefore non-coherent reception can be required for systems operating over fast fading channels.

In this study, we consider transmission of information over the Rayleigh fading channel and non-coherent reception, where each symbol experiences independent fading. In [50], Abou-Faycal *et al.* showed that the capacity achieving input distribution of this channel, subject to an average power constraint, is discrete with finite support. Hence finding the capacity is equivalent to a finite dimensional optimization problem. Motivated by this work, we investigate the structure of the capacity achieving input for non-coherent Rayleigh fading channels subject to practical power constrains induced by a non-linear power amplifier. In communication systems, a power amplifier is necessary to obtain enough signal power to combat background noise and fading. The characteristic of a power amplifier imposes power constraints on input signals. First, due to the limit on output power, there exists a peak power constraint on the transmit signal. Second, there is an average power constraint on the consumed power, which is required to operate a power amplifier. In general, the consumed power is greater than the output power due to the inefficiency of the amplifier. Assuming that the consumed power is a deterministic function of the output power, we show that the optimal input is also discrete with finite support.

1.2   Outline of Thesis

The rest of this thesis is organized as follows. In Chapter 2, we present results on the error exponent of the XMAC. We then analyze the performance of LDPC codes over the Gaussian XMAC via density evolution techniques in Chapter 3. In Chapter 4, we derive the outage probability of LDPC-coded systems for slow fading channels under the assumption that the transmitter knows only the channel statistics while the receiver has perfect or imperfect CSI. In Chapter 5, we propose a new frequency domain channel estimator based on the Slepian basis expansion which can compensate for the effects of a multipath fading channel. In Chapter 6, we investigate the capacity of non-coherent Rayleigh fading channels subject to power constraints induced by a non-linear power amplifier. We prove that the capacity achieving input distribution is discrete in amplitude with a finite number of mass points. Conclusions and discussions on future research are given in Chapter 7.

CHAPTER 2

Error Exponent of Exclusive-Or Multiple-Access Channels

In this chapter, we consider the problem of communicating over an exclusive-or multiple-access channel (XMAC) where a receiver wants to reconstruct the exclusive-or (XOR) of the incoming messages from two user nodes. By allowing an intermediate node to mix incoming data from multiple links, network coding can increase network throughput significantly. For this problem, we consider two possible network strategies. First, two users can transmit data through a multiple-access channel (MAC) so that the receiver recovers each user's message separately and then computes the XOR of the two messages. We call this strategy a MAC strategy. Next, the receiver can also reconstruct the XOR of the two concurrently transmitted messages directly from the channel output. We call this a physical layer network coding (PNC) strategy. In this study, we investigate the error exponent and the cutoff rate of the XMAC. Assuming a Gaussian XMAC, we show that the MAC strategy performs better (in terms of cutoff rate) than the PNC strategy in the low rate region while the PNC strategy performs better in the high rate region.
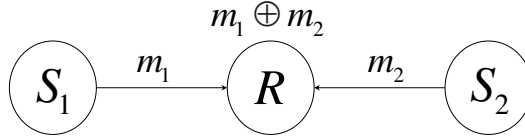
Figure 2.1: Exclusive-or multiple access channel

2.1 Introduction

Network coding has been proposed as a promising technique at the network layer of the protocol stack to improve the network capacity [1]-[3]. In contrast to conventional approaches to network operation, where an intermediate node replicates the received information and delivers it to its neighbor nodes, network coding allows an intermediate node to process incoming data from multiple sources. With network coding the required number of transmissions to send data from a source to a destination can be reduced [1]-[4]. One potential application of network coding would be heartbeat type of packets that are distributed throughout the network, in which individual node has limited battery power. In this application reducing the amount of time a node is transmitting or receiving can significantly enhance the lifetime of the network.

The typical example of network coding is illustrated in Fig. 2.1. An intermediate node receives messages from S_1 and S_2 and computes the exclusive-or (XOR) of the incoming messages from two user nodes. In standard network coding, each user transmits data to the receiver in a time-division multiple-access (TDMA) manner. The receiver then computes the XOR of the two packets. Recently there has been efforts to further reduce the transmission (and thus also the reception) times. In [4], physical layer network coding (PNC) was proposed where the XOR operation is performed at the physical layer by suitable modulation and demodulation. In PNC, the receiver maps simultaneously transmitted signals from two users into the XOR of the two users' data bits. We call this type of channel the *exclusive-or multiple-access channel* (XMAC). However, error control coding was not considered in [4]. If the intermediate node has

the ability to use error control coding then the XOR of the data can benefit from the coding gain.

We consider two network strategies: a multiple-access channel (MAC) strategy and a physical layer network coding (PNC) strategy. In the MAC strategy, two users send data through a MAC. Then the receiver estimates each user's message separately and computes the XOR of the two messages. In the PNC strategy, the receiver extracts the XOR of the incoming messages directly from the channel output. The capacity of the XMAC is still unknown except for special cases. In [6], the capacity for a specific class of MAC, called the *symmetric linear MAC* was found. They also found the achievable rate for reliable transmission of arbitrary functions of sources over arbitrary MACs. For arbitrary MACs, Nazer *et al.* [6] considered a systematic transmission where in the first phase, a multiple number of users send uncoded information bits using the PNC strategy and in the second phase they send parity bits using the MAC strategy. This can be seen as time-sharing between the MAC strategy and the PNC strategy. In contrast, in our PNC strategy all the coded bits are transmitted using the PNC strategy. Since the capacity of the XMAC is unknown in general, in this study we are interested in investigating the error exponent and the cutoff rate of the XMAC so that we can provide an insight into communication system design for the XMAC including modulation, coding and network strategy.

Since the capacity region and error exponents for the MAC are well studied in the literature [9],[11]-[15], we focus on the PNC strategy in our study. The challenge in the PNC strategy is that signals from two users can arrive with different carrier phases and at different times. In this study we assume that the symbol duration is sufficiently long so that the receiver is able to synchronize the arrival times of incoming symbols from two users. This can be easily accomplished by using an orthogonal frequency division multiplexing (OFDM) type of modulation so that higher data rates are achieved by using multiple frequencies but each symbol has a relatively long duration. Thus we

assume that two users' symbols are perfectly time synchronized in our study. Unlike time synchronization, it is not realistic to achieve phase synchronization in many practical systems. When phase synchronization is not possible, we study the impact of the relative phase difference on the system performance.

The remainder of this chapter is organized as follows. We address the problem of communicating over an XMAC in Section 2.2. Assuming the PNC strategy is applied, the error exponent of the XMAC is derived in Section 2.3. As a special case, we investigate the cutoff rate of an Gaussian XMAC with both MAC and PNC strategies in Section 2.4. The effect of phase difference between two signals on the cutoff rate is considered in Section 2.5. Numerical examples and discussions are provided in Section 2.6. Finally conclusions are given in Section 2.7.

2.2 Problem Formulation
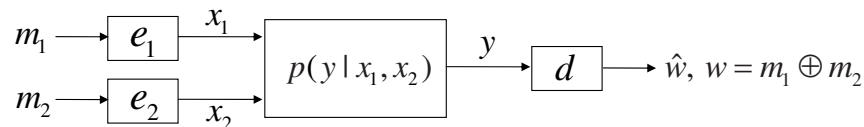
Figure 2.2: System description of an XMAC

We consider a communication system described in Fig. 2.2. In this system, two users transmit encoded messages. The channel probabilistically combines the encoded signals to produce a received signal. The receiver wants to extract from the received signal the XOR of the two messages. This is a special case of computation over a MAC where the receiver reconstructs a function of messages from a multiple number of users [6]. We assume that each user has 2^K possible messages and each message is a binary sequence of length K. Let $\boldsymbol{m}_i$ denote a message of the i-th user. We assume that $\boldsymbol{m}_1$ and $\boldsymbol{m}_2$ are independent and each message is uniform over $\{0,1\}^K$. At the i-th transmitter, the message $\boldsymbol{m}_i$ is encoded into a binary codeword $\boldsymbol{c}_i(\boldsymbol{m}_i)$ by an encoding

function e_i

$$e_i : \{0,1\}^K \rightarrow \mathcal{X}_i^N, \; i = 1,2, \qquad (2.1)$$

where $\mathcal{X}_i$ is the channel input alphabet of the i-th user. In this study, we assume $\mathcal{X}_1 = \mathcal{X}_2 = \{0,1\}$. Note that both channel codes have the same code rate and the same codeword length. Both users' codewords are transmitted to the receiver over a noisy channel with channel transition probability given by

$$p(\boldsymbol{y}|\boldsymbol{x_1},\boldsymbol{x_2}), \qquad (2.2)$$

where $\boldsymbol{x_i} \in \mathcal{X}_i$ and $\boldsymbol{y} \in \mathcal{Y}$ are vectors of length N corresponding to the channel input by the i-th user and the channel output at the receiver respectively and $\mathcal{Y}$ is the channel output alphabet. Given the channel output $\boldsymbol{y}$, the receiver estimates the XOR of the two transmitted messages by a decoding function d

$$d : \mathcal{Y}^N \rightarrow \{0,1\}^K. \qquad (2.3)$$

The error probability is defined as

$$\Pr\left(\boldsymbol{w} \neq \hat{\boldsymbol{w}}\right), \qquad (2.4)$$

where $\boldsymbol{w} = \boldsymbol{m_1} \oplus \boldsymbol{m_2}$, $\hat{\boldsymbol{w}} = d(\boldsymbol{y})$ and $\oplus$ denotes the bitwise XOR. A rate $R = K/N$ is said to be *achievable* if there exist encoding functions e_1, e_2 and a decoding function d such that error probability goes to zero as the codeword length goes to infinity.

As a general assumption, we assume that both users can cooperate in the sense that they are aware of each other's encoding function but not each other's message to be sent at any given time. One simple strategy to reconstruct the XOR of the two

messages, called a multiple-access channel (MAC) strategy, is that each user transmits its message and the receiver estimates each user's message independently as would be done in a MAC then creates the XOR of the two messages. Another possible network strategy, which is our main interest, is that two users send their messages through the common channel and the receiver computes the XOR of the two messages directly from the channel output. We call this type of strategy a physical layer network coding (PNC) strategy. In the PNC strategy, we consider the following cases:

- A random code is generated by each user independently of the other user.

- The same linear code is employed by both users.

In point-to-point communication systems, random codes are known to achieve Shannon limit performance. However, to the best of our knowledge, finding the best achievable performance of random codes in the network coding scenario is still an open problem. In [6]-[8], it has been shown that for some network coding problems, we can achieve fairly good performance close to the capacity upper bound with lattice codes by exploiting their linear structure.

2.3 Error Exponent: Physical Layer Network Coding Strategy

In this section, we investigate the error exponent of the XMAC when the PNC strategy is applied. For random codes, an upper bound on the error probability is obtained using Gallager's random coding technique [16]. For linear codes, we extend the Shulman-Feder bound [17] to the XMAC and obtain an upper bound on the average error probability. In our analysis, we assume that the channel is discrete but the extension to discrete input, continuous output channels is straightforward.

2.3.1 Random Codes

Consider an ensemble of random codes $\mathcal{E}_i$, where each code in the ensemble has 2^K binary codewords of length N and each codeword $\boldsymbol{x}$ is chosen at random according to the probability assignment on the channel input by the i-th user, $Q_i(\boldsymbol{x})$ for $i = 1, 2$. Suppose that the i-th user selects a codebook $C_i \in \mathcal{E}_i$ at random. With some abuse of notation, we will write

$$\mathcal{C}_1 \oplus \mathcal{C}_2 = \{\boldsymbol{x} : \boldsymbol{x} = \boldsymbol{x}_1 \oplus \boldsymbol{x}_2, \forall \boldsymbol{x}_1 \in \mathcal{C}_1, \forall \boldsymbol{x}_2 \in \mathcal{C}_2\}, \tag{2.5}$$

i.e., $\mathcal{C}_1 \oplus \mathcal{C}_2$ is a set of vectors of length N, each of which is a binary sum of a codeword in $\mathcal{C}_1$ and a codeword in $\mathcal{C}_2$. Now define a new code ensemble $\tilde{\mathcal{E}}$ as

$$\tilde{\mathcal{E}} = \{\mathcal{C} : \mathcal{C} = \mathcal{C}_1 \oplus \mathcal{C}_2, \ \forall \mathcal{C}_1 \in \mathcal{E}_1, \forall \mathcal{C}_2 \in \mathcal{E}_2\}. \tag{2.6}$$

Suppose that an arbitrary message $\boldsymbol{m}_i$ enters the i-th user's encoder and is encoded into a codeword $\boldsymbol{c}_i(\boldsymbol{m}_i)$. Let $\boldsymbol{w}_j$ be the j-th lexicographically smallest element of $\{0, 1\}^K$, e.g., $\boldsymbol{w}_1 = 000$ and $\boldsymbol{w}_2 = 001$ when $K = 3$. Let S_j denote a set of binary sequences as

$$S_j = \{x : \boldsymbol{x} = \boldsymbol{c}_1(\boldsymbol{m}_1) \oplus \boldsymbol{c}_2(\boldsymbol{m}_2), \ \boldsymbol{m}_1 \in \{0, 1\}^K, \ \boldsymbol{m}_2 \in \{0, 1\}^K, \ \boldsymbol{m}_1 \oplus \boldsymbol{m}_2 = \boldsymbol{w}_j\}. \tag{2.7}$$

Then S_j's are collectively exhaustive with respect to $\mathcal{C} \in \tilde{\mathcal{E}}$, i.e., $\mathcal{C} = \bigcup_j S_j$. Let $\boldsymbol{x}_{j,k}$ be the k-th element of S_j. Let us introduce the conditional probability $P(\boldsymbol{y}|\boldsymbol{x}_{j,k})$ as

$$P(\boldsymbol{y}|\boldsymbol{x}_{j,k}) = \sum_{(\boldsymbol{c}_1(\boldsymbol{m}_1), \boldsymbol{c}_2(\boldsymbol{m}_2)) \in T} P(\boldsymbol{y}|\boldsymbol{c}_1(\boldsymbol{m}_1), \boldsymbol{c}_2(\boldsymbol{m}_2)) \frac{Q_1(\boldsymbol{c}_1(\boldsymbol{m}_1))Q_2(\boldsymbol{c}_2(\boldsymbol{m}_2))}{Q_3(\boldsymbol{x}_{j,k})}, \tag{2.8}$$

where

$$T = \{(\boldsymbol{c}_1(\boldsymbol{m}_1), \boldsymbol{c}_2(\boldsymbol{m}_2)) : \boldsymbol{c}_1(\boldsymbol{m}_1) \oplus \boldsymbol{c}_2(\boldsymbol{m}_2) = \boldsymbol{x}_{j,k}\} \tag{2.9}$$

Table 2.1: Example: Codebooks C_1 and C_2

source	C_1	C_2
00	0100	0011
01	1101	1011
10	0010	0001
11	1010	0110

$$C = C_1 \oplus C_2$$

$S_1(00)$
0111, 0110,
0011

$S_2(01)$
1111, 1110,
0100

1100

1011

0010, 1001,
1001

0001, 0101

$S_4(11)$

$S_3(10)$
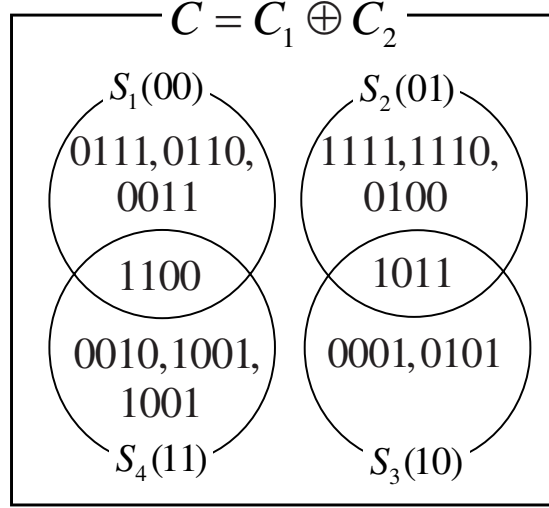
Figure 2.3: Codebook C

and

$$Q_3(\boldsymbol{x}_{j,k}) = \sum_{(\boldsymbol{c}_1(\boldsymbol{m}_1), \boldsymbol{c}_2(\boldsymbol{m}_2)) \in T} Q_1(\boldsymbol{c}_1(\boldsymbol{m}_1)) Q_2(\boldsymbol{c}_2(\boldsymbol{m}_2)). \tag{2.10}$$

Assuming that $\boldsymbol{y}$ is received, the decoding function d is defined as

$$d(\boldsymbol{y}) = \boldsymbol{w}_j, \tag{2.11}$$

if $\exists \boldsymbol{x}_{j,k} \in S_j$ s.t. $P(\boldsymbol{y}|\boldsymbol{x}_{j,k}) \geq P(\boldsymbol{y}|\boldsymbol{x}_{j',k'}) \ \forall \boldsymbol{x}_{j',k'} \notin S_j$.

For example, assume that each user generates a codebook as in table 2.1. Then the receiver generates a codebook $C = C_1 \oplus C_2$ as shown in Fig. 2.3. Each set S_i

is a collection of vectors which correspond to the identical XOR message. Given the channel output, the receiver computes the likelihood of each element in C. If the codeword 0100 is most probable, then the decoder decides the XOR bit is 01. If 1011 is most probable, the decoder selects one of 01 and 10 randomly. Note that this decoder is not optimal since it selects the most probable element $\boldsymbol{x}_{j,k}$ not the most probable XOR message which we are interested in. However this suboptimal decoder not only makes the analysis easier but also enables us to obtain a meaningful performance measure.

Given that the i-th user transmitted $\boldsymbol{m}_i$ resulting in $\boldsymbol{w}_j = \boldsymbol{m}_1 \oplus \boldsymbol{m}_2$, the probability of error averaged over the ensemble $\tilde{\mathcal{E}}$ can be expressed as

$$\bar{P}_{e,j} = \sum_{\boldsymbol{x}_{j,k}} \sum_{\boldsymbol{y}} Q_3(\boldsymbol{x}_{j,k}) P(\boldsymbol{y}|\boldsymbol{x}_{j,k}) \Pr(\text{error}|\boldsymbol{w}_j, \boldsymbol{x}_{j,k}, \boldsymbol{y}), \tag{2.12}$$

where $\Pr(\text{error}|\boldsymbol{w}_j, \boldsymbol{x}_{j,k}, \boldsymbol{y})$ is the probability of decoding error conditioned on the XOR message $\boldsymbol{w}_j$, selection of $\boldsymbol{x}_{j,k}$ and the channel output $\boldsymbol{y}$. To find an upper bound on the average error probability, we define the following events:

- $E_{j,j'} = \{(\mathcal{C}_1, \mathcal{C}_2, \boldsymbol{m}_1, \boldsymbol{m}_2, \boldsymbol{y}) : \boldsymbol{c}_1(\boldsymbol{m}_1) \oplus \boldsymbol{c}_2(\boldsymbol{m}_2) = \boldsymbol{x}_{j',k'}, \text{ for some } \boldsymbol{x}_{j',k'} \in S_{j'}, \\ P(\boldsymbol{y}|\boldsymbol{x}_{j',k'}) \geq P(\boldsymbol{y}|\boldsymbol{x}_{j,k}), \forall \boldsymbol{x}_{j,k} \in S_j \}$

- $E_{j,j',k'} = \{(\mathcal{C}_1, \mathcal{C}_2, \boldsymbol{m}_1, \boldsymbol{m}_2, \boldsymbol{y}) : \boldsymbol{c}_1(\boldsymbol{m}_1) \oplus \boldsymbol{c}_2(\boldsymbol{m}_2) = \boldsymbol{x}_{j',k'} \in S_{j'}, \\ P(\boldsymbol{y}|\boldsymbol{x}_{j',k'}) \geq P(\boldsymbol{y}|\boldsymbol{x}_{j,k}), \forall \boldsymbol{x}_{j,k} \in S_j \}$

- $E_{j,j',l,k'} = \{(\mathcal{C}_1, \mathcal{C}_2, \boldsymbol{m}_1, \boldsymbol{m}_2, \boldsymbol{y}) : \boldsymbol{c}_1(\boldsymbol{m}_1) \oplus \boldsymbol{c}_2(\boldsymbol{m}_2) = \boldsymbol{x}_{j',k'} \in S_{j'}, \\ P(\boldsymbol{y}|\boldsymbol{x}_{j',k'}) \geq P(\boldsymbol{y}|\boldsymbol{x}_{j,l}), \boldsymbol{x}_{j,l} \in S_j \}$.

Let $P_c(\cdot)$ denote a conditional probability conditioned on $\boldsymbol{w}_j, \boldsymbol{x}_{j,k}$ and $\boldsymbol{y}$. Observing that $E_{j,j'} = \bigcup_{k'} E_{j,j',k'}$ and $E_{j,j',k'} = \bigcap_l E_{j,j',l,k'} \subseteq E_{j,j',k,k'}$, the conditional error probability

$\Pr(\text{error}|\boldsymbol{w}_j, \boldsymbol{x}_{j,k}, \boldsymbol{y})$ in (2.12) is upper bounded by

$$
\begin{aligned}
\Pr(\text{error}|\boldsymbol{w}_j, \boldsymbol{x}_{j,k}, \boldsymbol{y}) \;\leq\; & P_c\left(\bigcup_{j'\neq j} E_{j,j'}\right) \leq \left(\sum_{j'\neq j} P_c\left(E_{j,j'}\right)\right)^{\rho_1}, \; 0 < \rho_1 \leq 1 \\
=\; & \left(\sum_{j'\neq j} P_c\left(\bigcup_{k'=1}^{|S_{j'}|} E_{j,j',k'}\right)\right)^{\rho_1} \\
\leq\; & \left(\sum_{j'\neq j}\left(\sum_{k'=1}^{|S_{j'}|} P_c\left(E_{j,j',k'}\right)\right)^{\rho_2}\right)^{\rho_1}, \; 0 < \rho_2 \leq 1 \\
=\; & \left(\sum_{j'\neq j}\left(\sum_{k'=1}^{|S_{j'}|} P_c\left(\bigcap_{l=1}^{|S_j|} E_{j,j',l,k'}\right)\right)^{\rho_2}\right)^{\rho_1} \\
\leq\; & \left(\sum_{j'\neq j}\left(\sum_{k'=1}^{|S_{j'}|} P_c\left(E_{j,j',k,k'}\right)\right)^{\rho_2}\right)^{\rho_1}, \qquad (2.13)
\end{aligned}
$$

where $|A|$ is the cardinality of a set A. From the definition of the event $E_{j,j',k,k'}$, for any $s > 0$ we have

$$
\begin{aligned}
P_c\left(E_{j,j',k,k'}\right) \;=\; & \sum_{\boldsymbol{x}_{j',k'}:P(\boldsymbol{y}|\boldsymbol{x}_{j',k'})\geq P(\boldsymbol{y}|\boldsymbol{x}_{j,k})} Q_3(\boldsymbol{x}_{j',k'}) \\
\leq\; & \sum_{\boldsymbol{x}_{j',k'}} Q_3(\boldsymbol{x}_{j',k'})\left(\frac{P(\boldsymbol{y}|\boldsymbol{x}_{j',k'})}{P(\boldsymbol{y}|\boldsymbol{x}_{j,k})}\right)^s. \qquad (2.14)
\end{aligned}
$$

Since $\boldsymbol{x}_{j',k'}$ is a dummy variable of summation in (2.14), the subscripts can be dropped. From (2.12)-(2.14) we have

$$
\begin{aligned}
\bar{P}_{e,j} \;\leq\; & \left(\sum_{j'\neq j}|S_{j'}|^{\rho_2}\right)^{\rho_1} \sum_{\boldsymbol{y}}\left(\sum_{\boldsymbol{x}'} Q_3(\boldsymbol{x}')P(\boldsymbol{y}|\boldsymbol{x}')^{1-s\rho_1\rho_2}\right) \\
& \times\left(\sum_{\boldsymbol{x}} Q_3(\boldsymbol{x})P(\boldsymbol{y}|\boldsymbol{x})^s\right)^{\rho_1\rho_2}. \qquad (2.15)
\end{aligned}
$$

21

By choosing $s = \frac{1}{1+\rho_1\rho_2}$, we can minimize (2.15) over s and the upper bound becomes

$$\bar{P}_{e,j} \leq \left(\sum_{j' \neq j}|S_{j'}|^{\rho_2}\right)^{\rho_1}\sum_{\boldsymbol{y}}\left(\sum_{\boldsymbol{x}}Q_3(\boldsymbol{x})P(\boldsymbol{y}|\boldsymbol{x})^{\frac{1}{1+\rho_1\rho_2}}\right)^{1+\rho_1\rho_2}. \tag{2.16}$$

After some manipulation, it can be shown that the random variables $|S_j|$'s are i.i.d with the following probability mass function

$$P(|S_j| = l) = \binom{2^N}{l}\sum_{m=1}^{l}(-1)^{l+m}\binom{l}{m}m^{2^K}2^{-N2^K}. \tag{2.17}$$

Lemma 2.1: If $R = \frac{K}{N} < \frac{1}{2}$, the cardinality of S_j converges to 2^K in probability as $N \to \infty$, i.e., for any arbitrarily small $\epsilon > 0$,

$$\lim_{N\to\infty}\Pr\left(||S_j| - 2^K| \geq \epsilon\right) = 0. \tag{2.18}$$

Proof: See Appendix A. ∎

Since for each $j \in \{1, \cdots, 2^K\}$ there exist 2^K pairs of $(\boldsymbol{m}_1, \boldsymbol{m}_2)$ which satisfy $\boldsymbol{m}_1 \oplus \boldsymbol{m}_2 = \boldsymbol{w}_j$, we have $|S_j| \leq 2^K$ and by Lemma 1, $|S_j| \approx 2^K$ when $0 < R < \frac{1}{2}$. Then the average error probability over all pairs of $(\boldsymbol{m}_1, \boldsymbol{m}_2)$ can be upper bounded by

$$\bar{P}_e \leq 2^{\rho_1(\rho_2+1)K}\sum_{\boldsymbol{y}}\left(\sum_{\boldsymbol{x}}Q_3(\boldsymbol{x})P(\boldsymbol{y}|\boldsymbol{x})^{\frac{1}{1+\rho_1\rho_2}}\right)^{1+\rho_1\rho_2}. \tag{2.19}$$

Suppose we have a discrete memoryless channel, i.e.,

$$P(\boldsymbol{y}|\boldsymbol{x}_1, \boldsymbol{x}_2) = \prod_{n=1}^{N}P(\boldsymbol{y}(n)|\boldsymbol{x}_1(n), \boldsymbol{x}_2(n)), \tag{2.20}$$

and choose the distributions $Q_1(\boldsymbol{x})$, $Q_2(\boldsymbol{x})$ and $Q_3(\boldsymbol{x})$ as

$$Q_i(\boldsymbol{x}) = \prod_{n=1}^{N}q_i(\boldsymbol{x}(n)), i = 1, 2, 3, \tag{2.21}$$

22

where $\boldsymbol{x}(n)$ is the n-th element of the sequence $\boldsymbol{x}$, q_1 (q_2) is a probability assignment on the channel input alphabet at the first (second) user and q_3 is a probability assignment on the XOR bit. Then we have

$$P(\boldsymbol{y}|\boldsymbol{x}) = \prod_{n=1}^{N} P(\boldsymbol{y}(n)|\boldsymbol{x}(n)), \tag{2.22}$$

where $P(\boldsymbol{y}(n)|\boldsymbol{x}(n))$ can be obtained by replacing each vector and probability assignments Q_i's with its n-th element and q_i's respectively in (2.8). Now the upper bound on the average error probability in (2.19) can be expressed as

$$
\begin{aligned}
\bar{P}_e &\leq 2^{\rho_1(\rho_2+1)K} \left(\sum_{y \in \mathcal{Y}} \left(\sum_{x=0}^{1} q_3(x) P(y|x)^{\frac{1}{1+\rho_1\rho_2}} \right)^{1+\rho_1\rho_2} \right)^{N} \\
&\leq 2^{-N(E_0(\rho,\boldsymbol{q}_3)-\rho_1(\rho_2+1)R)},
\end{aligned} \tag{2.23}
$$

where $P(y|x)$ denotes $P(\boldsymbol{y}(n) = y|\boldsymbol{x}(n) = x)$, $\rho = \rho_1\rho_2$ and $E_0(\rho, \boldsymbol{q}_3)$ is given by

$$E_0(\rho, \boldsymbol{q}_3) = -\log_2 \left(\sum_{y \in \mathcal{Y}} \left(\sum_{x=0}^{1} q_3(x) P(y|x)^{\frac{1}{1+\rho}} \right)^{1+\rho} \right). \tag{2.24}$$

Finally, the random coding error exponent can be obtained as

$$E_r(R) = \max_{\boldsymbol{q}_3} \max_{0<\rho_1,\rho_2\leq 1} \left(E_0(\rho, \boldsymbol{q}_3) - \rho_1(\rho_2 + 1)R \right). \tag{2.25}$$

The maximization in (2.25) is over all probability vectors $\boldsymbol{q}_3 = (q_3(0), q_3(1))$.

2.3.2 Linear Codes

The random coding exponent for the XMAC suffers from the fact that there exist exponentially many codewords for each XOR message $\boldsymbol{w}_j$. If the same binary linear code is applied at both transmitters, there is only one codeword assigned to each XOR

message $\boldsymbol{w}_j$. In [17], for point-to-point communication systems, an upper bound on the average error probability of binary linear codes was provided. We extend the results to the XMAC and obtain an upper bound on the average error probability.

***Lemma* 2.2**[17]: Consider a discrete memoryless channel with input $\boldsymbol{x}$, output $\boldsymbol{y}$ and transition probability $p(\boldsymbol{y}|\boldsymbol{x})$. Suppose that each codeword is selected independently with the distribution $Q(\boldsymbol{x})$ and the receiver decodes the received signal $\boldsymbol{y}$ into $\boldsymbol{c}(\boldsymbol{m}_i)$, one of the codewords. For any $i \neq j$, $\boldsymbol{x}$ and $\boldsymbol{x}'$, assume

$$\Pr(\boldsymbol{c}(\boldsymbol{m}_i) = \boldsymbol{x}, \boldsymbol{c}(\boldsymbol{m}_j) = \boldsymbol{x}') \leq \alpha \Pr(\boldsymbol{c}(\boldsymbol{m}_i) = \boldsymbol{x})\Pr(\boldsymbol{c}(\boldsymbol{m}_j) = \boldsymbol{x}'), \ \alpha \geq 1, \quad (2.26)$$

$$\Pr(\boldsymbol{c}(\boldsymbol{m}_i) = \boldsymbol{x}) \leq \beta Q(\boldsymbol{x}), \ \beta \geq 1, \quad (2.27)$$

where $Q(\boldsymbol{x}) = \prod_{n=1}^N q(\boldsymbol{x}(n))$. Then the average error probability is upper bounded by

$$\bar{P}_e \ \leq \ \alpha^\rho \beta^{1+\rho} 2^{-N(E_0(\rho, \boldsymbol{q}) - \rho R)}, \ 0 < \rho \leq 1. \quad (2.28)$$

Let $\mathcal{E}$ denote an ensemble of binary linear codes. Assume that both users transmit their messages using the same binary linear code $\mathcal{C} \in \mathcal{E}$ and each coded bit is mapped to one of the binary signals s_0 and s_1. Receiving the channel output $\boldsymbol{y}$, the receiver reconstructs the codeword corresponding to the XOR of two messages. Depending on the channel, the error probability may depend on the codeword which makes finding an upper bound on the average error probability complicated. In such a case, we randomize the signal mapping for each coded bit. The signal mapping can be different for each user. Then we find the average error probability over $\mathcal{E}$ and all possible signal mapping rules.

***Theorem* 2.1**: Let $\mathcal{E}_l$ be an ensemble of binary linear codes satisfying the following property:

$$\Pr\left(\boldsymbol{c}(\boldsymbol{m}_i) \oplus \boldsymbol{c}(\boldsymbol{m}_j) = \boldsymbol{x}\right) \leq \alpha 2^{-N}, \ \forall i \neq j, \ \alpha \geq 1, \ \forall \boldsymbol{x}. \quad (2.29)$$

24

Consider both users transmitting their information using the same binary linear code $\mathcal{C} \in \mathcal{E}_l$ over a binary input XMAC. Then the average error probability over $\mathcal{E}_l$ and all signal mapping rules is bounded by

$$\bar{P}_e \leq \alpha^\rho 2^{-N(E_0(\rho, \boldsymbol{q}) - \rho R)}, \; 0 < \rho \leq 1, \tag{2.30}$$

where $\boldsymbol{q}$ is the uniform distribution.

Proof: The proof is parallel to that of Lemma 1 in [17]. The random signal mapping is equivalent to adding (mod 2) a random vector to each codeword under a fixed signal mapping rule. Define a new ensemble $\tilde{\mathcal{E}}$ as

$$\tilde{\mathcal{E}} = \{\mathcal{C} \oplus \boldsymbol{v} : \forall \mathcal{C} \in \mathcal{E}_l, \; \forall \boldsymbol{v} \in \{0, 1\}^N\}, \tag{2.31}$$

where $\mathcal{C} \oplus \boldsymbol{v}$ denotes a code generated by adding a vector $\boldsymbol{v}$ to each codeword of $\mathcal{C}$. Now consider that the i-th user selects a code $\tilde{\mathcal{C}}_i = \mathcal{C} \oplus \boldsymbol{v}_i \in \tilde{\mathcal{E}}$. Assume that $\boldsymbol{v}_1$ and $\boldsymbol{v}_2$ are independent. Then receiving $\boldsymbol{y}$, the receiver decodes $\boldsymbol{y}$ into one of the codewords of $\tilde{\mathcal{C}}_3 = \mathcal{C} \oplus \boldsymbol{v}_3 \in \tilde{\mathcal{E}}$ where $\boldsymbol{v}_3 = \boldsymbol{v}_1 \oplus \boldsymbol{v}_2$. Using the fact that $\boldsymbol{v}_3$ is a random vector, it is easy to show that the followings are satisfied for all codebooks in $\tilde{\mathcal{E}}$:

$$\Pr(\tilde{\boldsymbol{c}}(\boldsymbol{m}_i) = \boldsymbol{x}) = 2^{-N}, \tag{2.32}$$

$$\Pr(\tilde{\boldsymbol{c}}(\boldsymbol{m}_i) = \boldsymbol{x} | \tilde{\boldsymbol{c}}(\boldsymbol{m}_j) = \boldsymbol{x}') \leq \alpha 2^{-N}. \tag{2.33}$$

Then we can see that (2.26) and (2.27) are satisfied with $\beta = 1$ and $Q(\boldsymbol{x}) = 2^{-N}$. Hence by applying Lemma 2.2 to the XMAC, we have (2.30). ∎

For any specific linear code $\mathcal{C}$ with weight distribution $A_l, \forall l \in \{1, \cdots, N\}$, generate a code ensemble $\mathcal{E}'$ by word permutation which changes the order of codewords. Then we can further enlarge code ensemble by symbol permutation which changes the order of symbols in each codeword. Let us call the new ensemble $\mathcal{E}''$. Then it was shown that

[17]

$$\Pr\left(\boldsymbol{c}''(\boldsymbol{m}_i) \oplus \boldsymbol{c}''(\boldsymbol{m}_j) = \boldsymbol{x}\right) = \frac{A_l}{(2^K - 1)\binom{N}{l}}. \tag{2.34}$$

Then by Theorem 2.1, the average error probability over $\mathcal{E}''$ and all signal mapping rules is upper bounded by

$$\bar{P}_e \ \leq \ 2^{-N(E_0(\rho,\boldsymbol{q}) - \rho R - \rho(\log_2 \alpha)/N)}, \ 0 < \rho \leq 1, \tag{2.35}$$

where $\boldsymbol{q}$ is the uniform distribution and α is given by

$$\alpha = \max_{0 < l \leq N} \frac{A_l 2^N}{(2^K - 1)\binom{N}{l}}. \tag{2.36}$$

For linear codes, the error exponent is given as

$$E_l(R) = \max_{0 < \rho \leq 1} \left(E_0(\rho, \boldsymbol{q}) - \rho R - \rho(\log_2 \alpha)/N\right). \tag{2.37}$$

Example 2.1: If we select a linear code whose weight distribution is close to average weight distribution of random linear code i.e., $A_l \approx 2^{K-N}\binom{N}{l}$, we have $\alpha \approx 1$.

Example 2.2: Suppose that we generate a parity check matrix such that each element is 1 with probability p and each element is independent of the other. Then for such linear codes, the weight distribution averaged over all possible parity check matrix is given by [19]

$$A_l = \left(\frac{1 + (2p - 1)^l}{2}\right)^{N-K} \binom{N}{l}. \tag{2.38}$$

Hence if we select a linear code whose weight distribution is close to (2.38), we have $\alpha \approx (4p^2 - 4p + 2)^{N-K}$.
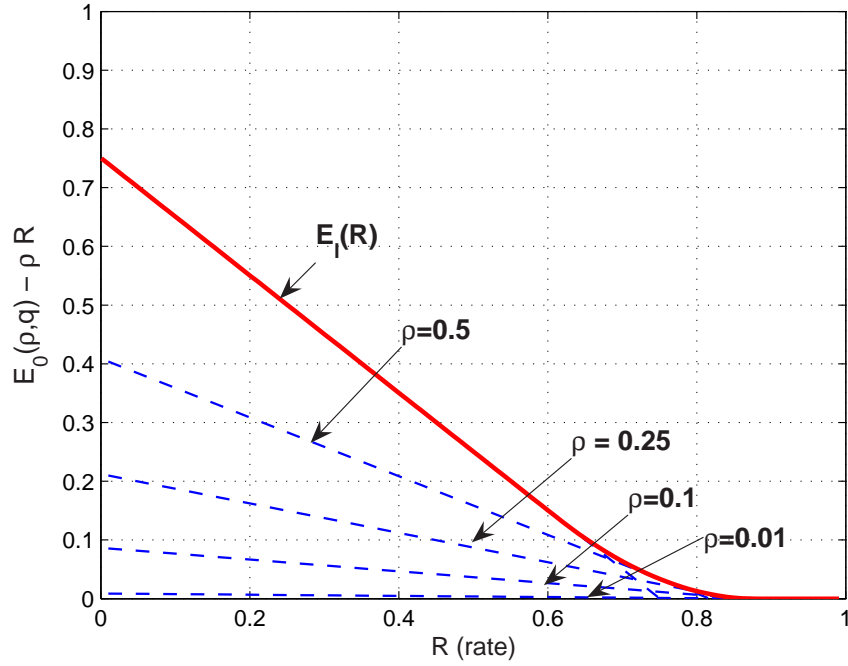
Figure 2.4: The error exponent $E_l(R)$ in the Gaussian XMAC with BPSK modulation and $E_s/N_0 = 3$ dB

Example 2.3: Consider a Gaussian XMAC where the channel output is given as

$$y = x_1 + x_2 + n, \tag{2.39}$$

where n is a Gaussian noise with zero mean and variance of $\frac{N_0}{2}$. Assume that binary phase-shift keying (BPSK) is used at each user node with the same signal power E_s and $\alpha = 1$ in (2.37). For this channel, the error exponent $E_l(R)$ is shown in Fig. 2.4. In Fig. 2.4, $E_0(\rho, \boldsymbol{q}) - \rho R$ is also plotted for various values of ρ.

In Fig. 2.5, error exponents with random codes and with random linear codes are compared for the Gaussian XMAC with BPSK modulation. For this channel, random linear codes show higher error exponent than random codes.
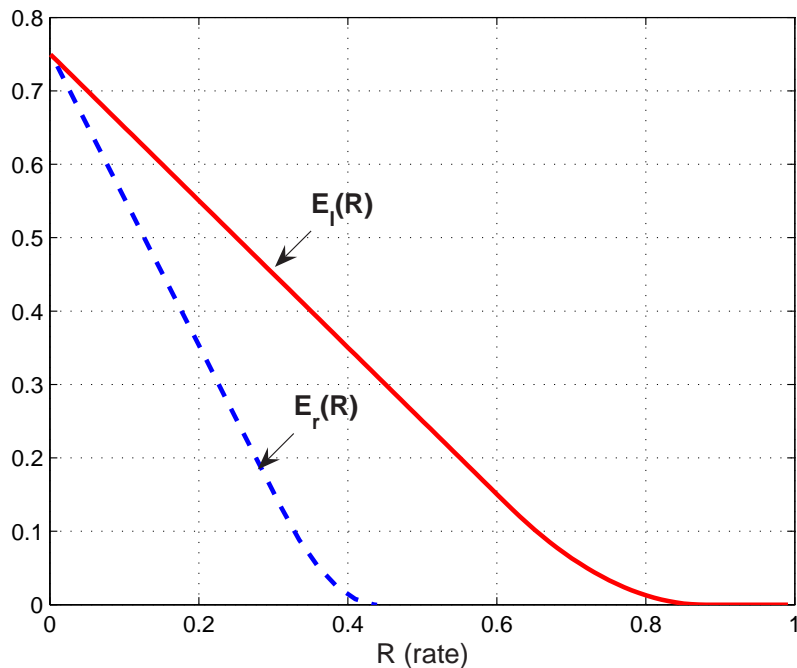
Figure 2.5: Error exponents, $E_r(R)$ and $E_l(R)$ in the Gaussian XMAC with BPSK modulation and $E_s/N_0 = 3$ dB

2.4 Cutoff Rate

In this section, we derive the cutoff rate when each user's signal is transmitted over a Gaussian XMAC. The cutoff rate, R_0 is a parameter for which there exists an upper bound on the average error probability of the form $\bar{P}_e \leq 2^{-N(R_0 - R)}$. The cutoff rate can be also seen as a lower bound on the capacity. If the uniform distribution on the XOR bit maximizes the error exponent with random codes, assuming $\alpha \approx 1$ in (2.36), we can see that the error exponent with linear codes is larger than the random coding error exponent. In general, however, it is not straightforward that one is larger than the other since the random coding exponent is maximized over all possible distributions on the XOR bit. In this study when we derive the cutoff rate, we restrict to the case of linear codes.

Assume that both users employ the same linear code whose weight distribution is close to that of random linear codes. Let R_0^{PNC} denote the cutoff rate in the PNC

strategy defined by

$$R_0^{PNC} = E_0(1, \boldsymbol{q}), \tag{2.40}$$

where $\boldsymbol{q}$ is the uniform distribution. Then by Theorem 2.1, any rate $R < R_0^{PNC}$ is achievable with a linear code. By applying the sphere packing bound to the XMAC and assuming channel input is uniform, it can be shown that R_0^{PNC} is the parameter for which there is the tightest upper bound on the average error probability of the form $\bar{P}_e \le 2^{-N(R_0^{PNC}-R)}$.

2.4.1 Binary Phase-shift Keying

Consider both users using BPSK modulation such that 0 is mapped into $\sqrt{E_s}$ and 1 is mapped into $-\sqrt{E_s}$. The receiver attempts to detect in each symbol interval the XOR signal which is one of $\{-2\sqrt{E_s}, 0, 2\sqrt{E_s}\}$. If 0 is detected, the receiver decides that one of the two users transmitted a 1 and the other transmitted a 0. On the other hand, if one of $\{-2\sqrt{E_s}, 2\sqrt{E_s}\}$ is detected, the receiver decides that both users transmitted the same bit. Assuming a Gaussian XMAC, the received signal y can be expressed as

$$y = x_1 + x_2 + n, \tag{2.41}$$

where x_i is a BPSK symbol of the i-th user and n is Gaussian noise with variance $\sigma^2 = \frac{N_0}{2}$. Assuming equal priors on the inputs, the conditional density of y, the received signal, given that the XOR bit $W = i$ is

$$p(y|W = i) = \begin{cases} \frac{1}{2\sqrt{2\pi}\sigma}\left(e^{\left(-\frac{(y-2\sqrt{E_s})^2}{2\sigma^2}\right)} + e^{\left(-\frac{(y+2\sqrt{E_s})^2}{2\sigma^2}\right)}\right), & i = 0, \\ \frac{1}{\sqrt{2\pi}\sigma}e^{-\frac{y^2}{2\sigma^2}}, & i = 1. \end{cases} \tag{2.42}$$

Then the cutoff rate can be simplifies as

$$
\begin{aligned}
R_0^{PNC} &= 1 - \log_2\left(1 + \int_{-\infty}^{\infty} \frac{1}{\sqrt{2\pi}} e^{-\frac{y^2}{2} - \frac{E_s}{\sigma^2}} \cosh^{\frac{1}{2}}\left(2\sqrt{\frac{E_s}{\sigma^2}} y\right) dy\right) \\
&= 1 - \log_2\left(1 + \int_{-\infty}^{\infty} \frac{1}{\sqrt{2\pi}} e^{-\frac{y^2}{2} - 2R\frac{E_b}{N_0}} \cosh^{\frac{1}{2}}\left(2\sqrt{2R\frac{E_b}{N_0}} y\right) dy\right), \quad (2.43)
\end{aligned}
$$

where E_b is the energy per information bit defined by $E_b = E_s/R$. From Theorem 2.1, there exist a linear code with arbitrarily small error probability provided $R < R_0^{PNC}$. For a fixed R, let $\left(\frac{E_b}{N_0}\right)^*$ denotes the minimum information bit signal-to-noise ratio (SNR) required to achieve the cutoff rate.

Lemma 2.3 (Low rate analysis - PNC strategy/BPSK): Assuming that each user transmits its data using the same linear code and BPSK modulation over an Gaussian XMAC, as $R_0^{PNC} \rightarrow 0^+$, $\left(\frac{E_b}{N_0}\right)^* \rightarrow \infty$.

Proof: See Appendix B. ∎

Both users can also transmit their own data in a multiple-access manner. In [10], based on the error exponent derived by Slepian and Wolf [11], the cutoff rate region of the MAC was introduced. Although there have been many results on the error exponent which improved the one of Slepian and Wolf [12]-[15], we follow the definition of the cutoff rate region introduced in [10]. The cutoff rate region of the MAC is defined as the convex hull of the union of the set of all rate pairs (R_1, R_2) satisfying [10]

$$
R_1 \leq -\log_2\left(\sum_y \sum_{x_2} q_2(x_2)\left(\sum_{x_1} q_1(x_1) P^{1/2}(y|x_1, x_2)\right)^2\right), \quad (2.44)
$$

$$
R_2 \leq -\log_2\left(\sum_y \sum_{x_1} q_1(x_1)\left(\sum_{x_2} q_2(x_2) P^{1/2}(y|x_1, x_2)\right)^2\right), \quad (2.45)
$$

and

$$R_1 + R_2 \leq -\log_2\left(\sum_y\left(\sum_{x_1}\sum_{x_2}q(x_1,x_2)P^{1/2}(y|x_1,x_2)\right)^2\right), \qquad (2.46)$$

where R_i is the i-th user's rate, $q(x_1,x_2) = q_1(x_1)q_2(x_2)$ and $q_i(x)$ is the distribution on the i-th user's channel input alphabet. When both users' code rates are the same, the cutoff rate with the MAC strategy, R_0^{MAC} can be obtained as

$$R_0^{MAC} = -\frac{1}{2}\log_2\left(\sum_y\left(\sum_{x_1,x_2}q(x_1,x_2)P^{1/2}(y|x_1,x_2)\right)^2\right). \qquad (2.47)$$

For BPSK case, the transition probability $P(y|x_1,x_2)$ is given as

$$p(y|x_1 = i, x_2 = j) = \frac{1}{\sqrt{2\pi}\sigma}\exp\left(-\frac{\left(y - (-1)^i\sqrt{E_s} - (-1)^j\sqrt{E_s}\right)^2}{2\sigma^2}\right), \qquad (2.48)$$

where $i,j \in \{0,1\}$. Assuming equal priors on the inputs, the cutoff rate in the MAC strategy R_0^{MAC} is

$$R_0^{MAC} = \frac{3}{2} - \frac{1}{2}\log_2\left(3 + 4e^{-\frac{E_b R}{N_0}} + e^{-\frac{4E_b R}{N_0}}\right). \qquad (2.49)$$

Lemma **2.4** (Low rate analysis - MAC strategy/BPSK): Assuming that each user transmits its data using the same linear code and BPSK modulation over an Gaussian XMAC, as $R_0^{MAC} \to 0^+$, $\left(\frac{E_b}{N_0}\right)^* \to 2\ln 2$.

Proof: See Appendix C. ∎

This result indicates that the minimum signal-to-noise ratio necessary to reach the cutoff rate when the rate goes to 0 is finite in the MAC strategy while it is infinite in the PNC strategy. Therefore the MAC strategy is more energy efficient than the PNC strategy in the low rate region. However, note that with binary input, the maximum achievable rate for the MAC strategy is less than 1 while it is 1 for the NC case. Hence

we cannot simply say that one network strategy outperforms the other.

2.4.2 Binary Frequency-shift Keying

Consider each user using binary frequency-shift keying (BFSK) modulation. The receiver attempts to detect in each symbol interval the presence of each of the possible two frequencies used by the transmitters. If each frequency is detected then the receiver knows that one of the two users transmitted a one and the other transmitted a zero. On the other hand if only one frequency is detected then the receiver knows that both users transmitted the same bit. If $x_i \in \{0, 1\}$ is the channel input by the i-th user and $x_i = j$, the i-th user transmits a signal $s_j(t)$ with energy E_s at frequency ω_j for T seconds:

$$s_j(t) = \sqrt{\frac{2E_s}{T}} \cos(\omega_j t). \tag{2.50}$$

Assuming a Gaussian XMAC, when $x_1 = j, x_2 = k$, the received signal can be represented as

$$r(t) = \sqrt{\frac{2E_s}{T}} \cos(\omega_j t) + \sqrt{\frac{2E_s}{T}} \cos(\omega_k t) + n(t), \tag{2.51}$$

where $n(t)$ is a Gaussian process with zero mean and two-sided spectral density $\frac{N_0}{2}$. The receiver computes four dimensional vector $\boldsymbol{y} = (y_{0c}, y_{0s}, y_{1c}, y_{1s})$ where

$$
\begin{aligned}
y_{ic} &= \sqrt{\frac{2}{T}} \int_0^T \cos(\omega_i t) r(t) dt, \\
y_{is} &= \sqrt{\frac{2}{T}} \int_0^T \sin(\omega_i t) r(t) dt.
\end{aligned}
$$

Conditioned on $x_1 = j, x_2 = k, \theta_1$ and θ_2, y_{ic} and y_{is} are Gaussian random variables with means

$$
\begin{aligned}
E\left[y_{ic}|x_1 = j, x_2 = k\right] &= \sqrt{E_s}\left(\delta_{i,j} + \delta_{i,k}\right), \\
E\left[y_{is}|x_1 = j, x_2 = k\right] &= 0,
\end{aligned}
$$

where $\delta_{i,j} = 1$ if $i = j$ or zero otherwise. The variances are the same as $\sigma^2 = \frac{N_0}{2}$. Assuming equal priors on the inputs, the conditional density of y given $W = i$ is

$$
p(\boldsymbol{y}|W = i) = \begin{cases} \frac{1}{8\pi^2\sigma^4}e^{\left(-\frac{\Omega+4E_s}{2\sigma^2}\right)}\left(e^{\frac{2\sqrt{E_s}y_{0c}}{\sigma^2}} + e^{\frac{2\sqrt{E_s}y_{1c}}{\sigma^2}}\right), & i = 0 \\ \frac{1}{4\pi^2\sigma^4}e^{\left(-\frac{\Omega+2E_s-2\sqrt{E_s}(y_{0c}+y_{1c})}{2\sigma^2}\right)}, & i = 1 \end{cases} \tag{2.52}
$$

where $\Omega = y_{0c}{}^2 + y_{0s}{}^2 + y_{1c}{}^2 + y_{1s}{}^2$. Then the cutoff rate R_0^{PNC} is given as

$$
\begin{aligned}
R_0^{PNC} &= 1 - \log_2\left(1 + \int_{-\infty}^{\infty}\int_{-\infty}^{\infty}\frac{1}{2\pi}e^{-\frac{y_0^2+y_1^2}{2}-R\frac{E_b}{N_0}}\cosh^{\frac{1}{2}}\left(\sqrt{2R\frac{E_b}{N_0}}(y_0 - y_1)\right)dy_0 dy_1\right) \\
&= 1 - \log_2\left(1 + \int_{-\infty}^{\infty}\frac{1}{2\sqrt{\pi}}e^{-\frac{y^2}{4}-R\frac{E_b}{N_0}}\cosh^{\frac{1}{2}}\left(\sqrt{2R\frac{E_b}{N_0}}y\right)dy\right). \tag{2.53}
\end{aligned}
$$

Lemma 2.5 (Low rate analysis - PNC strategy /BFSK): Assuming that each user transmits its data using the same linear code and BFSK modulation over an Gaussian XMAC, as $R_0^{PNC} \to 0^+$, $\left(\frac{E_b}{N_0}\right)^* \to \infty$.

Proof: See Appendix D. ∎

In the MAC strategy, two users transmit data through a MAC with transition

33

probability given by

$$p(\boldsymbol{y}|x_1 = 0, x_2 = 0) = \left(\frac{1}{\sqrt{2\pi}\sigma}\right)^4 e^{-\frac{(y_{0c}-2\sqrt{E_s})^2+y_{0s}^2+y_{1c}^2+y_{1s}^2}{2\sigma^2}},$$

$$p(\boldsymbol{y}|x_1 = 1, x_2 = 1) = \left(\frac{1}{\sqrt{2\pi}\sigma}\right)^4 e^{-\frac{y_{0c}^2+y_{0s}^2+(y_{1c}-2\sqrt{E_s})^2+y_{1s}^2}{2\sigma^2}},$$

$$p(\boldsymbol{y}|x_1 = 0, x_2 = 1) = P(\boldsymbol{y}|x_1 = 1, x_2 = 0)$$

$$= \left(\frac{1}{\sqrt{2\pi}\sigma}\right)^4 e^{-\frac{(y_{0c}-\sqrt{E_s})^2+y_{0s}^2+(y_{1c}-\sqrt{E_s})^2+y_{1s}^2}{2\sigma^2}}.$$

Assuming equal priors on the inputs, the cutoff rate in the MAC strategy, R_0^{MAC} can be computed as

$$R_0^{MAC} = \frac{3}{2} - \frac{1}{2}\log_2\left(3 + 4e^{-\frac{E_b R}{2N_0}} + e^{-\frac{2E_b R}{N_0}}\right). \tag{2.54}$$

Lemma 2.6 (Low rate analysis - MAC strategy/BFSK): Assuming that each user transmits its data using the same linear code and BFSK modulation over an Gaussian XMAC, as $R_0^{MAC} \to 0^+$, $\left(\frac{E_b}{N_0}\right)^* \to 4\ln 2$.

Proof: The proof is parallel to that of Lemma 2.4 and hence omitted. ∎

2.5 Effect of Relative Phase Difference

Due to the characteristic of wireless medium, it may be unrealistically stringent to assume that two users' signals arrive with identical phase. Here we investigate the impact of nonzero relative phase difference on the cutoff rate.

2.5.1 Binary Phase-shift Keying

We assume that phase of each user is random and phase information is perfectly known at the receiver. Then the received signal y can be represented as

$$\boldsymbol{y} = x_1 e^{j\theta_1} + x_2 e^{j\theta_2} + n = y_c + jy_s, \tag{2.55}$$

where θ_i is the i-th user's phase, n is a zero mean circularly symmetric complex Gaussian random variable with variance $\sigma^2 = \frac{N_0}{2}$ per dimension, y_c and y_s are real and imaginary part of $\boldsymbol{y}$ respectively. Then the conditional density of $\boldsymbol{y}$ given the XOR bit $W = i$ and phase information $\boldsymbol{\theta} = (\theta_1, \theta_2)$ is given by

$$p(\boldsymbol{y}|W = i, \boldsymbol{\theta}) = \frac{1}{2\pi\sigma^2} e^{(-\Gamma_i)} \cosh\left(\Lambda_i\right), \quad \text{for } i = 0, 1, \tag{2.56}$$

where

$$
\begin{aligned}
\Gamma_i &= \frac{y_c^2 + y_s^2 + 2E_s(1 + (-1)^i \cos(\theta_1 - \theta_2))}{2\sigma^2}, \quad \text{for } i = 0, 1, \\
\Lambda_i &= \frac{\sqrt{E_s}\left((\cos\theta_1 + (-1)^i \cos\theta_2)y_c + (\sin\theta_1 + (-1)^i \sin\theta_2)y_s\right)}{\sigma^2}, \quad \text{for } i = 0, 1.
\end{aligned}
$$

Letting $y_c' = \cos\left(\frac{\theta_1+\theta_2}{2}\right)y_c + \sin\left(\frac{\theta_1+\theta_2}{2}\right)y_s$ and $y_s' = -\sin\left(\frac{\theta_1+\theta_2}{2}\right)y_c + \cos\left(\frac{\theta_1+\theta_2}{2}\right)y_s$, by the change of variable we obtain an equivalent channel with input W, output $\boldsymbol{y}' = y_c' + jy_s'$ and transition probability

$$p(\boldsymbol{y}'|W = i, \boldsymbol{\theta}) = P(\boldsymbol{y}'|W = i, \phi) = \frac{1}{2\pi\sigma^2} e^{-\Gamma_i'} \cosh\left(\Lambda_i'\right), \quad \text{for } i = 0, 1, \tag{2.57}$$

where

$$\phi = \theta_1 - \theta_2,$$

$$\Gamma'_i = \frac{y_c'^2 + y_s'^2 + 2E_s(1 + (-1)^i \cos(\phi))}{2\sigma^2}, \quad \text{for } i = 0, 1,$$

$$\Lambda'_0 = \frac{2\sqrt{E_s} \cos\left(\frac{\phi}{2}\right) y_c'}{\sigma^2},$$

$$\Lambda'_1 = \frac{2\sqrt{E_s} \sin\left(\frac{\phi}{2}\right) y_s'}{\sigma^2}.$$

For a given ϕ, the cutoff rate $R_0^{PNC}(\phi)$ is given by

$$R_0^{PNC}(\phi) = 1 - \log_2\left(1 + \int_{\boldsymbol{y}'} \sqrt{(p(\boldsymbol{y}'|W=0,\phi)p(\boldsymbol{y}'|W=1,\phi))} d\boldsymbol{y}'\right).$$

Then it is guaranteed that there exists a channel code with arbitrarily small error probability regardless of ϕ if $R < \min_{0 \le \phi < 2\pi} R_0^{PNC}(\phi)$. It can be easily seen that the worst case occurs when $\cos\left(\frac{\phi}{2}\right) = \pm\sin\left(\frac{\phi}{2}\right)$, i.e., $\phi = \frac{\pi}{2}$ or $\frac{3\pi}{2}$. Note that $R_0^{PNC}(\phi)$ is maximized when $\cos\left(\frac{\phi}{2}\right)\sin\left(\frac{\phi}{2}\right) = 0$, i.e., $\phi = 0$ or π. We also notice that $R_0^{PNC}(\phi) = R_0^{PNC}(\phi + \pi)$.

2.5.2 Binary Frequency-shift Keying

Assuming a Gaussian XMAC, when $x_1 = j, x_2 = k$, the received signal can be represented as

$$r(t) = \sqrt{\frac{2E_s}{T}} \cos(\omega_j t + \theta_1) + \sqrt{\frac{2E_s}{T}} \cos(\omega_k t + \theta_2) + n(t). \tag{2.58}$$

The receiver computes four dimensional vector $\boldsymbol{y} = (y_{0c}, y_{0s}, y_{1c}, y_{1s})$ where

$$y_{ic} = \sqrt{\frac{2}{T}} \int_0^T \cos(\omega_i t) r(t) dt,$$

$$y_{is} = \sqrt{\frac{2}{T}} \int_0^T \sin(\omega_i t) r(t) dt.$$

36

Conditioned on $x_1 = j, x_2 = k$ and $\boldsymbol{\theta} = (\theta_1, \theta_2)$, y_{ic} and y_{is} are Gaussian random variables with means

$$E[y_{ic}|x_1 = j, x_2 = k, \boldsymbol{\theta}] = \sqrt{E_s}\left(\cos\theta_1\delta_{i,j} + \cos\theta_2\delta_{i,k}\right)$$

$$E[y_{is}|x_1 = j, x_2 = k, \boldsymbol{\theta}] = -\sqrt{E_s}\left(\sin\theta_1\delta_{i,j} + \sin\theta_2\delta_{i,k}\right),$$

where $\delta_{i,j} = 1$ if $i = j$ or zero otherwise. The variances are the same as $\sigma^2 = \frac{N_0}{2}$. Let us define a sufficient statistic $\boldsymbol{y}' = \left(y'_{0c}, y'_{0s}, y'_{1c}, y'_{1s}\right)$ as

$$y'_{ic} = \cos\left(\frac{\theta_1 + \theta_2}{2}\right)y_{ic} - \sin\left(\frac{\theta_1 + \theta_2}{2}\right)y_{is},$$

$$y'_{is} = \sin\left(\frac{\theta_1 + \theta_2}{2}\right)y_{ic} + \cos\left(\frac{\theta_1 + \theta_2}{2}\right)y_{is}.$$

By the change of variable we obtain an equivalent channel with input W, output $\boldsymbol{y}'$ and transition probability

$$p(\boldsymbol{y}'|W = i, \phi) = \begin{cases} \frac{1}{8\pi^2\sigma^4}e^{\left(-\frac{\Omega + 2E_s(1+\cos\phi)}{2\sigma^2}\right)}\left(e^{\frac{2\sqrt{E_s}y'_{0c}\cos\frac{\phi}{2}}{\sigma^2}} + e^{\frac{2\sqrt{E_s}y'_{1c}\cos\frac{\phi}{2}}{\sigma^2}}\right), & i = 0 \\ \frac{1}{4\pi^2\sigma^4}e^{\left(-\frac{\Omega + 2E_s - 2\sqrt{E_s}\left(y'_{0c}+y'_{1c}\right)\cos\frac{\phi}{2}}{2\sigma^2}\right)}\cosh\left(\frac{\sqrt{E_s}\left(y'_{0s}-y'_{1s}\right)\sin\frac{\phi}{2}}{\sigma^2}\right), & i = 1 \end{cases} \quad (2.59)$$

where $\Omega = {y'_{0c}}^2 + {y'_{0s}}^2 + {y'_{1c}}^2 + {y'_{1s}}^2$. Note that $R_0^{PNC}(\phi) = R_0^{PNC}(-\phi)$.

2.6 Numerical Results and Discussions

In this section, we compare MAC and PNC strategy with respect to the cutoff rate. In Fig. 2.6, the necessary information bit SNR to achieve the cutoff rate over a Gaussian XMAC with BPSK is plotted. In the range of code rate $R \lesssim 0.4$, we notice that the MAC strategy outperforms the PNC strategy. In the MAC strategy, the achievable rate is upper bounded by about 0.71 while the rate of 1 is achievable with the PNC strategy.

The numerical results indicate that in the PNC strategy, there exists an optimal code rate for which the energy per information bit necessary to achieve the cutoff rate is minimized. Similar results for the BFSK case are shown in Fig. 2.7. The cutoff rate can be further improved by using time-sharing between two strategies, i.e., each user exploits the MAC strategy for the first tN channel uses and the PNC strategy for the next $(1-t)N$ channel uses.

The error exponent of Slepian and Wolf [11], on which the cutoff rate region is based, does not count the possibility of time-sharing between two users. Therefore the cutoff rate with the MAC strategy, R_0^{MAC} dose not capture the performance of time-division multiple-access scheme. The performance with TDMA can be easily computed as follows. In the point-to-point communication system that employs BPSK modulation with symbol energy E_s , the cutoff rate R_0 is given by [22]

$$R_0 = 1 - \log_2 \left(1 + e^{-\frac{E_s}{N_0}} \right).$$

Consider that for a given time slot, each user transmits its own data using BPSK modulation such that 0 is mapped to $\sqrt{2E_s}$ and 1 is mapped to $-\sqrt{2E_s}$. Note that the average power used by each user is set to be the same as the NC and MAC cases for a fair comparison. Then the cutoff rate with TDMA, R_0^{TDMA} is given by

$$R_0^{TDMA} = \frac{1}{2} \left(1 - \log_2 \left(1 + e^{-\frac{2E_s}{N_0}} \right) \right), \text{binary antipodal signals.} \tag{2.60}$$

Similar to the BPSK case, for the BFSK modulation we can find the cutoff rate in the TDMA as follows. In point-to-point systems the cutoff rate with binary orthogonal signals is given as [22]

$$R_0 = 1 - \log_2 \left(1 + e^{-\frac{E_s}{2N_0}} \right). \tag{2.61}$$
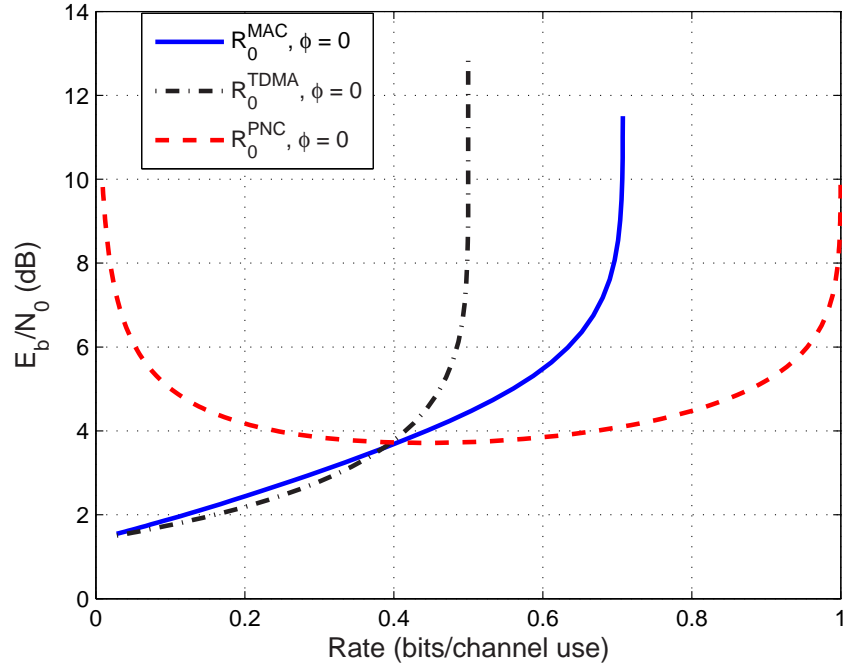
Figure 2.6: Necessary E_b/N_0 to reach the cutoff rate for the Gaussian XMAC with BPSK

Then assuming that symbol energy is $2E_s$ and time-sharing is applied, the cutoff rate can be expressed as

$$R_0^{TDMA} = \frac{1}{2}\left(1 - \log_2\left(1 + e^{-\frac{E_s}{N_0}}\right)\right), \text{binary orthogonal signals.} \qquad (2.62)$$

In Fig. 2.6 it can be seen that in case of BPSK, TDMA shows better performance than the MAC strategy in the low rate region. In the high rate region, the MAC strategy performs better than TDMA and the cutoff rate with TDMA is inherently limited by 0.5. For the BFSK case we can see the similar result in Fig. 2.7.

In Fig. 2.8 we show the cutoff rate when the PNC strategy is applied with BPSK for various values of the phase difference ϕ. Numerical results support our observation in Section V that the cutoff rate is maximized when the phase difference $\phi = 0$ and minimized when $\phi = \frac{\pi}{2}$. At the code rate $R = 0.5$, there is less than 1 dB difference in the required information bit SNR. In Fig. 2.9 the corresponding results for the

39
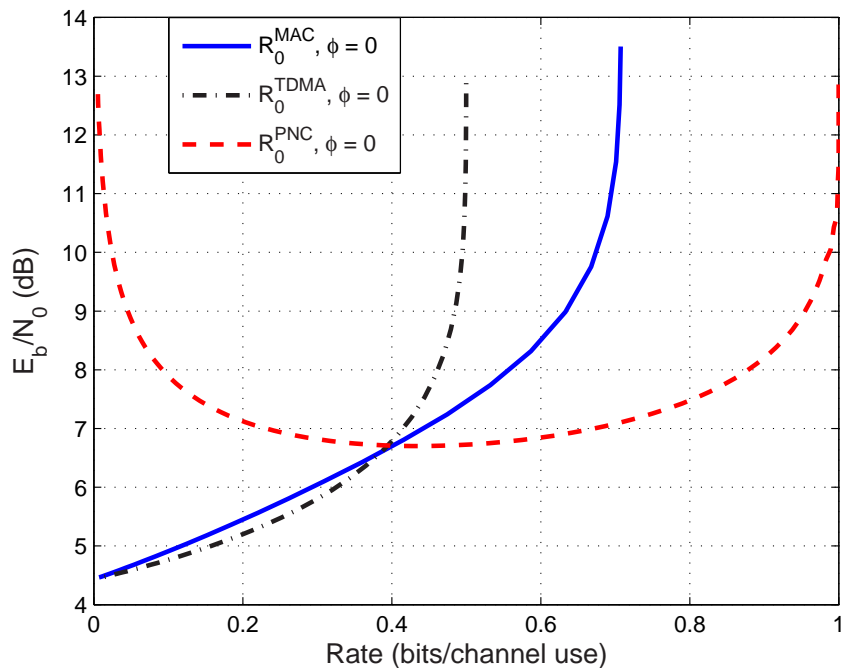
Figure 2.7: Necessary E_b/N_0 to reach the cutoff rate for the Gaussian XMAC with BFSK

BFSK case are shown. In the BFSK case, we have not shown that when the cutoff rate is maximized or minimized with respect to the phase difference. Instead we plot the cutoff rate for $\phi = 0, \frac{\pi}{2}$ and π.

In the Gaussian XMAC, we cannot simply say that one strategy is better than the other in general. In [6] it was indicated that when the channel is well matched to the function (XOR in our case) of users' information sources, the PNC strategy is advantageous over the MAC strategy. An example is that the channel output is given as $y = x_1 \oplus x_2 \oplus e$ where x_i is a binary input by the i-th user and e denotes a channel error, Bernoulli distributed with parameter ϵ. In this channel, $R_0^{PNC} = 1 - \log_2\left(1 + 2\sqrt{\epsilon(1-\epsilon)}\right)$ and $R_0^{MAC} = \frac{1}{2}R_0^{PNC}$. Note that the PNC strategy shows better performance than the MAC strategy regardless of the value of ϵ. For this special case, using Theorem 1 in [6], the capacity can be achieved with the PNC strategy and be computed as $C = 1 - h_B(\epsilon)$ where $h_B(\epsilon) = -\epsilon \log_2(\epsilon) - (1-\epsilon)\log_2(1-\epsilon)$.
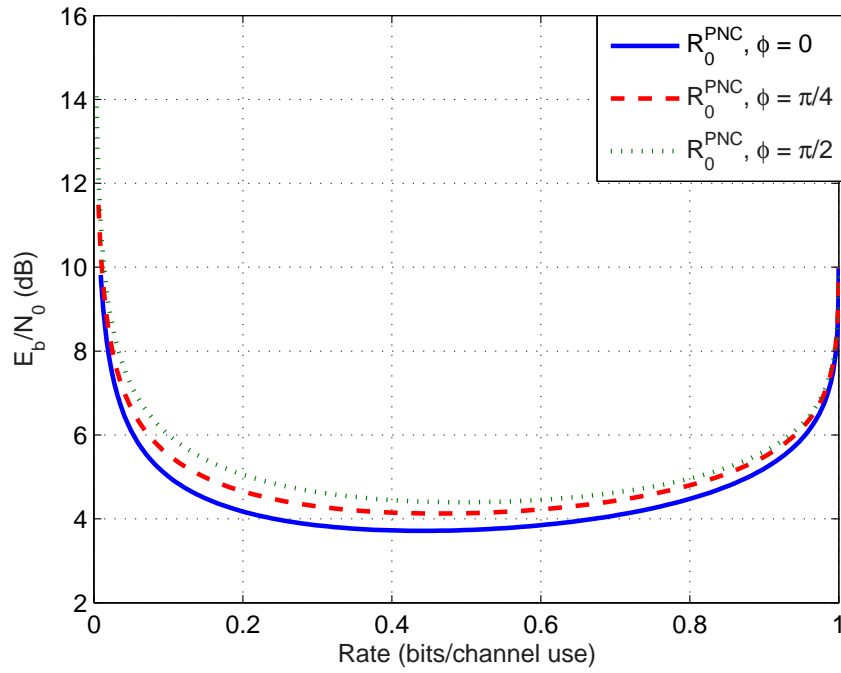
Figure 2.8: The effect of phase difference ϕ on the necessary E_b/N_0 to reach R_0^{PNC} for the Gaussian XMAC with BPSK
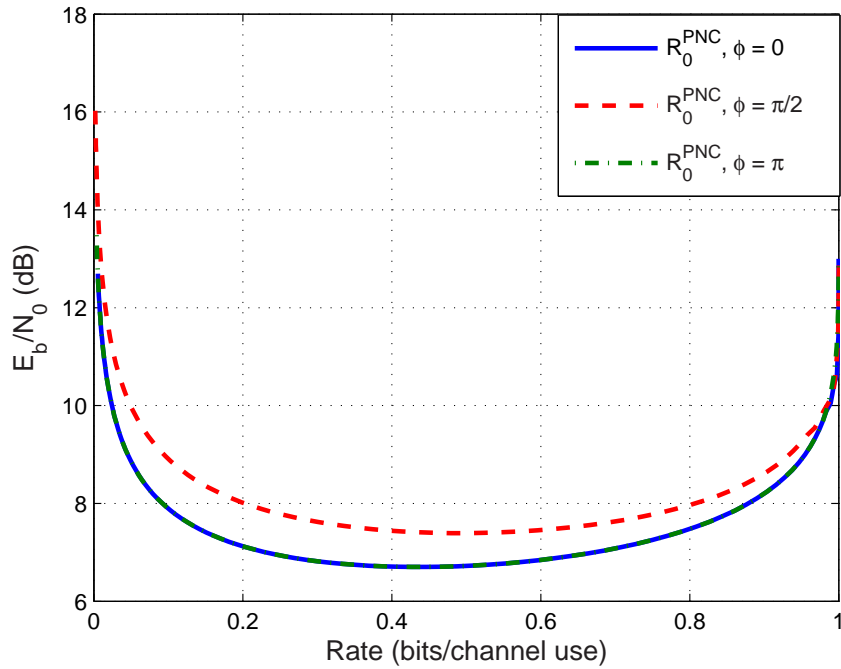
Figure 2.9: The effect of phase difference ϕ on the necessary E_b/N_0 to reach R_0^{PNC} for the Gaussian XMAC with BFSK

2.7   Conclusion

In this chapter, we have considered the XMAC as a typical example of network coding. For this type of channel, the error exponent and the cutoff rate were investigated. These metrics provide meaningful guidance for designing an efficient communication system in the XMAC. Two network strategies, the physical layer network coding (PNC) strategy and the multiple-access (MAC) strategy have been considered. For the PNC strategy, both random codes and linear codes were considered and an upper bound on the average error probability was derived for each case. For the Gaussian XMAC, analytical and numerical results indicate that in the low rate region, the MAC strategy performs better than the PNC strategy while in the high rate region the PNC strategy performs better. In the PNC strategy, the impact of relative phase difference of two users' signal on the performance has been evaluated. Although we assumed binary input channels, the methodology introduced in this chapter can be applied to the case of M-ary signaling where k coded bits are mapped to one of M signal waveforms.

Many aspects of the XMAC are still unexplored. Finding the maximal achievable rate of the XMAC is an open problem. The optimal performance in the XMAC is only known for very limited cases yet. Another interesting issue is related to coding and implementation. In point-to-point communications, turbo codes and low-density parity-check (LDPC) codes show capacity-approaching performance. Hence it will be interesting to examine the performance of such practical codes over the XMAC.

CHAPTER 3

Performance Analysis of LDPC Codes over Exclusive-Or Multiple-Access Channels

In the previous chapter, we investigated the error exponent and the cutoff rate of exclusive-or multiple-access channels (XMAC) where a common receiver reconstructs the exclusive-or (XOR) of incoming data from two users. If two transmitters apply the same binary linear code, the receiver can also apply error correction to the XOR of the transmitted data. In point-to-point communication systems, low-density parity-check (LDPC) codes are one of the most promising error correcting codes and achieve near Shannon limit performance. In this chapter, assuming each link is an additive white Gaussian noise channel, we evaluate noise thresholds of binary LDPC codes via density evolution. Both binary phase-shift keying (BPSK) and binary frequency-shift keying (BFSK) modulation schemes are considered. Numerical results shows that LDPC codes provide reliable performance very close to the achievable rate with linear codes found in Chapter 2.

3.1   Introduction

Originally introduced in wired networks, the concept of network coding has been extended to wireless networks in [4]. In [4], physical layer network coding (PNC) was

proposed. The idea is to recognize that the receiver does not need to determine each user's data bits but only the exclusive-or (XOR) of the two users' data bits. In PNC, two users send data simultaneously. Then the receiver maps the received signal into the XOR of the two messages. In this scheme, network coding is performed through proper modulation and demodulation techniques. However, channel coding was not considered in [4]. Without the coding, the energy would need to be increased significantly to achieve the same error probability. If the same error control is applied by each user then the intermediate node can also apply error correction to the XOR of the transmitted data. This can be accomplished if the same binary linear code is used at each user since the mod 2 sum of two codewords is also a codeword. Of interest is the performance with each user using advanced coding techniques such as turbo codes and low-density parity-check (LDPC) codes.

In point-to-point communication systems, it is well known that LDPC codes show excellent performance at rates very close to the Shannon limit over various channels in the literature [29]-[31]. Since the capacity of the XMAC is unknown in general, it is interesting to examine the performance of LDPC codes over the XMAC. In [29], the density evolution algorithm was introduced to analyze the performance of LDPC codes using the belief propagation algorithm. This method was extended to asymmetric channels in [25]. In this chapter, we analyze the performance of LDPC codes over the Gaussian XMAC by evaluating the threshold via the density evolution technique introduced in [25]. Both binary phase-shift keying (BPSK) and binary frequency-shift keying (BFSK) are considered.

The remainder of this chapter is organized as follows. We describe the communication system and channel model in Section 3.2. In Section 3.3, we review the density evolution technique for asymmetric channels. We then apply this technique to calculate thresholds on the Gaussian XMAC. Numerical examples are provided in Section 3.4 and we present the conclusion in Section 3.5.

3.2   System Model

In this section, we describe the system model and compute quantities necessary to apply density evolution techniques in Section 3.3. Consider the three-node network model described in Fig. 2.1. Two user nodes S_1 and S_2 generate independent binary messages $\boldsymbol{m}_1$ and $\boldsymbol{m}_2$ respectively. The common receiver R wants to reconstruct the XOR of the two messages from the received signal. Assume that both users apply the same binary LDPC code. Each user encodes its message $\boldsymbol{m}_i \in \{0,1\}^K$ into an LDPC codeword $\boldsymbol{c}_i$ of length N. Then each coded bit $x_k = i \in \{0,1\}$ of the k-th user corresponds to transmitting a signal $s_i^k(t)$. Both users' signals are transmitted simultaneously to the receiver over a noisy channel. Assuming $x_1 = i, x_2 = j$ and a Gaussian XMAC, the received signal $r(t)$ can be expressed as

$$r(t) = s_i^1(t) + s_j^2(t) + n(t), \tag{3.1}$$

where $n(t)$ is a white Gaussian noise process with two-sided spectral density $N_0/2$. Since LDPC codes are linear, the modulo 2 sum of any two codewords is also a codeword. The receiver decodes the received signal into a codeword $\boldsymbol{c}_w$ which corresponds to the XOR message $\boldsymbol{w}$ such as

$$
\begin{aligned}
\boldsymbol{c}_w &= \boldsymbol{c}_1 \oplus \boldsymbol{c}_2 = \boldsymbol{m}_1 G \oplus \boldsymbol{m}_2 G \\
&= (\boldsymbol{m}_1 \oplus \boldsymbol{m}_2) G \\
&= \boldsymbol{w} G,
\end{aligned}
$$

where G denotes the generator matrix of the LDPC code. Therefore the receiver can apply a decoder for the same error correction code used by each user to reconstruct $\boldsymbol{w}$.

3.2.1 BPSK

Assume that each user employs BPSK modulation. Then the transmitted signal for user k with data bit i, $s_i^k(t)$ is given as

$$s_i^k(t) = \sqrt{\frac{2E_s}{T}} \cos\left(2\pi f_c t + i\pi + \theta_k\right), \quad 0 \le t \le T \tag{3.2}$$

where E_s is the symbol energy, T is the symbol duration, f_c is the carrier frequency and θ_k is the carrier phase of the k-th user. We assume that θ_1 and θ_2 are fixed and known at the receiver. The receiver computes sufficient statistics $\boldsymbol{y} = (y_c, y_s)$ as

$$y_c = \sqrt{\frac{2}{T}} \int_0^T r(t) \cos\left(2\pi f_c t\right) dt,$$
$$y_s = \sqrt{\frac{2}{T}} \int_0^T r(t) \sin\left(2\pi f_c t\right) dt. \tag{3.3}$$

Conditioned on $\boldsymbol{x} = (x_1, x_2)$ and $\boldsymbol{\theta} = (\theta_1, \theta_2)$, y_c and y_s are independent Gaussian random variables with means

$$E\left[y_c|\boldsymbol{x}, \boldsymbol{\theta}\right] = \sqrt{E_s}\left((-1)^{x_1}\cos\theta_1 + (-1)^{x_2}\cos\theta_2\right),$$
$$E\left[y_s|\boldsymbol{x}, \boldsymbol{\theta}\right] = -\sqrt{E_s}\left((-1)^{x_1}\sin\theta_1 + (-1)^{x_2}\sin\theta_2\right),$$

and the same variance $N_0/2$. Assuming that each user's channel input is equiprobable and independent of the other, the conditional density of channel output $\boldsymbol{y}$ given $\boldsymbol{\theta}$ and the XOR bit $W = x_1 \oplus x_2$, $p(\boldsymbol{y}|W = i, \boldsymbol{\theta})$ is given by

$$p(\boldsymbol{y}|W = i, \boldsymbol{\theta}) = \sum_{(x_1,x_2):x_1 \oplus x_2 = i} \frac{p(\boldsymbol{y}|\boldsymbol{x}, \boldsymbol{\theta})}{2}. \tag{3.4}$$

46

The conditional density $p(\boldsymbol{y}|W = i, \boldsymbol{\theta})$ can be expressed for $i = 0, 1$ as

$$p(\boldsymbol{y}|W = i, \boldsymbol{\theta}) = \frac{1}{\pi N_0} e^{(-\Gamma_i)} \cosh(\Lambda_i), \tag{3.5}$$

where

$$\begin{aligned}
\Gamma_i &= \frac{y_c^2 + y_s^2 + 2E_s(1 + (-1)^i \cos(\theta_1 - \theta_2))}{N_0}, \\
\Lambda_i &= \frac{2\sqrt{E_s}(\cos\theta_1 + (-1)^i \cos\theta_2)y_c}{N_0} \\
&\quad - \frac{2\sqrt{E_s}(\sin\theta_1 + (-1)^i \sin\theta_2)y_s}{N_0}.
\end{aligned}$$

Letting $y_c' = \cos\left(\frac{\theta_1 + \theta_2}{2}\right)y_c - \sin\left(\frac{\theta_1 + \theta_2}{2}\right)y_s$ and $y_s' = \sin\left(\frac{\theta_1 + \theta_2}{2}\right)y_c + \cos\left(\frac{\theta_1 + \theta_2}{2}\right)y_s$, by change of variables we obtain the conditional density of the sufficient statistic $\boldsymbol{y}' = (y_c', y_s')$ given W and $\boldsymbol{\theta}$ as

$$\begin{aligned}
p(\boldsymbol{y}'|W = i, \boldsymbol{\theta}) &= p(\boldsymbol{y}'|W = i, \phi) \\
&= \frac{1}{\pi N_0} e^{-\Gamma_i'} \cosh(\Lambda_i'), \tag{3.6}
\end{aligned}$$

where

$$\begin{aligned}
\phi &= \theta_1 - \theta_2, \\
\Gamma_i' &= \frac{y_c'^2 + y_s'^2 + 2E_s(1 + (-1)^i \cos(\phi))}{N_0}, \quad \text{for } i = 0, 1, \\
\Lambda_0' &= \frac{4\sqrt{E_s}\cos\left(\frac{\phi}{2}\right)y_c'}{N_0}, \\
\Lambda_1' &= \frac{4\sqrt{E_s}\sin\left(\frac{\phi}{2}\right)y_s'}{N_0}.
\end{aligned}$$

Note that the conditional density depends on $\boldsymbol{\theta}$ only through the phase difference ϕ.

3.2.2   BFSK

When each user employs BFSK modulation, the transmitted signal $s_i^k(t)$ is given by

$$s_i^k(t) = \sqrt{\frac{2E_s}{T}} \cos\left(2\pi f_i t + \theta_k\right), \quad 0 \le t \le T. \tag{3.7}$$

The receiver computes sufficient statistics $\boldsymbol{y} = (y_{0c}, y_{0s}, y_{1c}, y_{1s})$ given by

$$
\begin{aligned}
y_{ic} &= \sqrt{\frac{2}{T}} \int_0^T \cos\left(2\pi f_i t\right) r(t) dt, \\
y_{is} &= \sqrt{\frac{2}{T}} \int_0^T \sin\left(2\pi f_i t\right) r(t) dt.
\end{aligned}
$$

Conditioned on $\boldsymbol{x} = (x_1, x_2)$ and $\boldsymbol{\theta} = (\theta_1, \theta_2)$, y_{ic} and y_{is} are independent Gaussian random variables with means

$$
\begin{aligned}
E\left[y_{ic} | \boldsymbol{x}, \boldsymbol{\theta}\right] &= \sqrt{E_s}\left(\cos\theta_1 \delta_{i,x_1} + \cos\theta_2 \delta_{i,x_2}\right) \\
E\left[y_{is} | \boldsymbol{x}, \boldsymbol{\theta}\right] &= -\sqrt{E_s}\left(\sin\theta_1 \delta_{i,x_1} + \sin\theta_2 \delta_{i,x_2}\right),
\end{aligned}
$$

where $\delta_{i,j} = 1$ if $i = j$ or zero otherwise. The variances are $N_0/2$. Similar to the BPSK case, let us define a sufficient statistic $\boldsymbol{y}' = \left(y_{0c}', y_{0s}', y_{1c}', y_{1s}'\right)$ as

$$
\begin{aligned}
y_{ic}' &= \cos\left(\frac{\theta_1 + \theta_2}{2}\right) y_{ic} - \sin\left(\frac{\theta_1 + \theta_2}{2}\right) y_{is}, \\
y_{is}' &= \sin\left(\frac{\theta_1 + \theta_2}{2}\right) y_{ic} + \cos\left(\frac{\theta_1 + \theta_2}{2}\right) y_{is}.
\end{aligned}
$$
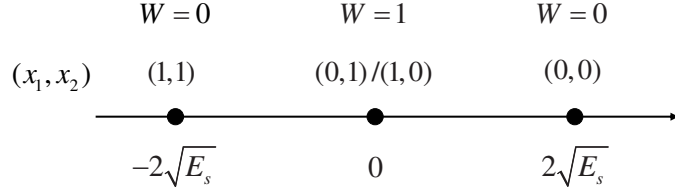
Figure 3.1: An example of signal constellations in the XMAC

By change of variables we obtain the conditional density of sufficient statistic $\boldsymbol{y}'$ given W and $\boldsymbol{\theta}$ as

$$p(\boldsymbol{y}'|W = i, \boldsymbol{\theta}) = p(\boldsymbol{y}'|W = i, \phi)$$
$$= \begin{cases} \frac{1}{2\pi^2 N_0^2} e^{\left(-\frac{\Omega + 2E_s(1 + \cos\phi)}{N_0}\right)} \left(e^{\frac{4\sqrt{E_s} y'_{0c} \cos\frac{\phi}{2}}{N_0}} + e^{\frac{4\sqrt{E_s} y'_{1c} \cos\frac{\phi}{2}}{N_0}} \right), & i = 0 \\ \frac{1}{\pi^2 N_0^2} e^{\left(-\frac{\Omega + 2E_s - 2\sqrt{E_s}\left(y'_{0c} + y'_{1c}\right) \cos\frac{\phi}{2}}{N_0}\right)} \cosh\left(\frac{2\sqrt{E_s}\left(y'_{0s} - y'_{1s}\right) \sin\frac{\phi}{2}}{N_0} \right), & i = 1 \end{cases} \quad (3.8)$$

where $\Omega = {y'_{0c}}^2 + {y'_{0s}}^2 + {y'_{1c}}^2 + {y'_{1s}}^2$ and $\phi = \theta_1 - \theta_2$.

3.3 Density Evolution

In [30], a density evolution technique was introduced to evaluate the asymptotic performance of LDPC codes. The density evolution technique tracks the density of messages passed through the underlying Tanner graph so that the performance of LDPC codes can be analyzed. This method depends on the channel symmetry assumption that the density of messages does not depend on codewords. However, in the XMAC, the density of messages can be codeword-dependent. An example of signal constellations in the XMAC is shown in Fig. 3.1. This is the case when both users employ BPSK modulation so that 0 and 1 are mapped into $\sqrt{E_s}$ and $-\sqrt{E_s}$ respectively and carrier phases $\theta_1 = \theta_2 = 0$. In this case the density of messages depends on the codeword transmitted. For such asymmetric channels, Wang *et al.* proposed a modified density

49

evolution technique [25]. This method keeps track of the density of messages averaged over all valid codewords. Using this density evolution technique, we can calculate the threshold, the maximum channel parameter for which the bit error probability under density evolution converges to zero.

Here we briefly review the density evolution technique for asymmetric channels. Let q^l be the message from a variable node to a check node in the l-th iteration. Then q^l is defined as

$$q^l = \ln \frac{p(\boldsymbol{y}^l | x = 0)}{p(\boldsymbol{y}^l | x = 1)}, \tag{3.9}$$

where $\boldsymbol{y}^l$ is the received signal on the tree-like subset of the Tanner graph spanned from the given variable node with depth $2l$. Let $f(q^l; x)$ be the density of the message q^l at the variable node corresponding to a coded bit x averaged over all valid codewords in the l-th iteration. Define the Chernoff bound on the error probability of message from a variable node corresponding to x in the l-th iteration as [25]

$$CBP^l(x) = \int e^{-\frac{(-1)^x q^l}{2}} f(q^l; x) dq^l. \tag{3.10}$$

The averaged Chernoff bound $\langle CBP^l \rangle$ can be expressed as

$$
\begin{aligned}
\langle CBP^l \rangle &= \frac{1}{2} \left(CBP^l(0) + CBP^l(1) \right) \\
&= CBP^l(0) = CBP^l(1).
\end{aligned}
\tag{3.11}
$$

In [25] for an LDPC code ensemble with a degree distribution pair $(\lambda(x), \rho(x))$ such as

$$\lambda(x) = \sum_{i=2}^{d_v} \lambda_i x^{i-1} \quad \text{and} \quad \rho(x) = \sum_{i=2}^{d_c} \rho_i x^{i-1}$$

where d_v and d_c denote the maximum variable degree and the maximum check degree

respectively, it was shown that $\lim_{l\to\infty} \langle CBP^l \rangle = 0$ if $\lambda_2 \rho'(1) \langle CBP^0 \rangle < 1$ and $\exists\ l'\ s.t.$ $\langle CBP^{l'} \rangle < \epsilon^*$ where ϵ^* is the smallest strictly positive root of the following equation:

$$\lambda \left(\rho'(1)\epsilon \right) \langle CBP^0 \rangle = \epsilon. \tag{3.12}$$

Rather than computing $\langle CBP^l \rangle$ directly, the following iterative upper bound on $\langle CBP^l \rangle$ can be used to check whether the error probability converges to zero or not [25]

$$\langle CBP^{l+1} \rangle \leq \langle CBP^0 \rangle \lambda \left(\rho'(1) \langle CBP^l \rangle \right). \tag{3.13}$$

Therefore we only need to compute $f(q^0; 0)$, the density of the initial message observed from the channel at a variable node corresponding to a coded bit 0. For more details we refer to [25]. Now we use this method to find the threshold on the Gaussian XMAC.

3.3.1 BPSK

From (3.6), the initial message q^0 is given as

$$
\begin{aligned}
q^0 &= \ln \frac{p(\boldsymbol{y}'|W=0,\phi)}{p(\boldsymbol{y}'|W=1,\phi)} \\
&= -\frac{4E_s \cos\phi}{N_0} + \ln\left(\cosh\left(\frac{4\sqrt{E_s}\cos\left(\frac{\phi}{2}\right) y_c'}{N_0} \right) \right) \\
&\quad - \ln\left(\cosh\left(\frac{4\sqrt{E_s}\sin\left(\frac{\phi}{2}\right) y_s'}{N_0} \right) \right).
\end{aligned}
\tag{3.14}
$$

assuming $W = 0$,

$$
\begin{aligned}
q^0 &= \ln \frac{p(\boldsymbol{y}'|W=0,\phi)}{p(\boldsymbol{y}'|W=1,\phi)} \\
&= -\frac{4E_s \cos\phi}{N_0} + \ln\left(\cosh\left(\frac{4\sqrt{E_s}\cos\left(\frac{\phi}{2}\right) y_c'}{N_0} \right) \right) - \ln\left(\cosh\left(\frac{4\sqrt{E_s}\sin\left(\frac{\phi}{2}\right) y_s'}{N_0} \right) \right).
\end{aligned}
$$

Let $A = \ln\left(\cosh\left(\frac{4\sqrt{E_s}\cos\left(\frac{\phi}{2}\right)y_c'}{N_0}\right)\right)$ and $B = \ln\left(\cosh\left(\frac{4\sqrt{E_s}\sin\left(\frac{\phi}{2}\right)y_s'}{N_0}\right)\right)$. Then assuming that the XOR bit W is 0, the corresponding density function of A, $f_A(a)$ can be obtained as

$$
\begin{aligned}
f_A(a) &= \frac{1}{8}\sqrt{\frac{N_0}{E_s\pi}}\sum_{k=0,1}\left|\frac{\sec\left(\frac{\phi}{2}\right)}{\tanh\left(\frac{4\sqrt{E_s}\cos\left(\frac{\phi}{2}\right)\alpha_k}{N_0}\right)}\right| \\
&\times \left(e^{-\frac{\left(\alpha_k - 2\sqrt{E_s}\cos\left(\frac{\phi}{2}\right)\right)^2}{N_0}} + e^{-\frac{\left(\alpha_k + 2\sqrt{E_s}\cos\left(\frac{\phi}{2}\right)\right)^2}{N_0}}\right),
\end{aligned}
\tag{3.15}
$$

where $\alpha_0 = \frac{N_0}{4\sqrt{E_s}\cos\left(\frac{\phi}{2}\right)}\ln\left(e^a + \sqrt{e^{2a} - 1}\right)$ and $\alpha_1 = \frac{N_0}{4\sqrt{E_s}\cos\left(\frac{\phi}{2}\right)}\ln\left(e^a - \sqrt{e^{2a} - 1}\right)$. Similarly given $W = 0$, the density function of B, $f_B(b)$ can be expressed as

$$
f_B(b) = \frac{1}{4}\sqrt{\frac{N_0}{E_s\pi}}\sum_{k=0,1}\left|\frac{e^{-\frac{\beta_k^2}{N_0}}\csc\left(\frac{\phi}{2}\right)}{\tanh\left(\frac{4\sqrt{E_s}\sin\left(\frac{\phi}{2}\right)\beta_k}{N_0}\right)}\right|,
\tag{3.16}
$$

where $\beta_0 = \frac{N_0}{4\sqrt{E_s}\sin\left(\frac{\phi}{2}\right)}\ln\left(e^b + \sqrt{e^{2b} - 1}\right)$ and $\beta_1 = \frac{N_0}{4\sqrt{E_s}\sin\left(\frac{\phi}{2}\right)}\ln\left(e^b - \sqrt{e^{2b} - 1}\right)$. Now the density function of the initial message q^0 given $W = 0$, $f(q^0; 0)$ can be computed as

$$
f(q^0; 0) = \int_0^\infty f_B\left(a - q^0 - \frac{4E_s\cos\phi}{N_0}\right)f_A(a)da.
\tag{3.17}
$$

When $\phi = 0$, the initial message q^0 is

$$
q^0 = -\frac{4E_s}{N_0} + \ln\left(\cosh\left(\frac{4\sqrt{E_s}y_c'}{N_0}\right)\right)
\tag{3.18}
$$

with the density function $f(q^0)$ as

$$
f(q^0; 0) = f_A\left(q^0 + \frac{4E_s}{N_0}\right).
\tag{3.19}
$$

When $\phi = \pi$, we have

$$q^0 = \frac{4E_s}{N_0} - \ln\left(\cosh\left(\frac{4\sqrt{E_s}\, y_s'}{N_0}\right)\right) \tag{3.20}$$

with the density function $f(q^0)$ as

$$f(q^0; 0) = f_B\left(-q^0 + \frac{4E_s}{N_0}\right). \tag{3.21}$$

3.3.2 BFSK

When both users employ BFSK modulation, from (3.8) the initial message q^0 can be expressed as

$$
\begin{aligned}
q^0 &= -\frac{2E_s \cos\phi}{N_0} + \ln\left(\cosh\left(\frac{2\sqrt{E_s}\cos\left(\frac{\phi}{2}\right)z_c}{N_0}\right)\right) \\
&\quad - \ln\left(\cosh\left(\frac{2\sqrt{E_s}\sin\left(\frac{\phi}{2}\right)z_s}{N_0}\right)\right),
\end{aligned} \tag{3.22}
$$

where $z_c = y_{0c}' - y_{1c}'$ and $z_s = y_{0s}' - y_{1s}'$. Note that given $W = 0$, the density functions of z_c and z_s are given by

$$f_{z_c}(z) = \frac{e^{-\frac{\left(z - 2\sqrt{E_s}\cos\frac{\phi}{2}\right)^2}{2N_0}} + e^{-\frac{\left(z + 2\sqrt{E_s}\cos\frac{\phi}{2}\right)^2}{2N_0}}}{2\sqrt{2\pi N_0}}, \tag{3.23}$$

$$f_{z_s}(z) = \frac{1}{\sqrt{2\pi N_0}} e^{-\frac{z^2}{2N_0}}. \tag{3.24}$$

In (3.22), let $M = \ln\left(\cosh\left(\frac{2\sqrt{E_s}\cos\left(\frac{\phi}{2}\right)z_c}{N_0}\right)\right)$ and $N = \ln\left(\cosh\left(\frac{2\sqrt{E_s}\sin\left(\frac{\phi}{2}\right)z_s}{N_0}\right)\right)$. Then from (3.22)-(3.24), the density function of M given $W = 0$ is

$$
\begin{aligned}
f_M(m) &= \frac{1}{4}\sqrt{\frac{N_0}{2E_s\pi}}\sum_{k=0,1}\left|\frac{\sec\left(\frac{\phi}{2}\right)}{\tanh\left(\frac{2\sqrt{E_s}\cos\left(\frac{\phi}{2}\right)\mu_k}{N_0}\right)}\right| \\
&\times \left(e^{-\frac{\left(\mu_k-2\sqrt{E_s}\cos\left(\frac{\phi}{2}\right)\right)^2}{2N_0}} + e^{-\frac{\left(\mu_k+2\sqrt{E_s}\cos\left(\frac{\phi}{2}\right)\right)^2}{2N_0}}\right),
\end{aligned}
$$

(3.25)

where $\mu_0 = \frac{N_0}{2\sqrt{E_s}\cos\left(\frac{\phi}{2}\right)}\ln\left(e^m + \sqrt{e^{2m}-1}\right)$ and $\mu_1 = \frac{N_0}{2\sqrt{E_s}\cos\left(\frac{\phi}{2}\right)}\ln\left(e^m - \sqrt{e^{2m}-1}\right)$. Similarly the density function of N given $W = 0$, $f_N(n)$ is given as

$$
f_N(n) = \frac{1}{2}\sqrt{\frac{N_0}{2E_s\pi}}\sum_{k=0,1}\left|\frac{e^{-\frac{\nu_k^2}{2N_0}}\csc\left(\frac{\phi}{2}\right)}{\tanh\left(\frac{2\sqrt{E_s}\sin\left(\frac{\phi}{2}\right)\nu_k}{N_0}\right)}\right|,
$$

(3.26)

where $\nu_0 = \frac{N_0}{2\sqrt{E_s}\sin\left(\frac{\phi}{2}\right)}\ln\left(e^n + \sqrt{e^{2n}-1}\right)$ and $\nu_1 = \frac{N_0}{2\sqrt{E_s}\sin\left(\frac{\phi}{2}\right)}\ln\left(e^n - \sqrt{e^{2n}-1}\right)$. Finally given $W = 0$, the density function of the message q^0, $f(q^0;0)$ is given by

$$
f(q^0;0) = \int_0^\infty f_N\left(n - q^0 - \frac{2E_s\cos\phi}{N_0}\right)f_M(m)dm.
$$

(3.27)

When $\phi = 0$, the initial message q^0 is

$$
q^0 = -\frac{2E_s}{N_0} + \ln\left(\cosh\left(\frac{2\sqrt{E_s}z_c}{N_0}\right)\right)
$$

(3.28)

with the density function $f(q^0)$ as

$$
f(q^0;0) = f_M\left(q^0 + \frac{2E_s}{N_0}\right).
$$

(3.29)

54

When $\phi = \pi$, q^0 is given as

$$q^0 = \frac{2E_s}{N_0} - \ln\left(\cosh\left(\frac{2\sqrt{E_s}z_s}{N_0}\right)\right) \tag{3.30}$$

with the density function

$$f(q^0; 0) = f_N\left(-q^0 + \frac{2E_s}{N_0}\right). \tag{3.31}$$

3.4   Numerical Results

In this section, we present numerical examples showing the performance of LDPC codes over the Gaussian XMAC. Based on the density evolution technique discussed in Section 3.3 and , we calculate the threshold of LDPC code codes. Using numerical optimization techniques called differential evolution, we found good distribution pairs with a maximum variable degree of 30 and a maximum check degree of 20. In our numerical analysis, we determine the threshold as the largest channel parameter for which the evolved average Chernoff bound $\langle CBP^l \rangle$ hits ϵ^*, the smallest strictly positive root of (3.12), in 300 iterations.

In the previous chapter, assuming that both users transmit their messages simultaneously using binary random linear codes, we derived the error exponent of the XMAC, $E_l(R)$ as

$$E_l(R) = \max_{0 < \rho \leq 1}\{E_0(\rho, Q) - \rho R\}, \tag{3.32}$$

where

$$E_0(\rho, Q) = -\log_2 \int_{\boldsymbol{y} \in \mathcal{Y}} \left(\sum_{W=0,1} Q(W)p(\boldsymbol{y}|W)^{\frac{1}{1+\rho}}\right)^{1+\rho} d\boldsymbol{y},$$
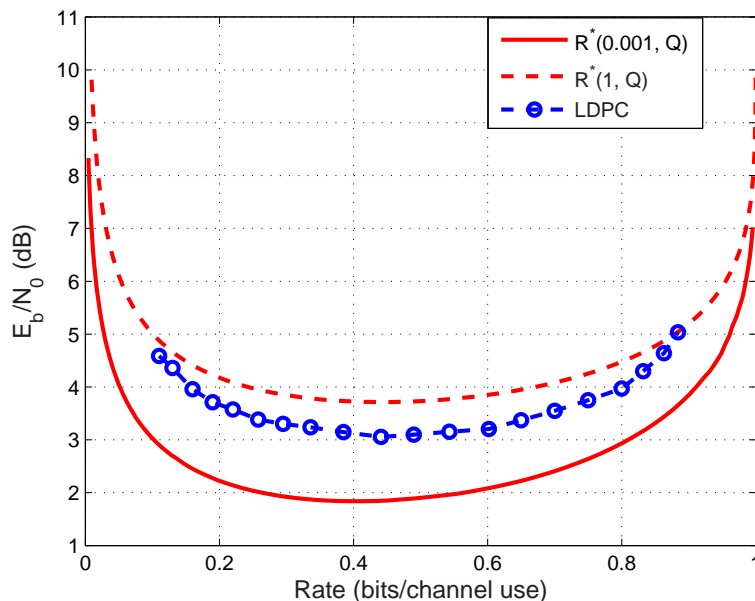
Figure 3.2: Performance of LDPC codes and $R^*(\rho, Q)$ with BPSK ($\phi = 0$)

Q is the uniform distribution on the XOR bit W and $\mathcal{Y}$ is the channel output alphabet. This implies that there exists a binary linear code such that the receiver can recover the XOR of the simultaneously transmitted data over the XMAC with arbitrarily small error probability if its code rate $R < \max_{Q} \max_{0 < \rho \leq 1} R^*(\rho, Q)$ where

$$R^*(\rho, Q) = \frac{E_0(\rho, Q)}{\rho}.$$

Note that given distribution Q, $R^*(\rho, Q)$ is a decreasing function of ρ.

In Fig. 3.2 we plot the signal-to-noise ratio (SNR) per information bit $E_b/N_0 = E_s/(N_0 R)$ as a function of code rate R for LDPC codes and compare it with $R^*(0.001, Q)$ and $R^*(1, Q)$ assuming BPSK modulation and uniform distribution on W. The phase difference ϕ is assumed to be zero. It shows that LDPC codes performs better than $R^*(1, Q)$. This is similar to the result in the point-to-point communication case where LDPC codes show reliable performance at rates above the cutoff rate. We can also see that the performance of LDPC codes is less than 1.5 dB away from $R^*(0.001, Q)$ over
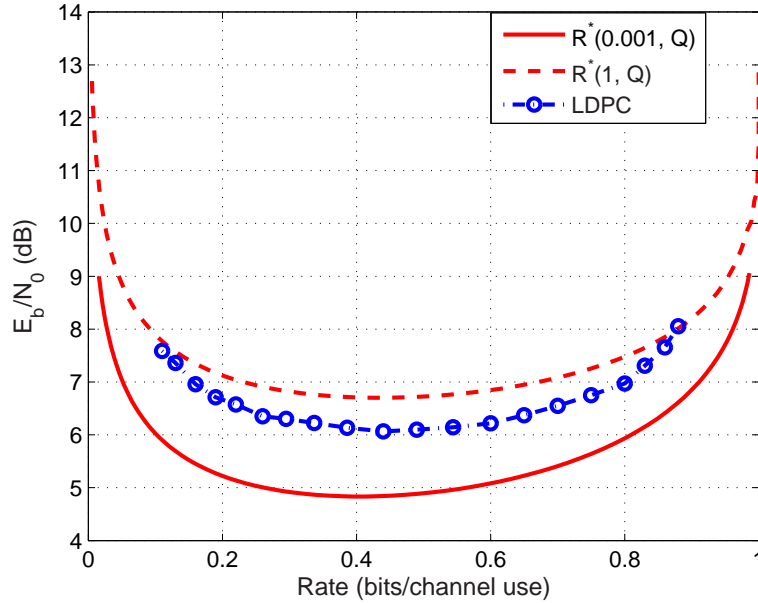
Figure 3.3: Performance of LDPC codes and $R^*(\rho, Q)$ with BFSK ($\phi = 0$)

wide range of rates. Similar results for BFSK case are shown in Fig. 3.3.

3.5   Conclusion

In this chapter, we considered the problem of reconstructing the XOR of simulta-
neously transmitted data from two users. This is a basic structure of wireless networks
where network coding can offer advantages over conventional routing. We investigated
the performance of binary LDPC codes on the Gaussian XMAC where the capacity
is not well established yet. Both BPSK and BFSK modulation schemes were consid-
ered. The noise thresholds of LDPC codes on the Gaussian XAMC were calculated via
the density evolution technique. Numerical results showed that the noise thresholds of
LDPC codes are very close to the values theoretically achievable with linear codes.

CHAPTER 4

Outage Probability of Low-Density Parity-Check (LDPC) Coded Systems

In this chapter, we study the outage probability of low-density parity-check (LDPC) coded systems for slow fading channels (nonergodic channels) under the assumption that the transmitter knows only the channel statistics while the receiver has perfect or imperfect channel side information (CSI) about the fading level. To reliably transmit information through fading channels, adequate signal-to-noise ratio (SNR) is essential. Therefore, outage probability is an important performance measure of wireless communication systems operating in a fading environment. We define the outage event as the set of channel realizations which results in unsuccessful decoding. The fading coefficient is assumed to be random but stays constant over a LDPC codeword. Based on a density evolution analysis, closed-form outage probabilities are derived for both Rayleigh and Rician fading channels. In many practical communication systems it is impossible to obtain perfect CSI. When channel estimation is required and imperfect the effect of channel estimation errors on the outage probability is investigated assuming the estimation error is Gaussian distributed. We further extend this work to the LDPC-coded direct-sequence code-division multiple-access (DS-CDMA) systems.

4.1 Introduction

The capacity of a fading channel is a performance measure which indicates the maximum rate of information flow at an arbitrarily small error probability. There have been many studies on the channel capacity of time-varying channels in the literature [26]-[28]. Goldsmith *et al.* [26] considered the capacity of fading channels with channel side information (CSI) at both transmitter and receiver and at the receiver alone. In [27], the capacity of time-varying channels was investigated under different assumptions of channel knowledge. In [28], bounds on the mutual information with imperfect CSI at the receiver were derived. For ergodic channels, *ergodic capacity* is a good performance measure which defines the maximum achievable rate based on averaging instantaneous mutual information over all channel realizations. However, in nonergodic channels, there is a nonzero probability that the channel experiences deep fading over a codeword transmission hence a given rate R cannot be supported by the channel. In such cases, outage probability, which is defined as the probability of signal-to-noise ratio (SNR) falling below an acceptable threshold, is a more meaningful performance measure in the design of wireless communication systems.

In this study, we investigate the outage probability of low-density parity-check (LDPC) codes over slow fading channels. Recently, LDPC codes have drawn significant attention due to their capacity-approaching error-correcting capabilities and simple decoding algorithm called belief propagation. In [29], the density evolution algorithm was introduced to analyze the performance of LDPC codes under belief propagation decoding. Density evolution techniques describe the evolution of message distributions that are passed on the Tanner graph of the code ensemble. In [30], density evolution was applied to irregular LDPC codes for various channels such as binary erasure channels, binary symmetric channels and additive white Gaussian channels. Then for each type of the channel, the stability condition was derived which can be interpreted as a sufficient condition so that the average error probability converges to zero as the number of

iterations tends to infinity. In [31], assuming perfect CSI at the receiver, the stability condition for uncorrelated Rayleigh fading channels was derived.

The aforementioned previous works considered fast fading channels (ergodic channels) where an infinitely long codeword can experience all the channel realizations during the transmission of a codeword. However, in slow fading channels (nonergodic channels) where a codeword may face deep fading during whole transmission time, reliable transmission at a constant rate is impossible. Therefore the outage probability can be a more important performance measure than capacity for nonergodic channels. We assume that the fading is fixed during the transmission of an LDPC codeword but varies randomly at the next transmission. We also assume that the statistics of fading process are known both at the transmitter and the receiver while the receiver obtains channel estimate. In this study, the outage is defined to be the case where the stability condition, a sufficient condition such that the error probability converges to zero as the number of iterations tends to infinity, does not hold due to fading. Under these assumptions, closed-form outage probabilities for Rayleigh and Rician fading channels are derived. In addition, the channel estimation error is modeled as Gaussian and the effect of imperfect CSI on the outage probability is investigated. We also consider LDPC-coded direct-sequence code-division multiple-access (DS-CDMA) systems. Using the same technique used for the single user case, we derived a closed-form outage probability, which is a function of the signal-to-interference ratio (SIR).

The remainder of this chapter is organized as follows. We outline the communication system and channel models in Section 4.2. In Section 4.3, we describe the outage model and derive an analytical expression for the outage probability over fading channels. In Section 4.4, we extend to the LDPC-coded CDMA systems and derive the corresponding outage probability. Finally conclusions are addressed in Section 4.5.

4.2   System Model

We consider data transmission over fading channels using binary LDPC codes with a degree distribution pair $(\lambda(t), \rho(t))$ such as

$$\lambda(t) = \sum_{i \geq 2}^{d_v} \lambda_i t^{i-1} \quad \text{and} \quad \rho(t) = \sum_{i \geq 2}^{d_c} \rho_i t^{i-1}$$

where λ_i is the fraction of edges connected to a variable node of degree i and ρ_i is the fraction of edges connected to a check node of degree i. The maximum variable degree and check degree are denoted by d_v and d_c respectively. The received signal can be expressed as

$$y = hx + n, \tag{4.1}$$

where x, h and n are the transmitted signal, a fading coefficient and a complex Gaussian noise with variance σ_n^2 per each dimension respectively. The channel fading coefficient h is a complex Gaussian random variable with independent real and imaginary parts each distributed as $\mathcal{N}(\mu/\sqrt{2}, \sigma_h^2)$. Let r and θ be the magnitude and the phase of h respectively. Then the magnitude r is Rician distributed with density function

$$p(r) = \frac{r}{\sigma_h^2} \exp\left(-\frac{(r^2 + \mu^2)}{2\sigma_h^2}\right) I_0\left(\frac{r\mu}{\sigma_h^2}\right), \tag{4.2}$$

where I_0 is the modified Bessel function of the first kind and zero order and μ represents specular component of the channel and the phase θ is uniformly distributed in the interval $(0, 2\pi]$. Since we focus on slow fading channels, h is assumed to be random but stay constant over an LDPC codeword. It is also assumed that the transmitter only knows the statistics of h and no other channel information is available at the transmitter. The transmitter is assumed to send its information at a constant code

rate and with a fixed power level. In this study, BPSK modulation is considered so that 0 and 1 are mapped into $\sqrt{E_s}$ and $-\sqrt{E_s}$ respectively.

At the receiver, for successful decoding, the receiver estimates h and obtains the channel estimate $\hat{h}$ which can be perfect or imperfect. The estimate $\hat{h}$ can be obtained by using pilot symbols. Then the channel realization h can be written as

$$h = \hat{h} + e, \tag{4.3}$$

where e denotes the channel estimation error. We assume that h and $\hat{h}$ are jointly Gaussian and the real (imaginary) components of h and $\hat{h}$ are correlated with correlation coefficient $\rho_{h,\hat{h}}$. We also assume that h and $\hat{h}$ are identically distributed with the same mean and variance. Since the estimation error e is a linear combination of jointly Gaussian random variables h and $\hat{h}$, it is a zero-mean circularly symmetric Gaussian random variable. In [32], it was shown that the channel estimation error is Gaussian distributed when the minimum mean-square error (MMSE) estimator is used. From (4.1) and (4.3), the received signal can be rewritten as

$$
\begin{aligned}
y &= hx + n \\
&= \hat{h}x + xe + n \\
&= \hat{h}x + w, \tag{4.4}
\end{aligned}
$$

where $w = xe + n$. Note that w is a zero-mean circularly symmetric Gaussian random variable with variance $\sigma_w^2 = 2E_s\sigma_h^2(1 - \rho_{h,\hat{h}}) + \sigma_n^2$ per dimension since x takes a value from the set $\{\sqrt{E_s}, -\sqrt{E_s}\}$ with equal probability and a sum of independent Gaussian random variables is also Gaussian. Let $\hat{r}$ and $\hat{\theta}$ be the magnitude and the phase of the estimate $\hat{h}$. Note that random variables r and $\hat{r}$ are identically distributed with the same density function given in (4.2) and $\hat{\theta}$ is uniform in $(0, 2\pi]$. Then the decision

statistic y' is given as

$$
\begin{aligned}
y' &= \operatorname{Re}\left\{ye^{-j\hat{\theta}}\right\} \\
&= \hat{r}x + \operatorname{Re}\left\{we^{-j\hat{\theta}}\right\} \\
&= \hat{r}x + w'.
\end{aligned}
\tag{4.5}
$$

The additive noise term w' is a zero-mean scalar Gaussian random variable with variance σ_w^2. Note that the channel estimation error is related to σ_w^2 in the form of $\rho_{h,\hat{h}}$.

4.3 Outage Probability

In this section, we first describe the outage model based on analytical tools such as density evolution and stability condition. Then we compute the outage probabilities for both Rayleigh and Rician fading channels.

4.3.1 Outage Model

The density evolution technique tracks messages passed through the underlying Tanner graph so that the performance of LDPC codes can be analyzed. Let u_0 be the initial message from a bit node to a check node and P_0 be the density function of u_0. Then for a given $\hat{r} = |\hat{h}|$, u_0 is defined as

$$
\begin{aligned}
u_0 &= \log\left(\frac{P(x = \sqrt{E_s}|y', \hat{r})}{P(x = -\sqrt{E_s}|y', \hat{r})}\right) \\
&= \frac{2y'\hat{r}\sqrt{E_s}}{\sigma_w^2}.
\end{aligned}
\tag{4.6}
$$

Assuming the all zero codeword is transmitted, a change of variable in (4.6) yields

$$
P_0(u_0|\hat{r}) = \frac{\sigma_w}{2\hat{r}\sqrt{2\pi E_s}}\exp\left(-\frac{\sigma_w^2}{8\hat{r}^2 E_s}\left(u_0 - \frac{2\hat{r}^2 E_s}{\sigma_w^2}\right)^2\right).
\tag{4.7}
$$

It is easy to show that $P_0(u_0|\hat{r})$ is symmetric as

$$
\begin{aligned}
P_0(u_0|\hat{r}) &= \frac{\sigma_w}{2r\sqrt{2\pi E_s}} \exp\left(-\frac{\sigma_w^2}{8\hat{r}^2 E_s}\left(u_0 - \frac{2\hat{r}^2 E_s}{\sigma_w^2}\right)^2\right) \\
&= \frac{\sigma_w}{2r\sqrt{2\pi E_s}} \exp\left(-\frac{\sigma_w^2}{8\hat{r}^2 E_s}\left(-u_0 - \frac{2\hat{r}^2 E_s}{\sigma_w^2}\right)^2 + u_0\right) \\
&= P_0(-u_0|\hat{r}) \exp(u_0).
\end{aligned}
\tag{4.8}
$$

In [30], it was also shown that with symmetric $P_0(u_0|\hat{r})$, the error probability converges to zero under density evolution if

$$
\lambda'(0)\rho'(1) < e^s,
\tag{4.9}
$$

where $s = -\log\left(\int_{-\infty}^{\infty} P_0(u_0|\hat{r}) e^{-u_0/2} du_0\right)$.

Definition 4.1: Let $(\lambda(t), \rho(t))$ be a distribution pair of an LDPC code. Then $R^*(\theta)$ is defined as

$$
R^*(\theta) = \max_{(\lambda(t),\rho(t))} \left(R = 1 - \frac{\sum_{i\geq 2}^{d_v} \frac{\rho_i}{i}}{\sum_{i\geq 2}^{d_c} \frac{\lambda_i}{i}} : \lambda'(0)\rho'(1) < \theta\right).
$$

The code rate $R^*(\theta)$ can be interpreted as the maximum achievable code rate of LDPC codes satisfying the stability condition given the channel condition which is parameterized by θ.

Lemma 4.1: $R^*(\theta)$ is a strictly increasing function of θ.

Proof: Suppose that $R^*(\theta)$ is not a strictly increasing function of θ. Then there exist $a > 0$ and an arbitrary small number $\epsilon > 0$ such that

$$
R^*(a) \geq R^*(a + \epsilon).
$$

Let $\lambda_a(t) = \sum_{i\geq 2}^{d_v} \lambda_{a,i} t^{i-1}$ and $\rho_a(t) = \sum_{i\geq 2}^{d_c} \rho_{a,i} t^{i-1}$ such that

$$R^*(a) = 1 - \frac{\sum_{i\geq 2}^{d_c} \frac{\rho_{a,i}}{i}}{\sum_{i\geq 2}^{d_v} \frac{\lambda_{a,i}}{i}} \quad \text{and} \quad \lambda_a{}'(0)\rho_a{}'(1) < a.$$

(Case1 : $\lambda_{a,2} \neq 0$) Consider the following distribution pair $(\lambda_b(t), \rho_b(t))$:

$$\lambda_b(t) = \lambda_a(t),$$

$$\rho_{b,i} = \begin{cases} \rho_{a,i} - \epsilon/\lambda_{a,2}, & \text{if } i = j \geq 2 \text{ and } \rho_{a,j} \neq 0 \\ \rho_{a,i} + \epsilon/\lambda_{a,2}, & \text{if } i = j+1 \geq 3 \\ \rho_{a,i}, & \text{else} \end{cases}.$$

Note that ϵ should be carefully chosen so that $\rho_{b,j} = \rho_{a,j} - \epsilon/\lambda_{a,2} > 0$. Then

$$\lambda_b'(0)\rho_b'(1) = \lambda_a'(0)\rho_a'(1) + \epsilon < a + \epsilon,$$

and the code rate $R(b)$ corresponding to the distribution pair $(\lambda_b(t), \rho_b(t))$ is given by

$$R(b) = 1 - \frac{\sum_{i\geq 2}^{d_c} \frac{\rho_{b,i}}{i}}{\sum_{i\geq 2}^{d_v} \frac{\lambda_{b,i}}{i}}.$$

By the assumption,

$$R(b) \leq R^*(a + \epsilon) \leq R^*(a).$$

However,

$$
\begin{aligned}
R(b) - R^*(a) &= \frac{\sum_{i \geq 2}^{d_c} \frac{\rho_{a,i}}{i}}{\sum_{i \geq 2}^{d_v} \frac{\lambda_{a,i}}{i}} - \frac{\sum_{i \geq 2}^{d_c} \frac{\rho_{b,i}}{i}}{\sum_{i \geq 2}^{d_v} \frac{\lambda_{b,i}}{i}} \\
&= \frac{1}{\sum_{i \geq 2}^{d_v} \frac{\lambda_{a,i}}{i}} \left(\frac{\epsilon}{j \lambda_{a,2}} - \frac{\epsilon}{(j+1)\lambda_{a,2}} \right) > 0,
\end{aligned}
$$

which is a contradiction.

(Case2 : $\lambda_{a,2} = 0$) Consider the following distribution pair $(\lambda_c(t), \rho_c(t))$:

$$
\lambda_c(t) = \lambda_a(t),
$$

$$
\rho_{c,i} = \begin{cases} \rho_{a,i} - \epsilon, & \text{if } i = j \geq 2 \text{ and } \rho_{a,j} \neq 0 \\ \rho_{a,i} + \epsilon, & \text{if } i = j + 1 \\ \rho_{a,i}, & \text{else} \end{cases} .
$$

Note that ϵ should be carefully chosen so that $\rho_{c,j} = \rho_{a,j} - \epsilon > 0$. Then the distribution pair $(\lambda_c(t), \rho_c(t))$ satisfies the stability condition as follows:

$$
\lambda_c'(0)\rho_c'(1) = \lambda_{a,2}\rho_c'(1) = 0 < a.
$$

If we define $R(c)$ as the code rate corresponding to the distribution pair $(\lambda_c(t), \rho_c(t))$, we have

$$
\begin{aligned}
R(c) - R^*(a) &= \frac{\sum_{i \geq 2}^{d_c} \frac{\rho_{a,i}}{i}}{\sum_{i \geq 2}^{d_v} \frac{\lambda_{a,i}}{i}} - \frac{\sum_{i \geq 2}^{d_c} \frac{\rho_{c,i}}{i}}{\sum_{i \geq 2}^{d_v} \frac{\lambda_{c,i}}{i}} \\
&= \frac{1}{\sum_{i \geq 2}^{d_v} \frac{\lambda_{a,i}}{i}} \left(\frac{\epsilon}{j} - \frac{\epsilon}{j+1} \right) > 0,
\end{aligned}
$$

which contradicts the definition of $R^*(a)$. By contradiction, we conclude that $R^*(\theta)$ is

a strictly increasing function of θ. ∎

Since the transmitter knows only the statistics of h, one simple strategy that the transmitter can select is to use an LDPC code of code rate $R^*(\delta)$ with a degree distribution pair $(\lambda^*(t), \rho^*(t))$ such that

$$R^*(\delta) = 1 - \frac{\sum_{i\geq 2}^{d_v} \frac{\rho_i^*}{i}}{\sum_{i\geq 2}^{d_c} \frac{\lambda_i^*}{i}}, \tag{4.10}$$

where

$$\delta = \left(\int_{-\infty}^{\infty} E(P_0(u_0|\hat{r}))e^{-u_0/2} du_0\right)^{-1}. \tag{4.11}$$

By the definition of $R^*(\theta)$ and Lemma 4.1, we assume

$$\lambda^{*\prime}(0)\rho^{*\prime}(1) = \left(\int_{-\infty}^{\infty} E(P_0(u_0|\hat{r}))e^{-u_0/2} du_0\right)^{-1}. \tag{4.12}$$

In (4.11) and (4.12), the density function of the initial message is marginalized with respect to $\hat{r}$ (this may be not an optimal choice in terms of minimizing outage probability). When the transmitted signal experiences deep fading, the stability condition may not be satisfied resulting in a decoding error. In this study, we define the outage as an event that SNR falls below an acceptable level thus the stability condition is violated. Then the outage probability P_{out}^{Rician} can be expressed as

$$\begin{aligned}
P_{out}^{Rician} &= \Pr\left(\lambda^{*\prime}(0)\rho^{*\prime}(1) \geq e^s\right) \\
&= \Pr\left(\delta \geq e^s\right).
\end{aligned} \tag{4.13}$$

4.3.2 Calculation of Outage Probability

Let $A = \int_{-\infty}^{\infty} E(P_0(u_0|\hat{r})) e^{-u_0/2} du_0$ and $B = \int_{-\infty}^{\infty} P_0(u_0|\hat{r}) e^{-u_0/2} du_0$. From (4.2) and (4.7), A can be computed as

$$
\begin{aligned}
A &= \frac{\sigma_w}{\sigma_h^2 \sqrt{2\pi E_s}} \int_0^{\infty} \left(\int_0^{\infty} \exp\left(-\frac{\sigma_w^2}{8\hat{r}^2 E_s} u_0^2 \right) du_0 \right) \\
&\quad \times \exp\left(-\frac{\hat{r}^2 E_s}{2\sigma_w^2} \right) \exp\left(-\frac{(\hat{r}^2 + \mu^2)}{2\sigma_h^2} \right) I_0\left(\frac{\hat{r}\mu}{\sigma_h^2} \right) d\hat{r} \\
&= \frac{1}{\sigma_h^2} \exp\left(-\frac{\mu^2}{2\sigma_h^2} \right) \int_0^{\infty} \hat{r} \exp\left(-\frac{(E_s\sigma_h^2 + \sigma_w^2)\hat{r}^2}{2\sigma_w^2 \sigma_h^2} \right) I_0\left(\frac{\hat{r}\mu}{\sigma_h^2} \right) d\hat{r}. \quad (4.14)
\end{aligned}
$$

Using $I_0(z) = \sum_{k=0}^{\infty} \frac{\left(\frac{z^2}{4} \right)^k}{k!^2}$,

$$
A = \frac{1}{\sigma_h^2} \exp\left(-\frac{\mu^2}{2\sigma_h^2} \right) \sum_{k=0}^{\infty} \frac{\left(\frac{\mu^2}{4\sigma_h^4} \right)^k}{k!^2} \int_0^{\infty} \hat{r}^{2k+1} \exp\left(-\frac{(E_s\sigma_h^2 + \sigma_w^2)\hat{r}^2}{2\sigma_w^2 \sigma_h^2} \right) d\hat{r}. \quad (4.15)
$$

Letting $\Delta = \frac{E_s\sigma_h^2 + \sigma_w^2}{2\sigma_h^2 \sigma_w^2}$ and $t = \Delta \hat{r}^2$ yields

$$
\begin{aligned}
A &= \frac{1}{\sigma_h^2} \exp\left(-\frac{\mu^2}{2\sigma_h^2} \right) \sum_{k=0}^{\infty} \frac{\left(\frac{\mu^2}{4\sigma_h^4} \right)^k}{k!^2} \int_0^{\infty} \hat{r}^{2k+1} \exp\left(-\Delta\hat{r}^2 \right) d\hat{r} \\
&= \frac{1}{\sigma_h^2} \exp\left(-\frac{\mu^2}{2\sigma_h^2} \right) \sum_{k=0}^{\infty} \frac{\left(\frac{\mu^2}{4\sigma_h^4} \right)^k}{k!^2} \frac{1}{2\Delta^{k+1}} \int_0^{\infty} t^k e^{-t} dt. \quad (4.16)
\end{aligned}
$$

Using $\int_0^{\infty} t^k e^{-t} dt = k!$ yields

$$
A = \frac{1}{\sigma_h^2} \exp\left(-\frac{\mu^2}{2\sigma_h^2} \right) \sum_{k=0}^{\infty} \frac{\mu^{2k} \sigma_w^{2k+2}}{k! 2^k \sigma_h^{2k-2} (E_s\sigma_h^2 + \sigma_w^2)^{k+1}}. \quad (4.17)
$$

Next, B can be calculated as

$$
\begin{aligned}
B &= \int_0^\infty \frac{\sigma_w}{\hat{r}\sqrt{2\pi E_s}} \exp\left(-\frac{\sigma_w^2}{8\hat{r}^2 E_s}\left(u_0 - \frac{2\hat{r}^2 E_s}{\sigma_w^2}\right)^2\right) e^{-u_0/2} du_0 \\
&= \frac{\sigma_w}{\hat{r}\sqrt{2\pi E_s}} \exp\left(-\frac{\hat{r}^2 E_s}{2\sigma_w^2}\right) \int_0^\infty \exp\left(-\frac{\sigma_w^2 u_0^2}{8\hat{r}^2 E_s}\right) du_0 \\
&= \exp\left(-\frac{\hat{r}^2 E_s}{2\sigma_w^2}\right).
\end{aligned}
\tag{4.18}
$$

From (4.13), (4.17) and (4.18), the outage probability P_{out}^{Rician} is given by

$$
\begin{aligned}
P_{out}^{Rician} &= \Pr\left(A^{-1} \ge B^{-1}\right) = \Pr\left(\frac{\sigma_h^2 \exp\left(\frac{\mu^2}{2\sigma_h^2}\right)}{\sum_{k=0}^\infty \frac{\mu^{2k}\sigma_w^{2k+2}}{k!2^k\sigma_h^{2k-2}(E_s\sigma_h^2+\sigma_w^2)^{k+1}}} \ge \exp\left(\frac{\hat{r}^2 E_s}{2\sigma_w^2}\right)\right) \\
&= \Pr(\hat{r} \le \alpha) \\
&= \int_0^\alpha \frac{\hat{r}}{\sigma_h^2} \exp\left(\frac{-(\hat{r}^2+\mu^2)}{2\sigma_h^2}\right) I_0\left(\frac{\hat{r}\mu}{\sigma_h^2}\right) d\hat{r} \\
&= 1 - \int_\alpha^\infty \frac{\hat{r}}{\sigma_h^2} \exp\left(\frac{-(\hat{r}^2+\mu^2)}{2\sigma_h^2}\right) I_0\left(\frac{\hat{r}\mu}{\sigma_h^2}\right) d\hat{r} \\
&= 1 - Q\left(\frac{\mu}{\sigma_h}, \frac{\alpha}{\sigma_h}\right),
\end{aligned}
\tag{4.19}
$$

where $Q(a,b)$ denotes Marcum's Q function and α is given by

$$
\alpha = \sqrt{\frac{2\sigma_w^2}{E_s} \log\left(\frac{\sigma_h^2 \exp\left(\frac{\mu^2}{2\sigma_h^2}\right)}{\sum_{k=0}^\infty \frac{\mu^{2k}\sigma_w^{2k+2}}{k!2^k\sigma_h^{2k-2}(E_s\sigma_h^2+\sigma_w^2)^{k+1}}}\right)}.
\tag{4.20}
$$

In case of Rayleigh fading, i.e., when $\mu = 0$, (4.17) becomes

$$
A = \frac{\sigma_w^2}{E_s\sigma_h^2 + \sigma_w^2}.
\tag{4.21}
$$

Then the corresponding outage probability $P_{out}^{Rayleigh}$ can be computed as

$$
\begin{aligned}
P_{out}^{Rayleigh} &= \Pr\left(\lambda'(0)\rho'(1) > \exp\left(\frac{\hat{r}^2 E_s}{2\sigma_w^2}\right)\right) \\
&= \Pr\left(1 + \frac{E_s \sigma_h^2}{\sigma_w^2} \geq \exp\left(\frac{\hat{r}^2 E_s}{2\sigma_w^2}\right)\right) \\
&= \Pr(\hat{r} \leq \beta) \\
&= \int_0^{\beta} \frac{\hat{r}}{\sigma_h^2} \exp\left(-\frac{\hat{r}^2}{2\sigma_h^2}\right) d\hat{r} \\
&= 1 - e^{-\frac{\beta^2}{2\sigma_h^2}},
\end{aligned}
\tag{4.22}
$$

where β is given by

$$
\beta = \sqrt{\frac{2\sigma_w^2}{E_s} \log\left(1 + \frac{E_s \sigma_h^2}{\sigma_w^2}\right)}.
\tag{4.23}
$$

4.3.3 Numerical Examples

In this section, we present a set of numerical results for the outage probability of fading channels in the presence of channel estimation error. Fig. 4.1 shows the outage probability of Rician fading channels as a function of the average received SNR for various values of Rician factor $K = \frac{\mu^2}{2\sigma_h^2}$. Note that for different SNR levels, different LDPC codes are used according to (4.12). The effect of channel estimation error on the outage probability is illustrated in Fig. 4.2 and Fig. 4.3 for Rayleigh and Rician fading channels respectively. We can see that the performance loss due to imperfect channel information is significant for wide range of SNR. It can be seen that at high SNR, small channel estimation errors induce high outage probability. This is because the transmitted signal is severely corrupted by the error term due to inaccurate channel estimation. Table 4.1 shows the outage probabilities of both Rayleigh and Rician fading channels for various $\rho_{h,\hat{h}}$ at SNR of 30 dB. An interesting observation is that even when $\rho \approx 1 (< 1)$, incorrect channel information induces considerable performance
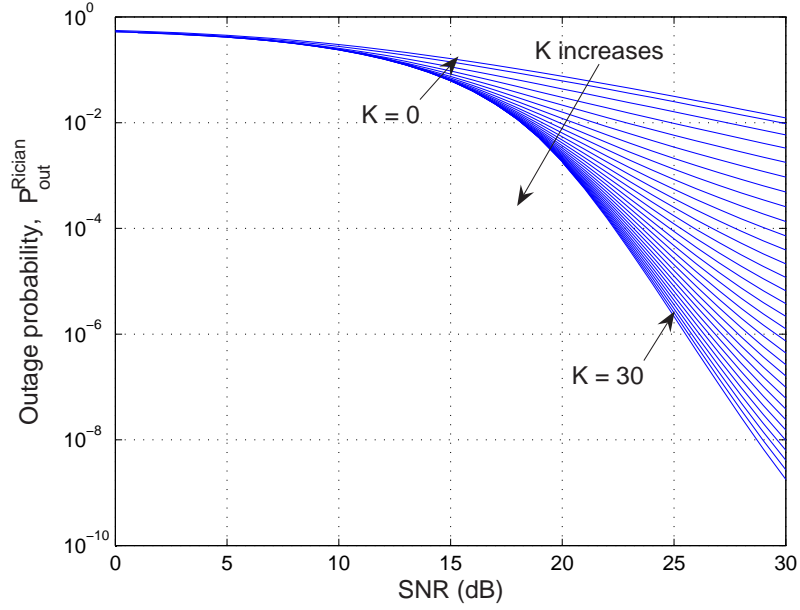
Figure 4.1: Outage probability of Rician fading channels versus average received SNR with perfect CSI ($\sigma_h^2 = 0.5$)

loss compared to when $\rho_{h,\hat{h}} = 1$. For example, in case of the Rician channel, if we increase $\rho_{h,\hat{h}}$ by 0.01 from 0.99 to 1, the outage probability can be reduced by 77%. This observation coincides with the results in [33] which indicated that to avoid severe performance degradation due to imperfect CSI, the second moment of the estimation error should be negligible compared to the reciprocal of the SNR.

Table 4.1: Outage Probability for various values of $\rho_{h,\hat{h}}$ ($\sigma_h^2 = 0.5, \mathrm{SNR} = 30$ dB)

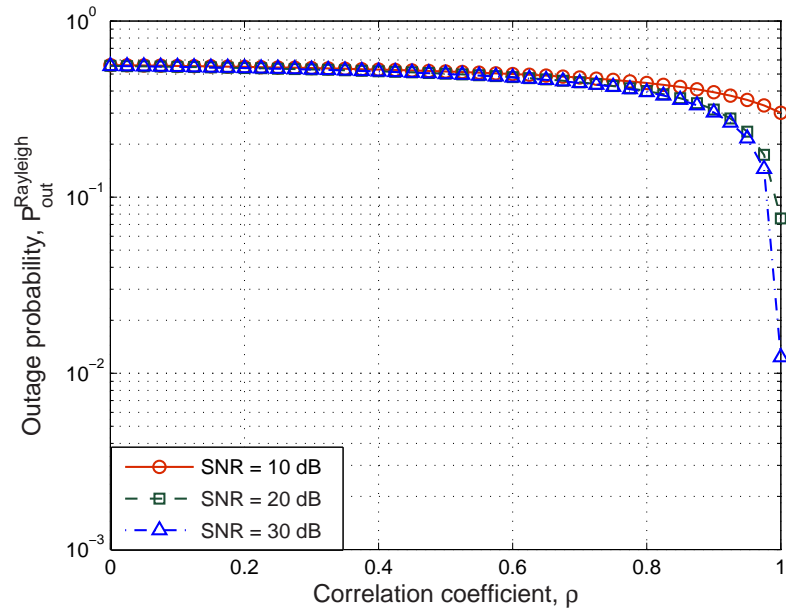| $\rho_{h,\hat{h}}$	$P_{out}^{Rayleigh}$	P_{out}^{Rician} ($K = 1$)
1	1.24×10^{-2}	9.60×10^{-3}
0.99	8.10×10^{-2}	4.17×10^{-2}
0.98	1.26×10^{-1}	6.67×10^{-2}
0.97	1.62×10^{-1}	8.79×10^{-2}
0.96	1.91×10^{-1}	1.07×10^{-1}
0.95	2.16×10^{-1}	1.24×10^{-1}

Figure 4.2: Outage probability of a Rayleigh fading channel versus correlation coefficient $\rho_{h,\hat{h}}$ $(\sigma_h^2 = 0.5)$
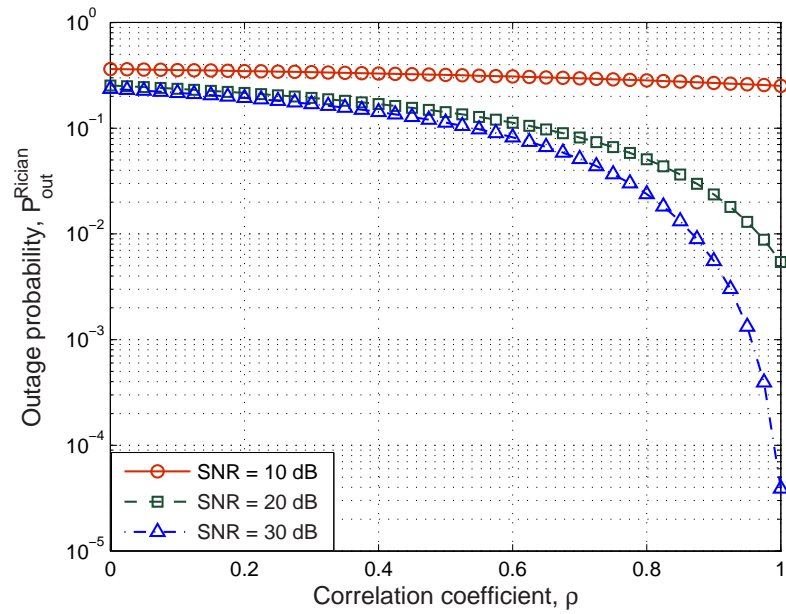

Figure 4.3: Outage probability of a Rician fading channel versus correlation coefficient $\rho_{h,\hat{h}}$ $(\sigma_h^2 = 0.5, K = 10)$

4.4 Outage Probability of LDPC-Coded DS-CDMA Systems

In this Section, we derive the closed-form outage probability of LDPC coded direct-sequence code-division multiple-access (DS-CDMA) systems. Both Rayleigh and Rician fading channels are considered. The channel coefficient is also assumed to be random but stays constant over a LDPC codeword. We also investigate the effect of the system load to the outage probability. Based on an asymptotic analysis for large CDMA systems with processing gain N, i.e. number of active users $K \to \infty$ with a fixed system load $L = \frac{K}{N}$, the outage probability is expressed as a function of system load L.

4.4.1 System Model

We consider a synchronous DS-CDMA system with K users. The transmitted signal from the k-th user is of the form

$$s_k(t) = A_k a_k(t) b_k(t) \cos(2\pi f_c t + \theta_k),\tag{4.24}$$

where A_k is the amplitude of the transmitted signal, $a_k(t)$ is the random spreading signal, $b_k(t)$ is the data signal, f_c is the carrier frequency, and θ_k is the carrier phase. The spreading signal $a_k(t)$ can be written as

$$a_k(t) = \sum_{l=-\infty}^{\infty} a_l^{(k)} \psi(t - lT_c)\tag{4.25}$$

where $\{a_l^{(k)}\}$ is the signature sequence with $a_l^{(k)} \in \{\pm 1\}$, and $\psi(t)$ is the chip waveform with the chip duration T_c. Every signature sequence $\{a_l^{(k)}\}$ is assumed to be random.

The k-th user's data signal $b_k(t)$ can be expressed as

$$b_k(t) = \sum_{j=-\infty}^{\infty} b_j^{(k)} P_T(t - jT), \tag{4.26}$$

where $P_T(t)$ is the rectangular waveform defined as

$$P_T(t) = \begin{cases} 1, & 0 \le t < T \\ 0, & \text{otherwise.} \end{cases} \tag{4.27}$$

where $T = NT_c$ is the symbol duration and N is the processing gain. The j-th LDPC-coded bit of the k-th user is defined as $b_j^{(k)}$ taking values from $\{-1, 1\}$. If we assume the use of rectangular chip waveform, $a_k(t)$ is then expressed as

$$a_k(t) = \sum_{l=-\infty}^{\infty} a_l^{(k)} P_{T_c}(t - lT_c). \tag{4.28}$$

The k-th user's signal $s_k(t)$ is transmitted over a fading channel whose impulse response is given by

$$h_k(t) = r_k e^{j\beta_k} \delta(t - \tau_k) \tag{4.29}$$

where r_k is Rician with the probability density function

$$f_R(r) = \frac{r}{\sigma_h^2} \exp\left(\frac{-(r^2 + \mu^2)}{2\sigma_h^2} \right) I_0\left(\frac{r\mu}{\sigma_h^2} \right), \tag{4.30}$$

where μ is the specular component of the channel and σ_h^2 is the variance of the diffuse component. The random variable β_k represents the phase introduced by the channel, which is uniformly distributed over $[0, 2\pi)$. We assume that the receiver has perfect channel side information (CSI) but the transmitter only knows the statistic of the

channel. The received signal is given by

$$r(t) = \sum_{k=1}^{K} r_k A_k b_k(t) a_k(t) \cos(2\pi f_c t + \phi_k) + n(t), \quad (4.31)$$

where $\phi_k = \beta_k + \theta_k$ and is assumed to be an uniform random variable over $[0, 2\pi)$. We assume that the channel is slow fading so that r_k remains constant over a LDPC codeword. We also assume that the receiver knows the exact value of r_k while the transmitter knows only the distribution of r_k.

4.4.2 Outage Probability

Without loss of generality, we assume that the first user is the desired user and each user is time synchronous to its own receiver, i.e. individual users are coherently demodulated. Letting $T_c = 1$ (hence $T = N$) and $A_k = 2$ $\forall k$, the decision statistic for user 1 is now given by [36]

$$
\begin{aligned}
Z_1 &= \int_0^T r(t) a_1(t) \cos(w_c t) dt. \\
&= r_1 b_0^{(1)} N + \sum_{k=2}^{K} r_k W_k \cos(\phi_k) + n_1, \quad (4.32)
\end{aligned}
$$

where

$$W_k = b_{-1}^{(k)} R_{k,1}(\tau_k) + b_0^{(k)} \widehat{R}_{k,1}(\tau_k)$$

with the continuous-time partial cross-correlation functions defined as

$$R_{k,i}(\tau) = \int_0^\tau a_k(t - \tau) a_i(t) dt$$

$$\widehat{R}_{k,i}(\tau) = \int_\tau^T a_k(t - \tau) a_i(t) dt,$$

and n_1 is a Gaussian random variable with zero mean and variance $N_0 N/4$. The variance of the multiple-access interference (MAI) term $\sum_{k=2}^{K} r_k W_k \cos(\phi_k)$ is $\frac{N(2\sigma_h^2+\mu^2)(K-1)}{3}$. If we approximate the MAI as Gaussian, the variance of the interference plus noise is given by

$$\sigma_I^2 = \frac{N_0 N}{4} + \frac{N(2\sigma_h^2 + \mu^2)}{3}(K-1).$$

From now on, we simplify the notation and write the decision statistic as

$$Z_1 = r_1 x + I, \tag{4.33}$$

where $x = b_0^{(1)} N$ and $I = \sum_{k=2}^{K} r_k W_k \cos(\phi_k) + n_1$.

Let u_0 be the initial message from a bit node to a check node and P_0 be the density function of u_0. Assuming the all zero codeword is transmitted, u_0 is defined as

$$
\begin{aligned}
u_0 &= \log\left(\frac{P(x = N|Z, r_1)}{P(x = -N|Z, r_1)} \right) \\
&= \frac{2 Z r_1 N}{\sigma_I^2}.
\end{aligned}
\tag{4.34}
$$

We also have

$$P_0(u_0|r_1) = \frac{\sigma_I}{2r\sqrt{2\pi N^2}} \exp\left(-\frac{\sigma_I^2}{8r^2 N^2}\left(u_0 - \frac{2r^2 N^2}{\sigma_I^2} \right)^2 \right). \tag{4.35}$$

The outage probability P_{out} is defined as the event where the stability condition is violated. Following the same technique in Section 4.3, we have

$$
\begin{aligned}
P_{out} &= \Pr(\lambda'(0)\rho'(1) > e^s) \\
&= \Pr\left(\left(\int_{-\infty}^{\infty} E(P_0(u_0|r_1)) e^{-u_0/2} du_0 \right)^{-1} > \exp\left(\frac{r_1^2 N^2}{2\sigma_I^2} \right) \right) \\
&= 1 - Q\left(\frac{\mu}{\sigma_h}, \frac{\beta}{\sigma_h} \right),
\end{aligned}
\tag{4.36}
$$

where $Q(a, b)$ denotes Marcum's Q function and β is given by

$$\beta = \sqrt{\frac{2\sigma_I^2}{N^2} \log \left(\frac{\exp\left(\frac{\mu^2}{2\sigma_h^2}\right)}{\sum_{i=0}^{\infty} \frac{\mu^{2i} \sigma_I^{2i+2}}{i! 2^i \sigma_h^{2i} (N^2 \sigma_h^2 + \sigma_I^2)^{i+1}}} \right)}. \tag{4.37}$$

If we define the system load $L = \frac{K}{N}$ and use $\sigma_I^2 = \frac{N_0 N}{4} + \frac{N(2\sigma_h^2 + \mu^2)}{3}(K-1)$, (4.37) can be written as

$$\beta = \sqrt{\frac{N_0}{2N} + \frac{4\sigma_h^2 + 2\mu^2}{3}\left(L - \frac{1}{N}\right)\left(\frac{\mu^2}{2\sigma_h^2} - \log C\right)}, \tag{4.38}$$

where

$$C = \sum_{k=0}^{\infty} \frac{\mu^{2i}}{i! 2^i \sigma_h^{2i}} \left(\frac{\frac{N_0}{4N} + \frac{(2\sigma_h^2 + \mu^2)}{3}\left(L - \frac{1}{N}\right)}{\sigma_h^2 + \frac{N_0}{4N} + \frac{(2\sigma_h^2 + \mu^2)}{3}\left(L - \frac{1}{N}\right)} \right)^{i+1}.$$

Based on the asymptotic analysis for large CDMA systems, i.e. $K \to \infty$ with $L = \frac{K}{N} < \infty$, we have

$$\begin{aligned}
\beta^* &= \lim_{K \to \infty, L = \frac{K}{N}} \beta \\
&= \sqrt{\frac{(4\sigma_h^2 + 2\mu^2)L}{3}\left(\frac{\mu^2}{2\sigma_h^2} - \log C\right)}.
\end{aligned} \tag{4.39}$$

In the Rayleigh fading case, letting $\mu = 0$ results in

$$\begin{aligned}
\beta^* &= \lim_{K \to \infty, L = \frac{K}{N}} \beta \\
&= \sqrt{\frac{4\sigma_h^2 L}{3} \log\left(1 + \frac{3}{2L}\right)}.
\end{aligned} \tag{4.40}$$

Then corresponding outage probability P_{out}^* can be expressed as

$$
\begin{aligned}
P_{out}^* &= \lim_{K \to \infty, L=\frac{K}{N}} P_{out} \\
&= 1 - \exp\left(-\frac{(\beta^*)^2}{2\sigma_h^2}\right) \\
&= 1 - \exp\left(-\frac{2L}{3}\log\left(1+\frac{3}{2L}\right)\right).
\end{aligned}
\tag{4.41}
$$

4.4.3 Numerical Examples
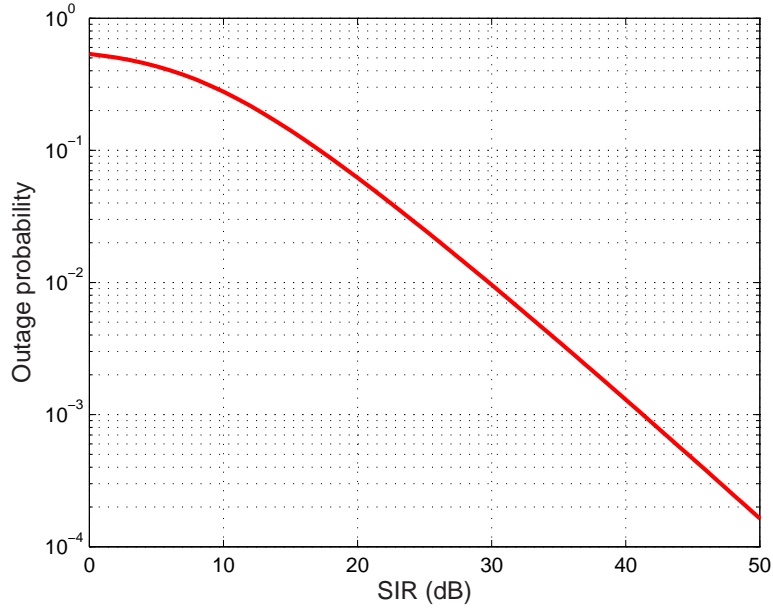
Figure 4.4: Outage probability versus SIR : Rician fading ($\sigma_h^2 = 0.5$, $\mu^2 = 1$, N=64)

Fig. 4.4 shows the relation between the outage probability and signal-to-interference ratio (SIR) defined as $SIR = \frac{N^2(2\sigma_h^2+\mu^2)}{\sigma_I^2}$. The effect of the system load L on the outage probability for both Rayleigh and Rician channels are shown in Fig. 4.5 and Fig. 4.6 respectively where E_s denotes the transmit energy per data symbol. In both Fig. 4.5 and Fig. 4.6, the outage probability saturates as the transmit power increases due to high interference level.
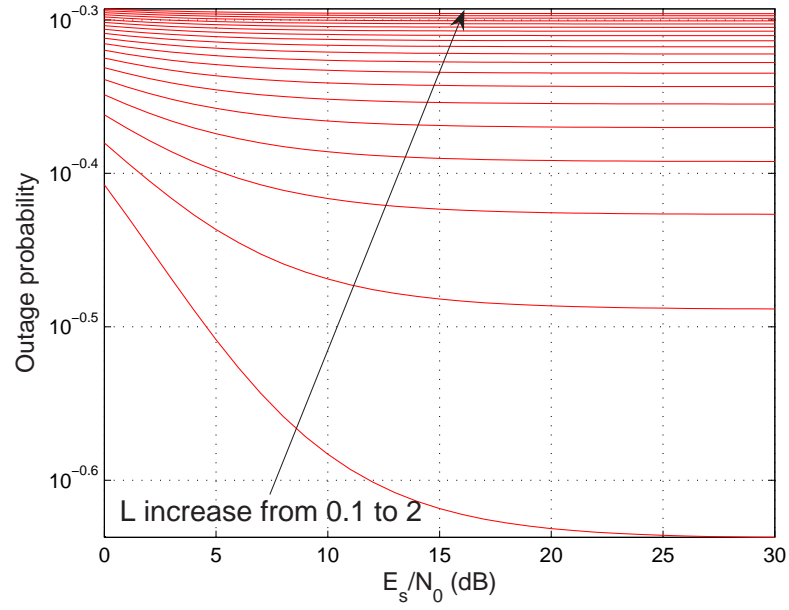
78

Figure 4.5: Outage probability versus E_s/N_0 : Rician fading ($\sigma_h^2 = 0.5, \mu^2 = 1, N = 64, L = \frac{K}{N}$)
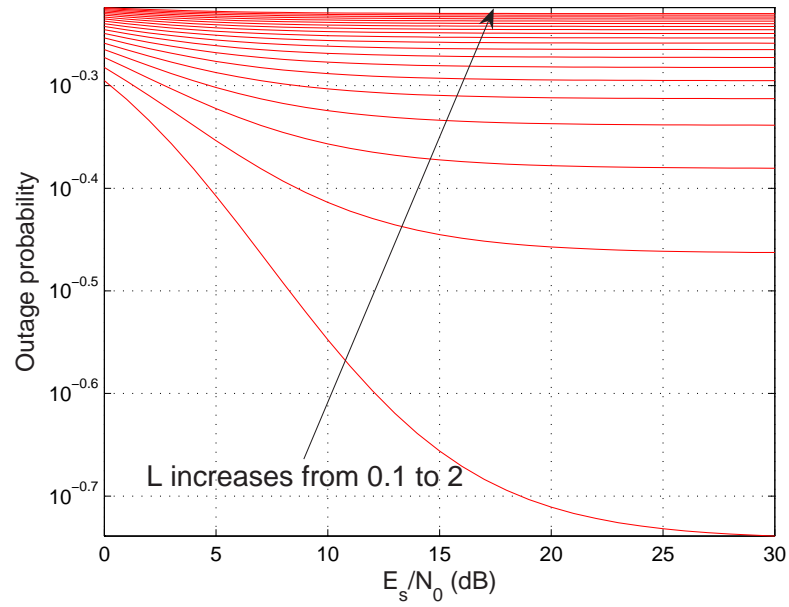
Figure 4.6: Outage probability versus E_s/N_0 : Rayleigh fading ($\sigma_h^2 = 0.5, N = 64, L = \frac{K}{N}$)

4.5 Conclusion

We have studied the outage probability of LDPC-coded communication systems over slow and flat fading channels. Based on the stability condition, the outage probability is defined as the probability of the stability condition is violated. The transmitter was assumed to know the statistics of fading channel while the receiver has perfect or imperfect CSI. We assumed that the transmitter selects an LDPC code according to the stability condition computed by marginalizing the density function of the initial message with respect to the channel coefficient. We also investigated the effect of channel estimation error on the outage probability. Numerical examples were presented illustrating the relationship between outage probability and quality of channel. We extended this work to the LDPC-coded CDMA systems and the corresponding outage probability was derived. In addition to fading channels, the methodology introduced in this study is also applicable to cases where there are other parameters (such as estimated timing, estimated frequency shift and Doppler) that are not accurate and can be modeled as fixed for the duration of a transmission but may randomly vary from one transmission to the next.

CHAPTER 5

Frequency Domain Channel Estimation for OFDM Based on the Slepian Basis Expansion

In this chapter we propose a low complexity frequency domain channel estimator for pilot-symbol-assisted (PSA) orthogonal frequency division multiplexing (OFDM) systems in a low mobility environment. We consider a situation where the receiver needs to estimate multipath channel with low complexity when only limited channel information is available. The proposed scheme relies on a recently proposed model, the Slepian basis expansion model, where Slepian sequences are used to exploit channel correlation in time. However, in slow fading channels, the length of the required Slepian sequence is very long and thus decoding complexity increases. To achieve accurate channel estimation with low complexity, we propose to utilize the Slepian sequences to exploit the frequency correlation of the channel. Simulation results show that the proposed channel estimator outperforms the channel estimator based on the exponential basis expansion model where the channel is approximated as a linear combination of complex exponential functions.

5.1 Introduction

Orthogonal frequency division multiplexing (OFDM) has been applied broadly in wireless communication systems such as digital video broadcasting (DVB) [37] and wireless local area networks (LANs) [38] due to its advantages of converting frequency selective fading channels into multiple frequency flat fading subchannels and mitigating the inter-symbol interference (ISI). Although ISI can be avoided by inserting a cyclic prefix, the transmitted signal on each subcarrier is affected by fading. Therefore, accurate estimates of the channel condition is required for successful decoding at the receiver.

Many channel estimation schemes for OFDM systems have been proposed in the literature [39]-[43]. Pilot-symbol-assisted (PSA) channel estimation is one approach where the transmitter sends known pilot symbols to allow the receiver to reliably estimate the channel at the expense of spectral efficiency. In [41], a low rank approximation to the frequency domain linear mean squared error (LMMSE) estimator was proposed using singular value decomposition. Wiener filter based channel estimators have been proposed in [42]. In [43], a minimum mean square error (MMSE) channel estimator exploiting both time and frequency correlation was presented. However, all the previously mentioned channel estimation schemes require the channel statistics which are time varying and often unavailable in practice. When there exists a channel mismatch, the performance of such estimators can be degraded or limited by an error floor.

The basis expansion model (BEM) has been studied to model doubly selective channels (both time and frequency) [40]. This model approximates doubly selective channels as a linear combination of a finite number of complex exponentials. Based on the BEM, channel estimation can be performed with low complexity and with limited channel information such as the maximum Doppler frequency and the maximum delay spread. In [39], Slepian sequences were used as a basis instead of complex exponentials and it was shown that this new basis allows more accurate representation of wireless channels in

a high mobility environment. However, in a low mobility scenario, the length of the required Slepian sequences should be very long to accurately represent wireless channels, which increases decoding delay and complexity.

In this study, we propose a new frequency domain channel estimator based on the Slepian basis expansion which can compensate for the effects of a multipath fading channel with low complexity in a low mobility environment. We assume that the receiver only knows the maximum delay spread but not other channel information such as the channel distribution and the delay profile. We consider a PSA-OFDM system. The channel frequency response is expanded over Slepian sequences in the frequency domain. Then the channel is estimated via least square estimation.

The rest of this chapter is organized as follows. We introduce an OFDM system and a multipath channel model in Section 5.2. In Section 5.3, we describe the properties of Slepian sequences and time domain channel estimation using the Slepian basis expansion. We propose a frequency domain channel estimator based on the Slepian basis expansion in Section 5.4. The performance of the proposed scheme is evaluated via computer simulation in Section 5.5. Finally, the conclusion is given in Section 5.6.

5.2 System Model

We consider an OFDM system so that a frequency selective channel is converted into N_s subchannels. Let B_w denote the total system bandwidth. Then the subchannel bandwidth is $B_s = B_w/N_s$. We assume that the subchannel bandwidth B_s, is much less than the channel coherence bandwidth $B_c \approx 1/\tau_{max}$, where τ_{max} is the maximum delay spread. Therefore, each subchannel can be assumed to be frequency flat fading. We also assume that the maximum delay spread is known at the receiver. At the transmitter, information bits are mapped into a set of constellation points. After inserting pilot symbols according to a specific pattern, subcarrier symbols $X[n, 1]$, $X[n, 2]$, $\cdots$,

$X[n, N_s]$ make up a single OFDM symbol at the n-th time slot. The N_s subchannel symbols are sent to an inverse discrete Fourier transform (IDFT) block which performs a N_s-point IDFT as

$$x[n, k] = \frac{1}{N_s} \sum_{i=1}^{N_s} X[n, i] e^{j2\pi ki/N_s}, \quad k = 1, \cdots, N_s. \tag{5.1}$$

After adding a cyclic prefix to avoid ISI between the OFDM symbols, each OFDM symbol of duration T_s is transmitted through the frequency selective channel which has the following impulse response

$$h(t, \tau) = \sum_{l=1}^{L} \alpha_l(t) e^{j\theta_l(t)} \delta(\tau - \tau_l), \tag{5.2}$$

where L is the number of resolvable multipath components, $\alpha_l(t)$ and $\theta_l(t)$ are the amplitude and phase of the l-th path whose delay is τ_l (hence $\tau_L = \tau_{max}$) and $\delta(\cdot)$ denotes the Kronecker delta function. We assume that the receiver has no information about the statistics of $\alpha_l(t)$ and $\theta_l(t)$. Furthermore, the channel correlation in time and frequency is assumed to be unknown a priori so that it cannot be utilized to estimate the channel. The frequency response of the channel is given by

$$H(t, f) = \int_{-\infty}^{\infty} h(t, \tau) e^{-j2\pi f\tau} d\tau. \tag{5.3}$$

At the receiver, the baseband signal is first sampled. After passing through a matched filter, the cyclic prefix is removed. Then the discrete Fourier transform (DFT) is applied and the received sample at time n through the k-th subchannel is given by

$$Y[n, k] = H[n, k] X[n, k] + W[n, k], \quad k = 1, \cdots, N_s, \tag{5.4}$$

where $H[n, k]$ and $W[n, k]$ are the DFT of the channel impulse response and additive

white Gaussian noise (AWGN), respectively. The channel frequency response $H[n, k]$ can be expressed as [44]

$$
\begin{aligned}
H[n, k] &\triangleq H(nT_s, kB_s) \\
&= \int_{-\infty}^{\infty} h(nT_s, \tau) e^{-j2\pi kB_s\tau} d\tau \\
&= \int_{-\infty}^{\infty} \sum_{l=1}^{L} \alpha_l(nT_s) e^{j\theta_l(nT_s)} \delta(\tau - \tau_l) e^{-j2\pi kB_s\tau} d\tau \\
&= \sum_{l=1}^{L} \alpha_l(nT_s) e^{j\theta_l(nT_s)} e^{-j2\pi kB_s\tau_l}.
\end{aligned} \tag{5.5}
$$

In (5.5), $H[n, k]$ lies on the subspace spanned by a set of complex exponentials. Therefore with the knowledge of every tap delay τ_l, $H[n, k]$ can be exactly represented with finite number of complex exponentials. However, it may be computationally complex to estimate each tap delay or impractical to obtain both the exact value of each tap delay and the number of resolvable paths at the receiver. We assume that the receiver knows the maximum delay spread but not each tap delay. In this case, without knowing the exact values of τ_l's, $H[n, k]$ cannot be expanded accurately using complex exponentials, which causes significant performance degradation.

5.3 Slepian Basis Expansion Model

5.3.1 Slepian Sequences

Slepian described a set of orthogonal functions that simultaneously optimize energy concentration in time and frequency when either or both have a definite limit [45]. Let us consider the Slepian sequences of length N, $v[n]$, which are bandlimited to the frequency range $[-\nu_{max}, \nu_{max}]$. Such sequences are the eigenvectors of the following

eigenvalue equation

$$\sum_{l=1}^{N} \frac{\sin(2\pi\nu_{max}(l-n))}{\pi(l-n)} v_i[l] = \lambda_i(\nu_{max}, N)v_i[n]. \tag{5.6}$$

The eigenvectors are normalized so that:

$$\sum_{n=1}^{N} (v_i[n])^2 = 1. \tag{5.7}$$

The eigenvalue, λ_i indicates the fraction of energy contained in the band $[-\nu_{max}, \nu_{max}]$ of the corresponding eigenvector. The eigenvalues are ordered according to their values starting with the largest one: $1 \geq \lambda_1 \geq \cdots \geq \lambda_N \geq 0$. Then $v_i[k]$ is the i-th most time concentrated Slepian sequence. In [45], Slepian proved that time concentration measure λ_i is close to 1 for $i \leq \lceil 2\nu_{max}N \rceil + 1$ and decreases rapidly to 0 for $i > \lceil 2\nu_{max}N \rceil + 1$. Therefore only $\lceil 2\nu_{max}N \rceil + 1$ Slepian sequences are enough to approximate time and frequency concentrated functions.

5.3.2 Time Domain Channel Estimator Using Slepian Basis

In [39], observing that the variation of wireless channels in the frequency domain is upper bounded by the maximum Doppler frequency, Zemen and Mecklenbräuker first applied the Slepian sequences to the BEM for channel estimation. When the Slepian basis expansion is applied to OFDM systems, the existing scheme utilizes the channel correlation over the time domain and channel estimation for each subchannel is performed independently. The authors showed that the channel estimator based on the Slepian basis expansion outperforms the channel estimator using exponential basis. Let $h(t, \tau)$ and f_{max} be the channel impulse response and the maximum Doppler frequency respectively. After sampling is performed at the receiver and observing N channel

realizations, the sequence of the sampled channel realizations can be expressed as

$$\mathbf{h} = [h[1], \cdots, h[N]], \quad h[n] \triangleq h(nT_s, 0). \tag{5.8}$$

Since $h(t, \tau)$ is bandlimited over $[-f_{max}, f_{max}]$ and sampled with sampling period T_s, $\mathbf{h}$ is bandlimited over $[-f_{max}T_s, f_{max}T_s]$. Therefore, $\mathbf{h}$ can be approximated as a superposition of the Slepian sequences $v_i[n]$ of length N which are bandlimited to $[-f_{max}T_s, f_{max}T_s]$ as

$$h[n] \approx \sum_{i=1}^{D} v_i[n]\gamma_i, \quad n = 1, \cdots, N, \tag{5.9}$$

where $D = \lceil 2f_{max}T_sN \rceil + 1$. Thus, to estimate $h[n]$, we only need to find suitable complex coefficients γ_i. In a high mobility environment, the channel estimator based on Slepian basis expansion model shows very low mean-square-error (MSE) with low complexity. However, when the relative mobility between the transmitter and the receiver is small (i.e., when the Doppler frequency is small), the existing scheme requires very long Slepian sequences to accurately model the channel. This is because any sequence peaky in the frequency domain is spread widely in the time domain.

Fig. 5.1 shows that for a given length of Slepian sequences, as the maximum normalized Doppler bandwidth, $\nu_{max} = f_{max}T_s$ decreases, the measure of time concentration, λ_i decreases, which means the Slepian basis expansion requires longer sequences to accurately model the channel. It can be seen from Fig. 5.2 that to increase λ_i, the length of the Slepian sequences should be increased for a given ν_{max}. This implies we need to observe more samples to estimate the channel, which causes long decoding delay and high decoding complexity. Therefore, in a low mobility environment, the existing Slepian basis expansion model cannot represent the channel effectively. By utilizing the channel correlation over the frequency domain, such channels can be represented more accurately and efficiently.
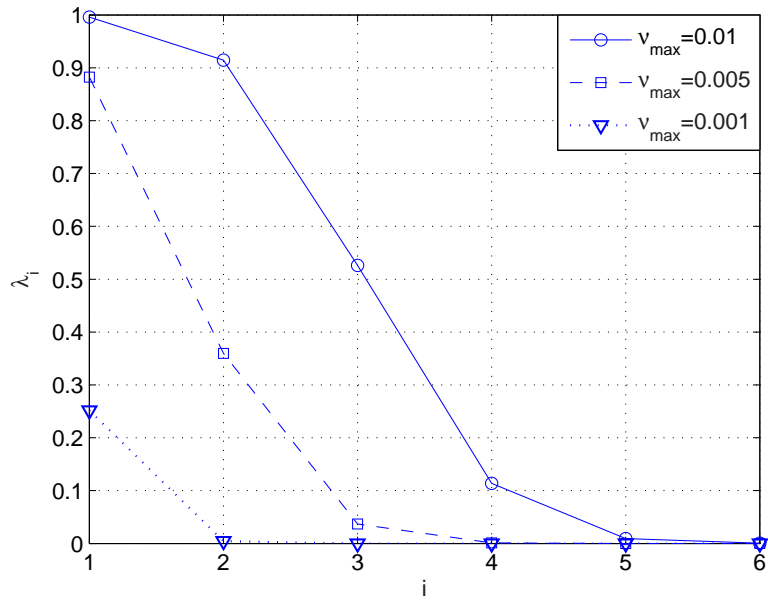
Figure 5.1: λ_i's for different normalized Doppler bandwidth ν_{max}'s when Slepian sequence length is 128.

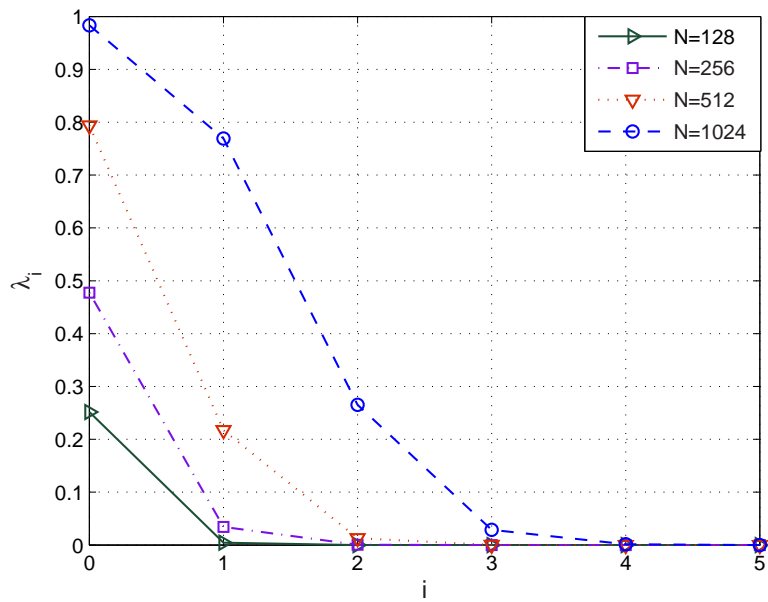Figure 5.2: λ_i's for different Slepian sequence lengths with normalized Doppler bandwidth $\nu_{max} = 0.001$.

5.4 Frequency Domain Channel Estimation Based on Slepian Basis Expansion

Since we focus on a low mobility environment, from now on we omit the time index. Let $\mathbf{H} = \{H[1], \cdots, H[N_s]\}$. Note that $\mathbf{H}$ is a sequence in the frequency domain. Since the IDFT of $H(f)$ is limited to $[0, \tau_{max}]$ and $H[k]$ is the channel frequency response sampled at the k-th subcarrier frequency with sampling period of B_s, the inverse DFT of $\mathbf{H}$ is limited to $[0, \tau_{max}B_s]$. Therefore $\mathbf{H}$ is both time and frequency concentrated. In order to represent $\mathbf{H}$, it is desirable to find basis functions which are also time and frequency concentrated so that $\mathbf{H}$ can be spanned by them. To construct such a basis, we first consider the Slepian sequences of length N_s that are bandlimited to $[-\frac{\tau_{max}B_s}{2}, \frac{\tau_{max}B_s}{2}]$. Let $v_i[k]$ be the i-th most time concentrated Slepian sequence. Then by the duality between time- and frequency-domain and the time shift property of DFT, a desired basis function $u_i[k]$ can be easily found as

$$u_i[k] \;\; = \;\; v_i[k]e^{-j\pi k\tau_{max}B_s}, \;\; k = 1, \cdots, N_s. \tag{5.10}$$

Note that the IDFT of $u_i[k]$ is concentrated in $[0, \tau_{max}B_s]$ as desired. From [45], among $u_i[k]$, only $\lceil \tau_{max}B_sN_s \rceil + 1$ sequences are highly concentrated in $[0, \tau_{max}B_s]$. Hence $D = \lceil \tau_{max}B_sN_s \rceil + 1$ sequences are enough to approximate $\mathbf{H}$ as

$$H[k] \;\; \approx \;\; \hat{H}[k] = \sum_{i=1}^{D} u_i[k]\gamma_i, \;\; k = 1, \cdots, N_s, \tag{5.11}$$

where $u_i[k]$ is the i-th most time-concentrated sequence and γ_i is the corresponding complex coefficient. Then the received sample can be represented as

$$
\begin{aligned}
Y[k] &= H[k]X[k] + W[k] \\
&\approx \hat{H}[k]X[k] + W[k] \\
&= \sum_{i=1}^{D} u_i[k]\gamma_i X[k] + W[k], \ k = 1, \cdots, N_s.
\end{aligned} \tag{5.12}
$$

The basis expansion coefficients γ_i can be estimated according to the least square method. Let $\{X[k]\}_{k \in P}$ be a set of pilot symbols where P is an index set of pilot symbols and J pilot symbols are inserted among N_s subchannels to estimate channel (i.e., the cardinality of P is J). Pilot symbols can be optimally designed to minimize MSE of the channel estimator. In our study, pilot symbols are evenly spaced over N_s subchannels and have equal energy. We define

$$
\begin{aligned}
\mathbf{Y} &= [Y[k_1], \cdots, Y[k_J]]^T, \\
\mathbf{U} &= \begin{bmatrix} u_1[k_1] & u_2[k_1] & \cdots & u_D[k_1] \\ u_1[k_2] & u_2[k_2] & \cdots & u_D[k_2] \\ \vdots & \vdots & \ddots & \vdots \\ u_1[k_J] & u_2[k_J] & \cdots & u_D[k_J] \end{bmatrix}, \\
\Gamma &= [\gamma_1, \cdots, \gamma_D]^T, \quad \text{for } k_1, \cdots, k_J \in P,
\end{aligned} \tag{5.13}
$$

where the superscript T denotes the transpose of a vector. Letting $X[k] = 1$, $\forall k \in P$, the least square estimates of γ_i are given by

$$
\begin{bmatrix} \hat{\gamma}_1 \\ \hat{\gamma}_2 \\ \vdots \\ \hat{\gamma}_D \end{bmatrix} = \hat{\Gamma} = (\mathbf{U}^H \mathbf{U})^{-1} \mathbf{U}^H \mathbf{Y}, \tag{5.14}
$$

where the superscript H denotes the Hermitian of a matrix.

In (5.14), it is required to compute an inverse of matrix of size $D \times D$ where $D = \lceil \tau_{max} B_s N_s \rceil + 1$. Since we assume that the coherence bandwidth of the channel B_c is much larger than the subchannel bandwidth B_s, we have

$$B_c \approx \frac{1}{\tau_{max}} \approx \rho B_s, \tag{5.15}$$

where $\rho \gg 1$. Hence we obtain

$$\begin{aligned} D &= \lceil \tau_{max} B_s N_s \rceil + 1 \\ &\approx \lceil N_s / \rho \rceil + 1. \end{aligned} \tag{5.16}$$

To evaluate the complexity of this scheme, we consider an actual system as an example. In IEEE 802.11a 5 GHz wireless LAN standard, the total system bandwidth of 300 MHz is divided into 20 MHz channels which are assigned to different user [46]. In 802.11a, the number of subcarriers N_s is 64. Therefore we have the subchannel bandwidth, $B_s = 312.5$ kHz, the maximum delay spread, $\tau_{max} \approx 0.8$ μs and the channel coherence bandwidth, $B_c \approx 1.25$ MHz (i.e., $\rho = 4$). In this example, we have $D = 17$ and it requires low complexity to estimate the channel with high accuracy.

5.5 Performance Evaluation

We illustrate the merits of the proposed channel estimator in terms of MSE by comparing with the exponential basis expansion model through computer simulation. The performance of our scheme is also compared with the case where the receiver has the perfect knowledge of each tap delay of the channel. In our simulations, the following parameters are used:

- Total system bandwidth : $B_w = 20$ MHz

- Number of subcarriers : $N_s = 64$

- Subchannel bandwidth : $B_s = 312.5$ kHz

- OFDM symbol duration : $T_s = 3.2$ μs

Fig. 5.3 shows two test channels considered in simulations. The maximum delay spread of the two test channels are 0.2 μs and 0.425 μs. The corresponding coherence bandwidths are 5 MHz and 2.35 MHz, respectively. Note that for each test channel, the coherence bandwidth is lager than the subchannel bandwidth so that each subchannel can be assumed frequency flat. To evaluate the performance of the proposed scheme, the mean square error (MSE) is introduced as

$$MSE = \frac{1}{N_s} \sum_{k=1}^{N_s} E\{|H[k] - \hat{H}[k]|^2\}. \tag{5.17}$$

To calculate the MSE, we average over 3000 channel realizations in our simulations.

Since we assume that the receiver only knows the maximum delay, for the exponential basis expansion model, the following complex exponentials with frequencies equally spaced between $[0, \tau_{max}B_s]$ are used as basis functions:

$$u_i^{exp}[k] = \frac{1}{\sqrt{N_s}} e^{-j2\pi kB_s\tau_{max}\frac{i}{D}}. \tag{5.18}$$

When each tap delay is perfectly known at the receiver, the following complex exponentials are used to approximate the channel:

$$u_i^{perfect}[k] = \frac{1}{\sqrt{N_s}} e^{-j2\pi kB_s\tau_i}, \tag{5.19}$$

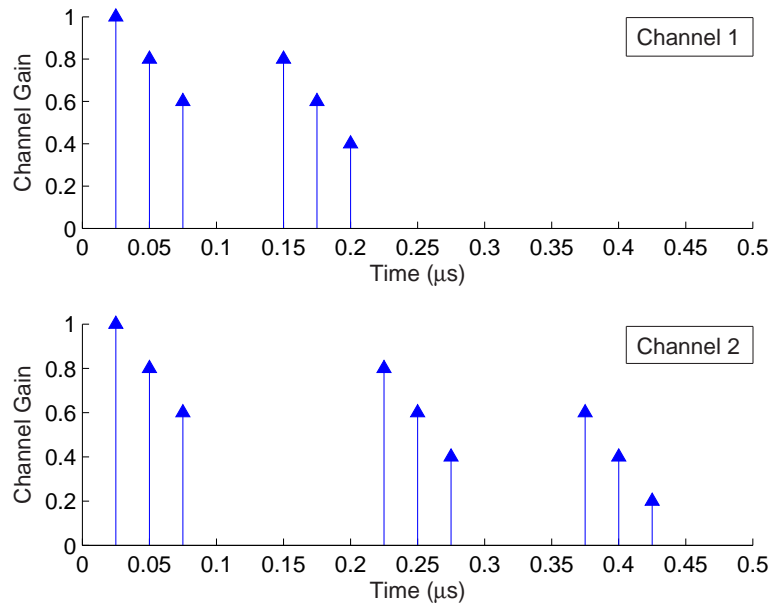where τ_i denotes the delay of the i-th path.
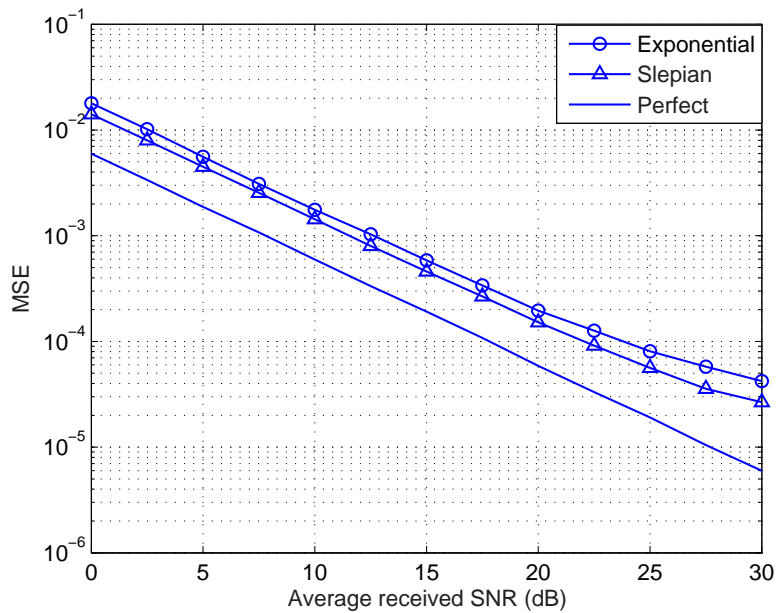
Figure 5.3: Test channels

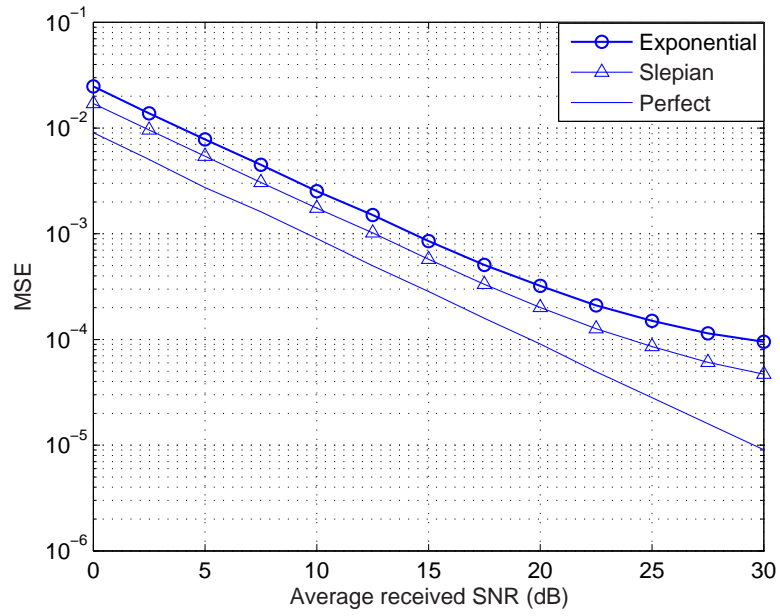Figure 5.4: MSE for test channel 1 with 16 pilot symbols

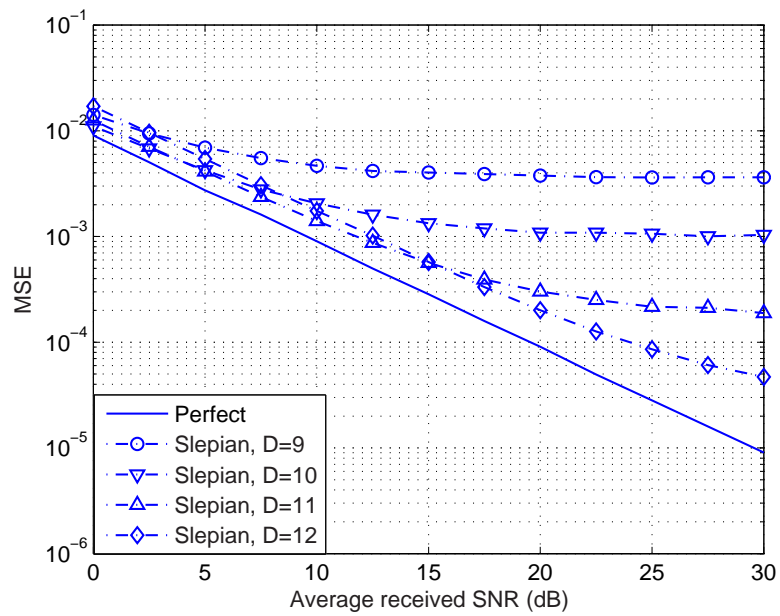Figure 5.5: MSE for test channel 2 with 16 pilot symbols

Figure 5.6: MSE's using different number of Slepian basis functions for test channel 2 with 16 pilot symbols ($\lceil \tau_{max} B_s N_s \rceil + 4 = 12$)

The performance of the channel estimators for the test channel 1 and 2 are compared in Fig. 5.4 and Fig. 5.5 in terms of MSE versus average signal-to-noise-ratio (SNR). For a fair comparison, $\lceil \tau_{max} B_s N_s \rceil + 4$ basis functions are used for both the Slepian basis expansion and the exponential basis expansion. For the two test channels, the Slepian basis expansion shows lower MSE's than the exponential basis expansion. However when each tap delay is exactly known at the receiver, exponential basis expansion shows better performance than Slepian basis expansion and the performance gap between these two schemes increases as the average received SNR increases. This is because the Slepian sequences cannot represent the channel components orthogonal to the subspace spanned by the Slepian sequences. Compared to this, with the exact tap delay information, the channel can be exactly represented with complex exponentials whose exponents are well chosen according to the given channel information. Fig. 5.6 shows the performance of Slepian basis expansion for test channel 2 using different numbers of basis functions. It can be seen that the more Slepian sequences are used, the lower MSE we can obtain over a wide range of SNR.

5.6   Conclusion

We proposed a frequency domain channel estimator for PSA-OFDM systems which requires only the knowledge of the maximum delay spread and operates with low complexity in a low mobility environment. Observing that the channel frequency response is both time- and frequency-concentrated, we applied Slepian sequences to represent channel frequency response. Slepian sequences are suitably chosen according to the maximum delay spread τ_{max} and the number of subcarriers N_s. The channel coefficients are first projected into a subspace spanned by Slepian sequences and then the least square method is applied to estimate channel coefficients. The proposed scheme does not depend on the statistics of multipath channels. Hence it can be applied to

various channels and perform with high accuracy. We have compared the performance of Slepian basis expansion and exponential basis expansion through computer simulation. Slepian basis expansion shows better performance compared to exponential basis expansion. The impact of the number of basis functions on the MSE was also investigated.

CHAPTER 6

Capacity of Non-coherent Rayleigh Fading Channels under Practical Power Constraints

In this chapter, we study the capacity of the non-coherent Rayleigh fading channel subject to power constraints induced by a power amplifier. In practical communication systems, a power amplifier is necessary to obtain enough signal power to combat background noise, fading and jamming. Due to the limit on power amplification, there exists a peak power constraint on the transmitted power. Furthermore, since power is a limited resource, there is an average power constraint on the consumed power which is needed to operate an amplifier. Given these power constraints, we prove that the capacity achieving input distribution for the non-coherent Rayleigh fading channel is discrete in amplitude with a finite number of mass points. Therefore computing the capacity is reduced to a finite dimensional optimization problem.

6.1   Introduction

Finding the capacity of communication channels subject to practical input constraints is a classic problem in information theory. The most frequently considered constraint is an average power constraint. Shannon [47] showed that for a scalar additive Gaussian channel subject to an average power constraint, Gaussian input distribution

achieves the capacity.

There have been many studies finding the capacity of the channel subject to an average power constraint. However, there has not been much attention to the capacity of the channel subject to a peak power constraint. A peak power constraint was first considered by Shannon in the scalar Gaussian channel [47]. For this channel, Shannon derived lower and asymptotic upper bounds on the capacity. Later, Smith showed that for the scalar additive Gaussian channel with average and peak power limited inputs, the capacity achieving input distribution is discrete and the number of mass points is finite [48]. This result is surprising because the capacity can be achieved with discrete input distributions, which is not possible for the Gaussian channel subject to an average power constraint. In [49], Shamai *et al.* considered quadrature Gaussian channels with both average and peak power constraints. For this channel, they showed that the capacity achieving input distribution is also discrete with a finite number of mass points. In [50], Abou-Faycal *et al.* considered Rayleigh fading channels assuming that neither the transmitter nor the receiver has channel side information. Subject to an average power constraint, they showed that the capacity achieving input distribution is discrete. This result indicates the fact that the discreteness of an optimal input distribution is not induced only by a peak power constraint.

In the previous research, the characteristic of a power amplifier has not been considered, which has to be considered to reflect practical power constraints. A power amplifier is an important device in communication systems, providing enough transmit signal level for reliable communication. Since the power amplifier has a limit on the output power level, there is a peak power constraint on the transmitted (output) power. To operate a power amplifier, we need DC power called consumed power. In general, the consumed power is greater than the transmitted power because of the power loss associated with amplifier inefficiency. Hence, there is an average power constraint on the consumed power.
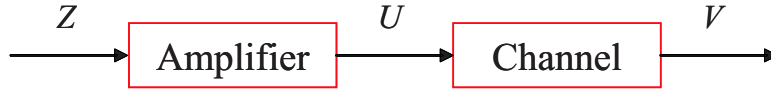
Figure 6.1: System model

In our study, we show that the capacity achieving input distribution for the non-coherent Rayleigh fading channel subject to power constraints induced by a power amplifier is also discrete with a finite number of mass points. We assume that a power amplifier operates in the region where the amplified signal is a bijective function of the input signal. This assumption is reasonable since most power amplifiers operate such that there is an one-to-one correspondence between the input power and the output power. Next, we assume that the consumed power is a function of the transmitted power which has a Taylor series convergent to the function at every point in the real line. The outline of this chapter is as follows. In Section 6.2, we describe the system model and set up a mathematical model that specifies the characteristic of a power amplifier. In Section 6.3, we prove the discreteness of the capacity achieving input distribution. We also show that for a given peak power constraint, there exists an average power constraint level at which the capacity does no longer increase. In Section 6.4, numerical results are presented. Section 6.5 concludes this chapter.

6.2   System Description

In this section, we introduce the communication system model which is analyzed through this chapter. In Fig. 6.1, the system model is described where Z, U and V denote the power amplifier input, the channel input (i.e., the power amplifier output) and the channel output respectively. With this model, we are interested to find the optimal input distribution of Z which maximizes the mutual information $I(Z;V)$. Consider the following channel,

$$V = HU + N, \tag{6.1}$$

where H is the fading coefficient and N is the channel noise. The random variables H and N are assumed to be independent complex circular Gaussian random variables with mean zero and variance σ_H^2 and σ_N^2 respectively. Furthermore we assume that both the transmitter and the receiver know only the statistics of H not the exact value of H. Conditioned on the channel input U, the channel transition probability is given by

$$p(v|u) = \frac{1}{\pi(\sigma_H^2|u|^2 + \sigma_N^2)} \exp\left(\frac{-|v|^2}{\sigma_H^2|u|^2 + \sigma_N^2}\right). \tag{6.2}$$

Note that the density $p(v|u)$ depends on V only through $|V|^2$ and hence $|V|^2$ is a sufficient statistic for V. Given the channel input U, $|V|^2$ is chi-square distributed with two degrees of freedom as

$$p(|v|^2|u) = \frac{1}{\sigma_H^2|u|^2 + \sigma_N^2} \exp\left(\frac{-|v|^2}{\sigma_H^2|u|^2 + \sigma_N^2}\right). \tag{6.3}$$

Fig. 6.2 shows the characteristic of a non-linear power amplifier which imposes practical constraints on the channel input. Let P_{in} and P_{out} denote input and output power of the power amplifier respectively. Define P_{dc} be the consumed power which is necessary to operate a power amplifier. As shown in Fig. 6.2, due to the characteristic of the power amplifier, there exists a peak power constraint on the output power. Since the average power is a limited resource in the system, there also exists an average power constraint on the consumed power in practical communication systems. Thus we have corresponding power constraints as

$$P_{out} = |U|^2 \leq P_p, \tag{6.4a}$$
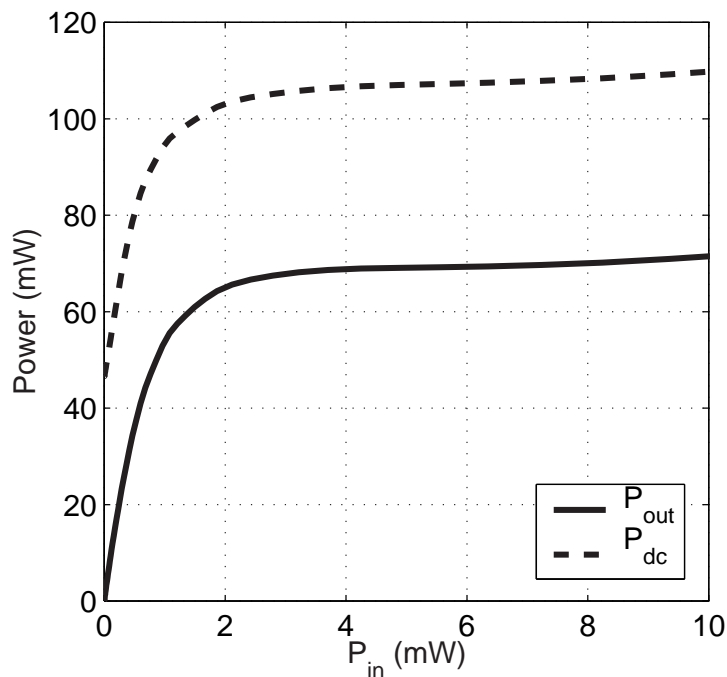
Figure 6.2: The characteristic of a non-linear power amplifier

$$E(P_{dc}) \leq P_a, \tag{6.4b}$$

where P_p and P_a denote a peak power constraint and an average power constraint respectively. Compared to this amplifier model, classic average power constraint models do not consider the effects of a power amplifier so that there exist an average power constraint on the transmitted power not on the consumed power. However it is necessary to consider the characteristic of the power amplifier to accurately reflect the physical limitation in communication systems.

We first assume that a power amplifier operates in the region where the power amplifier output is a bijective function of the power amplifier input. This assumption yields

$$I(Z; V) = I(U; V). \tag{6.5}$$

101

The optimal distribution of U can be determined directly from the optimal distribution of Z.

Next, we assume that the consumed power P_{dc} can be expressed as a function of the transmitted power P_{out} which has a Taylor series convergent to the function at every point in the real line. Then the transmitted power P_{out} can be expressed as

$$
\begin{aligned}
P_{dc} &= f(P_{out}) \\
&= \sum_{n=0}^{\infty} a_n (P_{out} - x_0)^n, \quad \forall x_0 \in \mathbb{R} \quad P_{out} \in [0, \sqrt{P_p}],
\end{aligned}
\tag{6.6}
$$

where the coefficients a_n's are real numbers and the series is convergent in a neighborhood of x_0. Letting $Y = \frac{|V|^2}{\sigma_N^2}$ and $X = \frac{|U|\sigma_H}{\sigma_N}$ in (6.3), an equivalent channel model can be obtained with the transition probability given as

$$
p(y|x) = \frac{1}{1+x^2} \exp\left(\frac{-y}{1+x^2}\right).
\tag{6.7}
$$

Now the original problem is equivalent to finding the optimal distribution on X which maximizes $I(X;Y)$ subject to the following power constraints:

$$
X^2 \leq \frac{\sigma_H^2}{\sigma_N^2} P_p.
\tag{6.8a}
$$

$$
E\left(f\left(\frac{\sigma_N^2}{\sigma_H^2} X^2\right)\right) \leq P_a.
\tag{6.8b}
$$

6.3 Capacity-achieving Input Distribution

6.3.1 Discreteness of the Optimal Input Distribution

We extend the work of Abou-Faycal *et al.* [50] to the non-coherent Rayleigh fading channel subject to constraints induced by a power amplifier. For simplicity of calcula-

tion, assume $\sigma_H^2 = \sigma_N^2 = 1$ where σ_H^2 and σ_N^2 denote the variance of fading and noise respectively. Note that since we assume that consumed power can be expressed as a function of transmitted power which has a Taylor series convergent to the function at every point, it also has a Taylor series around -1. Let $\mathbb{F}_{ap}$ be a set of all input distribution functions F such that

$$\int_0^{\sqrt{P_p}} \sum_{n=0}^\infty a_n(x^2+1)^n dF(x) \leq P_a \tag{6.9a}$$

and

$$F(x) = 0 \ \forall x < 0, \ F(x) = 1 \ \forall x \geq \sqrt{P_p}, \tag{6.9b}$$

where a_n's are real numbers. Define $I(F)$ be the mutual information between channel input and output induced by an input distribution F. Then the capacity of this channel is given by

$$C = \sup_{F \in \mathbb{F}_{ap}} I(F). \tag{6.10}$$

The following theorems are used to find the optimal input distribution.

Theorem **6.1**[Optimization theorem][48],[52]: Let f be a continuous, weakly differentiable and strictly concave mapping from a compact and convex space Ω to $\mathbb{R}$. Then followings are true.

- $C = \sup_{x \in \Omega} f(x) = f(x_0)$ for some unique $x_0 \in \Omega$.

- A necessary and sufficient condition for $f(x_0) = C$ is $f'_{x_0}(x) \leq 0 \quad \forall x \in \Omega$, where $f'_{x_0}(x)$ is the weak derivative of f at x_0.

The definition of weak differentiability is given as follows.

Definition **6.1**[Weak differentiability][48],[50]: Let $\mathbb{F}$ be a convex space and f be a mapping from $\mathbb{F}$ into the real line $\mathbb{R}$. Let F_0 be a fixed element of $\mathbb{F}$ and θ be a real

103

number in $[0, 1]$. Suppose there exits a map $f'_{F_0} : \mathbb{F} \to \mathbb{R}$ such that

$$f'_{F_0}(F) = \lim_{\theta \to 0} \frac{f((1 - \theta)F_0 + \theta F) - f(F_0)}{\theta}, \quad \forall F \in \mathbb{F}. \tag{6.11}$$

Then f is said to be weakly differentiable in $\mathbb{F}$ at F_0 and f'_{F_0} is the weak derivative in $\mathbb{F}$ at F_0. If f is weakly differentiable in $\mathbb{F}$ at for all $F_0 \in \mathbb{F}$, f is said to be weakly differentiable in $\mathbb{F}$.

Theorem **6.2**[Lagrangian theorem][48], [52]: Let f and g be concave mappings from a convex metric space Ω to $\mathbb{R}$. Assume there exists $x_0 \in \Omega$ such that $g(x_0) < 0$. Define

$$C = \sup_{\substack{x \in \Omega \\ g(x) \leq 0}} f(x). \tag{6.12}$$

If C is finite, then there exists a constant $\lambda \geq 0$ such that

$$C = \sup_{x \in \Omega}[f(x) - \lambda g(x)]. \tag{6.13}$$

Furthermore, if the supremum is achieved in (6.12) at $x_0 \in \Omega$, it is achieved by x_0 in (6.13) and $\lambda g(x_0) = 0$.

We first apply the Lagrangian theorem to our problem and obtain an equivalent expression for the capacity. Let $\mathbb{F}_p$ be a set of distribution functions F which satisfy the peak power constraint (6.11b). It was shown that $\mathbb{F}_p$ is convex and compact by Smith [48]. The convexity of $\mathbb{F}_p$ is straightforward by definition. The compactness comes from the fact that by Helley's weak compactness theorem [56], [57], $\mathbb{F}_p$ is weakly compact and on a finite interval, weak and complete convergence are equivalent. Define a mapping $g : \mathbb{F}_p \to \mathbb{R}$ by $g(F) = \int \sum_{n=0}^{\infty} a_n(x^2 + 1)^n dF(x) - P_a$. The mutual information $I(F)$ is shown to be strictly concave [50]. Since $g(F)$ is linear in $\mathbb{F}_p$, for any $\lambda \in \mathbb{R}$, $I(F) - \lambda g(F)$ is strictly concave in $\mathbb{F}_p$. Observing the capacity C is finite, by the Lagrangian theorem,

the capacity can be expressed as

$$C = \sup_{F \in \mathbb{F}_p} \left(I(F) - \lambda g(F) \right). \tag{6.14}$$

Now we apply the optimization theorem to obtain the necessary and sufficient condition for the optimality. In [50], $I(F)$ is shown to be continuous and weakly differentiable. It is clear that $g : \mathbb{F}_p \to \mathbb{R}$ is continuous and further weakly differentiable in $\mathbb{F}_p$ as $g'_{F_1}(F_2) = g(F_2) - g(F_1)$. Thus $I(F) - \lambda g(F)$ is continuous and weakly differentiable. Now by the optimization theorem, there exists a unique $F^* \in \mathbb{F}_p$ such that

$$C = I(F^*) - \lambda g(F^*). \tag{6.15}$$

The necessary and sufficient condition that the optimal input X^* with distribution $F^* \in \mathbb{F}_p$ achieves the capacity C is that there exists a $\lambda \geq 0$ such that

$$\lambda \Big(\sum_{n=0}^{\infty} a_n (x^2 + 1)^n - P_a \Big) + C - \int_0^{\infty} p(y|x) \log \frac{p(y|x)}{p(y; F^*)} dy \leq 0, \forall x \in [0, \sqrt{P_p}] \tag{6.16}$$

where the equality holds if x is in the support of X^* and the marginal density $p(y; F)$ is given by

$$p(y; F) = \int p(y|x) dF(x). \tag{6.17}$$

***Theorem* 6.3**[Discreteness of the optimal input distribution]: The capacity achieving input distribution of a memoryless Rayleigh fading channel subject to power constrains induced by a power amplifier is discrete in amplitude with a finite number of mass points.

Proof: Following the technique used in [50], we prove the discreteness of the optimal input distribution. Let us first assume that the capacity achieving input distribution

105

has an amplitude which is continuous or discrete with an infinite number of mass points. Now, let us consider the following change of variable

$$s = \frac{1}{1 + x^2}.$$

(6.18)

Then from (6.7), we have

$$p(y|s) = s \exp(-sy), \quad s \in \left[\frac{1}{1 + P_p}, 1\right]$$

(6.19)

and (6.16) becomes

$$\lambda \left(\sum_{n=0}^{\infty} a_n \left(\frac{1}{s}\right)^n - P_a\right) + C - \log s + 1 + \int_0^{\infty} s \exp(-sy) \log p(y; F^*) dy \leq 0.$$

(6.20)

The equality in (6.20) holds if and only if $s \in S_{S^*}$ where S_{S^*} denotes the support of the random variable $S^* = \frac{1}{(1 + X^{*2})}$. Since X^* is assumed to be continuous or discrete with an infinite number of mass points, S_{S^*} is an infinite set. Note that S_{S^*} is bounded as $S_{S^*} \subset \left[\frac{1}{1 + P_p}, 1\right]$. Then by the Bolzano-Weierstrass theorem [54], S_s^* has a limit point in $\left[\frac{1}{1 + P_p}, 1\right]$. Let $h(s)$ be the left-hand side of (6.20). Now let us extend $h(s)$ to the complex domain and define $h(z)$ as

$$h(z) = \lambda \left(\sum_{n=0}^{\infty} a_n \left(\frac{1}{z}\right)^n - P_a\right) + C - \log z + 1 + \int_0^{\infty} z \exp(-zy) \log p(y; F^*) dy.$$

(6.21)

Choosing $\log z$ as the principal branch of the logarithm [54], $h(z)$ is analytic in the domain $Re(z) > 0$. Furthermore by the optimization theorem,

$$h(z) = 0 \quad \forall z \in S_{S^*}$$

(6.22)

Since $h(z)$ is analytic and zero on S_{S^*} which has a limit point in $Re(z) > 0$, by the

identity theorem [54] we have

$$h(z) = 0 \ \forall z \ \text{s.t. } Re(z) > 0. \tag{6.23}$$

From (6.21) and (6.23), we have

$$\int_0^\infty \exp(-zy) \log p(y; F^*) dy$$

$$= -\frac{1}{z} \left(\lambda \sum_{n=0}^\infty a_n \left(\frac{1}{z} \right)^n - \lambda P_a + C - \log z + 1 \right), \ \forall z \ \text{s.t. } Re(z) > 0. \tag{6.24}$$

Note that the left-hand side of (6.24) is the Laplace transform of $\log p(y; F^*)$. Taking the inverse Laplace transform of both sides,

$$\log p(y; F^*) = -\lambda \sum_{n=0}^\infty a_n \left(\frac{y^n}{n!} \right) + \lambda P_a - C - C_E - \log y - 1 \ \ \forall z \ \text{s.t. } Re(z) > 0, \tag{6.25}$$

where C_E is the Euler's constant defined as

$$C_E = -\int_0^\infty \exp(-y) \log y \, dy \approx 0.5772.$$

Hence from (6.25), $p(y; F^*)$ should be of the form

$$p(y; F^*) = K \frac{\exp\left(-\lambda \sum_{n=0}^\infty a_n \frac{y^n}{n!}\right)}{y}, \tag{6.26}$$

where $K = \exp(\lambda P_a - C - C_E - 1) < \infty$. However this is not a proper distribution because $\int p(y; F^*) dy$ can not be 1. This can be shown as follows. Let us select a constant M such that $T = \max_{0 \le y \le M} \lambda \sum_{n=0}^\infty a_n \frac{y^n}{n!} < \infty$. Such M exists since $\lambda \sum_{n=0}^\infty a_n \frac{y^n}{n!}$ is

continuous and zero at $y = 0$. Then we obtain

$$
\begin{aligned}
\int_0^\infty p(y; F^*) dy &= K \int_0^\infty \frac{\exp\left(-\lambda \sum_{n=0}^\infty a_n \frac{y^n}{n!}\right)}{y} dy. \\
&\geq K \int_0^M \frac{\exp\left(-T\right)}{y} dy \\
&= \infty.
\end{aligned}
\tag{6.27}
$$

By contradiction, the capacity achieving input distribution is discrete in amplitude with a finite number of mass points. ∎

6.3.2 Capacity Saturation Point

It was shown that the capacity of non-coherent Rayleigh fading channels, subject to an average power constraint, increases as the average power constraint increases [50]. However if there is a peak power constraint also, there exist a capacity saturation point at which the capacity does not increase any more.

Theorem **6.4**[Existence of a capacity saturation point]: The capacity of non-coherent Rayleigh fading channels, subject to average and peak power constraints, for a fixed peak power constraint, there exist a capacity saturation point where the capacity does no longer increase even if the average power constraint increases.

Proof: In [50], it was shown that the optimal input distribution of non-coherent Rayleigh fading channels subject to an average power constraint has a mass point at zero. This result follows directly from the fact that the amplitude of the optimal input distribution is discrete with a finite number of mass points. By theorem 6.3, even with power constraints induced by a power amplifier, the amplitude of the optimal input distribution is also discrete with a finite number of mass points. Following [50], it can be easily shown that there exists a mass point at zero when a power amplifier is

considered. Now let us assume that there does not exist a capacity saturation point. Equivalently, for a fixed peak power constraint, the capacity increases as the average power constraint increases. Then the capacity is maximized when the average power constraint is the same as the peak power constraint. This is possible if and only if

$$x = \sqrt{P_p} \text{ with probability 1.} \tag{6.28}$$

In this case, there is not a mass point at zero which contradict the existence of a mass point at zero. Therefore there exist a capacity saturation point. ∎

6.4 Numerical Results

In this section, we numerically compute the capacity of non-coherent Rayleigh fading channels. Since the number of mass points is unknown, we first set the number of mass points to 2 (one mass point at zero and another at $x > 0$) and find the input distribution which maximizes the mutual information. Then we check if the necessary and sufficient condition for optimality (6.16) is satisfied or not. If this condition is violated, then we increase the number of mass points by one and repeat the previous steps.

Fig. 6.3 shows that the capacity subject only to an average power constraint and subject to both average and peak power constraints. The peak power constraint is fixed to 10 dB. In Fig. 6.3, we assume that the consumed power P_{dc} is the same as the transmitted power P_{out}. It can be seen that there exists a capacity saturation point around at $P_a = 6.5$ dB when there are both average and peak power constraints. In contrast, with an average power constraint only, the capacity increases steadily. Based on the numerical results, the existence of a capacity saturation point can be interpreted as follows. From numerical results it can be checked that when the average power constraint, $P_a \lesssim 6.5$ dB, the average power corresponding the optimal distribution is the same as P_a. However when $P_a \gtrsim 6.5$ dB, the average power corresponding to the
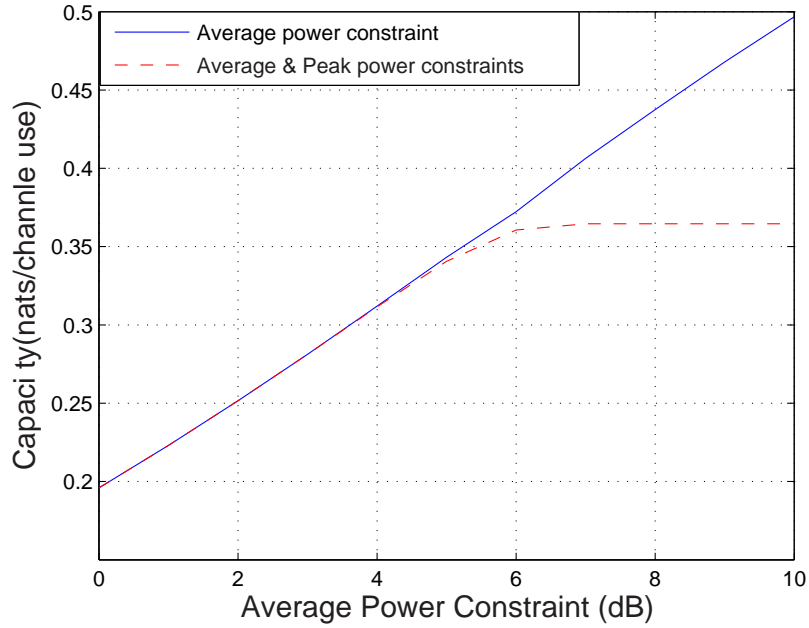
Figure 6.3: The capacity of non-coherent Rayleigh fading channels subject to an average power constraint and subject to both average and peak power constraints (peak power constraint is fixed to 10 dB, $\sigma_H^2 = \sigma_N^2 = 1$).

optimal distribution is less than the allowed average power, P_a. By the Lagrangian theorem, the capacity is achieved only if

$$\lambda \left(\int x^2 dF(x) - P_a \right) = 0. \tag{6.29}$$

When $P_a \gtrsim 6.5$ dB, we have

$$\left(\int x^2 dF(x) - P_a \right) \neq 0,$$

which implies $\lambda = 0$. Since λ represents the sensitivity of the objective to small perturbations of constraints, $\lambda = 0$ means that the capacity does not change any more even when the average power constraint increases.

The saturation point also occurs when a power amplifier is considered. A simple amplifier model is shown in Fig. 6.4. In this case, we model consumed power, P_{dc}, is
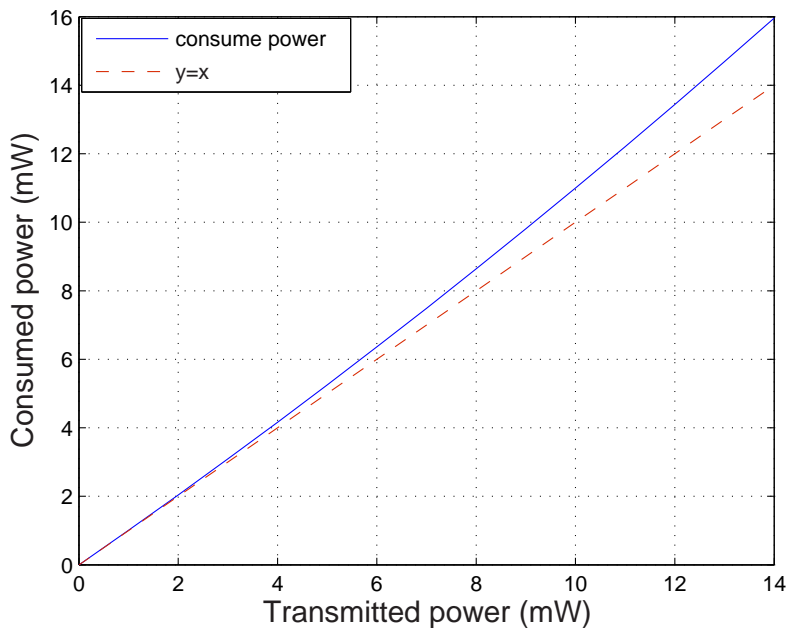
Figure 6.4: Consumed power modeling, $P_{dc} = P_{out} + 0.01P_{out}^2$.

a function of transmitted power, P_{out} such that $P_{dc} = P_{out} + 0.01P_{out}^2$. This function has a Taylor series at every point as the assumption in Section 6.2. Fig. 6.5 shows the capacity of non-coherent Rayleigh fading channels under the amplifier model which is shown in Fig. 6.4.

In Fig. 6.6, two different input signals are shown: 16-QAM and numerically optimized input X^* with two mass points $(p(0) = 0.6017, p(3.16) = 0.3983)$. Both constellations satisfy the average power constraint $P_a = 6$ dB and the peak power constraint $P_p = 10$ dB. Let I_{QAM} and I_{X^*} denote mutual information with respect to 16-QAM and input signal X^* respectively. When $\sigma_H^2 = \sigma_N^2 = 1$, $I_{X^*} = 0.3606$ (nats/channel use) which is 3 times larger than $I_{QAM} = 0.1149$ (nats/channel use).
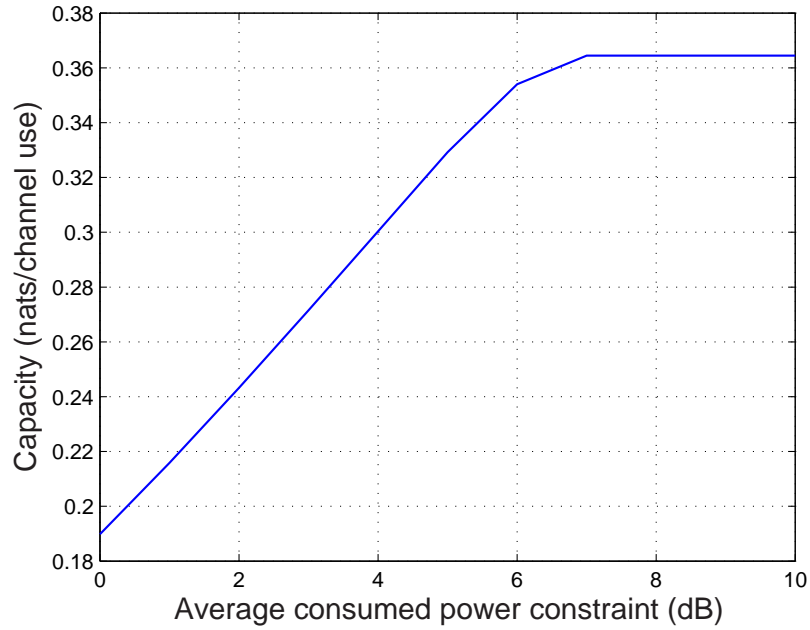
Figure 6.5: The capacity of non-coherent Rayleigh fading channels with the amplifier model in Fig. 6.4. ($\sigma_H^2 = \sigma_N^2 = 1$)
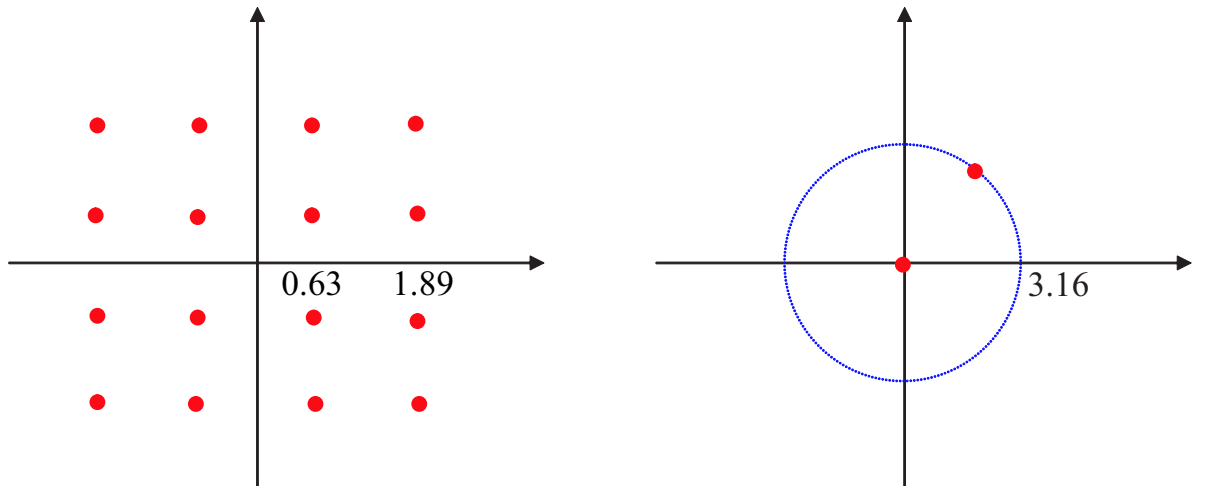

Figure 6.6: Two input signals: 16-QAM and X^*. ($I_{QAM} = 0.1149$ (nats/channel use), $I_{X^*} = 0.3606$ (nats/channel use), $\sigma_H^2 = \sigma_N^2 = 1$)

6.5 Conclusion

In this chapter, we considered the non-coherent Rayleigh fading channel subject to power constraints induced by a non-linear power amplifier which is not considered before. A non-linear power amplifier imposes a peak power constraint on transmitted power and an average power constraint on consumed power. It was assumed that consumed power is a function of transmitted power which has a Taylor series at every point in the real line. With this assumption, it was established that the optimal input distribution is discrete in amplitude with a finite number of mass points. Then finding capacity is reduced to a finite dimensional optimization problem and the corresponding optimal distribution can be found. Furthermore we have shown that a capacity saturation point exists which implies that even though the average power increases over a saturation point, the capacity remains the same.

CHAPTER 7

Conclusions

In this thesis, we have considered important problems regarding the performance limit of physical layer network coding and the communication system design in a fading environment. In Chapter 2, we have considered the exclusive-or multiple-access channel (XMAC) where physical layer network coding can provide advantages over conventional store-and-forward. We have investigated the error exponent for this type of channel which provides a measure of how fast the error probability decay exponentially as a function of codeword length. Two different operations at the receiver, the multiple-access (MAC) strategy and the physical layer network coding (PNC) strategy were considered. Since the MAC strategy has been well studied in the literature, we mainly focused on the PNC strategy. With PNC strategy, we derived error exponents for both random codes and linear codes. We also studied the cutoff rate of the XMAC and evaluated the cutoff rate of the Gaussian XMAC. It has been shown that the PNC strategy shows better performance in terms of the cutoff rate than the MAC strategy in the high rate region while the MAC performs better in the low rate region.

Although we investigated the theoretical performance limit of PNC over the XMAC, it is also important to evaluate the performance of practical channel codes combined with network coding. In Chapter 3, we have evaluated the threshold of low-density parity-check (LDPC) codes over the XMAC via density evolution methods. Assuming that both users employ the same LDPC codes, the XOR data can also be protected by

error correcting codes since LDPC codes are linear. Numerical results were presented to show that LDPC codes provide reliable performance near theoretically achievable rates discussed in Chapter 2. We also considered the case where two incoming signals from two users arrive at the receiver with different phase.

Other research topics considered in this thesis have been concerned with transmission over fading channels. In Chapter 4, we have derived the outage probability of LDPC-coded systems. In fading channels, in addition to the ergodic capacity which characterizes the long-term average achievable rate limit of a fading channel, outage probability is another important performance measure since practical codeword lengths are finite due to transmission delay constraints. We assumed that an outage occurs when signal-to-interference-plus-noise ratio (SINR) falls below an acceptable threshold so that the message passing decoder fails to decode successfully. Assuming channel state is fixed for the duration of an LDPC codeword but varies in the next transmission, we derived the outage probability for both Rayleigh and Rician fading channels. We also investigated the effect of imperfect channel side information (CSI) at the receiver on the outage probability. We have also applied this method to LDPC-coded code-division multiple-access (CDMA) systems.

In Chapter 5, we have proposed an efficient frequency domain channel estimation scheme for orthogonal frequency division multiplexing (OFDM) systems. Although it has been known that Slepian sequences are suitable to represent time-varying channels, in slow fading channels, the length of required Slepian sequences for accurate channel estimation is very long. This increases decoding complexity and delay at the receiver. Motivated by this observation, we proposed a channel estimator which exploits channel correlation in frequency domain using Slepian sequences. In the proposed scheme, channel coefficients are projected into a subspace spanned by Slepian sequences and then estimated by the least square method. Our scheme performs with high accuracy and requires only the knowledge of the maximum delay spread of the channel. Simulation

results were provided to demonstrate that the proposed channel estimator outperforms channel estimators using exponential basis expansion.

In Chapter 6, we have studied the capacity achieving input of the non-coherent Rayleigh fading channel subject to power constraints induced by a non-linear power amplifier. Due to the limit on the amplification level, there exists a peak power constraint on the transmitted power. Furthermore we have noted that there exists an average power constraint on the power needed to operate a power amplifier, called consumed power which can be different from the transmitted power. Assuming that the consumed power is a function of the transmitted power which has a Taylor series at every point in the real line, we have shown that the capacity achieving input is discrete with finite support. Hence we can compute the capacity using finite dimensional optimization.

There are a number of important issues remaining to be explored regarding practical implementation of physical layer network coding. An area of future research is to investigate the performance of physical layer network coding in a fading environment. In fading channels, more problems can be encountered. Since the receiver needs to reconstruct the XOR of the two transmitted signals, it is required to obtain accurate CSI of both links for successful decoding. The imperfect CSI of either link may cause severe performance degradation. Therefore it is important to study the effect of imperfect CSI on the achievable rate. It is also interesting to study the performance of network coding with non-coherent reception.

Another interesting direction of future research is to examine the combination of network coding with routing and medium access control. Joint design of network coding with protocols such as routing and scheduling can enable a node to determine whether interference from other users can be used to increase throughput or is to be avoided.

APPENDICES

APPENDIX A

Proof Of Lemma 2.1

For any arbitrarily small $\epsilon > 0$,

$$\lim_{N \to \infty} \Pr\left(||S_j| - 2^K| \geq \epsilon\right)$$

$$\leq \lim_{N \to \infty} \Pr\left(|S_j| \neq 2^K\right)$$

$$= 1 - \lim_{N \to \infty} \Pr\left(|S_j| = 2^K\right)$$

$$= 1 - \lim_{N \to \infty} \left(\binom{2^N}{2^K} \sum_{m=1}^{2^K} (-1)^{2^K + m} \binom{2^K}{m} m^{2^K} \cdot 2^{-N2^K}\right)$$

using $\sum_{m=1}^{l} (-1)^m \binom{l}{m} m^l = (-1)^l \cdot l!$,

$$= 1 - \lim_{N \to \infty} \left(\binom{2^N}{2^K} (2^K)! \cdot 2^{-N2^K}\right)$$

$$= 1 - \lim_{N \to \infty} \left(\frac{2^N \cdot (2^N - 1) \cdots (2^N - (2^K - 1))}{2^{N2^K}}\right)$$

$$= 1 - \lim_{N \to \infty} \left(\prod_{i=0}^{2^K - 1} \left(1 - \frac{i}{2^N}\right)\right)$$

$$\leq 1 - \lim_{N \to \infty} e^{\ln\left(1 - \frac{2^K - 1}{2^N}\right)^{2^K}}$$

$$= 1 - e^{\lim_{N \to \infty} \ln\left(1 - \frac{2^K - 1}{2^N}\right)^{2^K}} \tag{A.1}$$

Let z denotes the exponent in (A.1). Then, we have

$$
\begin{aligned}
z &= \lim_{N \to \infty} \ln \left(1 - \frac{2^K - 1}{2^N} \right)^{2^K} \\
&= \lim_{N \to \infty} 2^{NR} \ln \left(1 - 2^{-N(1-R)} + 2^{-N} \right)
\end{aligned}
$$

using L'Hôpital's rule,

$$
\begin{aligned}
&= \lim_{N \to \infty} \frac{\left(1 - \frac{1}{R}\right) 2^{-N(1-2R)} + \frac{1}{R} 2^{-N(1-R)}}{1 - 2^{-N(1-R)} + 2^{-N}} \\
&= \begin{cases} 0, & 0 < R < \frac{1}{2}, \\ -1, & R = \frac{1}{2}, \\ -\infty, & \frac{1}{2} < R < 1. \end{cases}
\end{aligned} \tag{A.2}
$$

Therefore from (A.1) and (A.2) we have

$$
\lim_{N \to \infty} \Pr \left(||S_j| - 2^K| \geq \epsilon \right) \leq \begin{cases} 0, & 0 < R < \frac{1}{2}, \\ 1 - \frac{1}{e}, & R = \frac{1}{2}, \\ 1, & \frac{1}{2} < R < 1. \end{cases} \tag{A.3}
$$

$\blacksquare$

APPENDIX B

Proof of Lemma 2.3

For convenience, let us introduce new random variables and a function as follows:

$$\mu = \left(\frac{E_b}{N_0}\right)^*, \tag{B.1a}$$

$$\nu = R, \tag{B.1b}$$

$$\lambda = \mu\nu = R\left(\frac{E_b}{N_0}\right)^*, \tag{B.1c}$$

$$g(\lambda) = \int_{-\infty}^{\infty} \frac{1}{\sqrt{2\pi}} e^{-\frac{y^2}{2}} \cosh^{\frac{1}{2}}\left(2\sqrt{2\lambda}y\right) dy. \tag{B.1d}$$

Then from (2.43) we have the following relation

$$\nu = 1 - \log_2\left(1 + e^{-2\lambda}g(\lambda)\right). \tag{B.2}$$

We first show $\nu \to 0^+$ as $\lambda \to 0^+$. Since $\cosh^{\frac{1}{2}}\left(2\sqrt{2\lambda}y\right)$ is non-decreasing with regard to λ, by the monotone convergence theorem, we have

$$
\begin{aligned}
\lim_{\lambda \to 0^+} g(\lambda) &= \lim_{\lambda \to 0^+} \int_{-\infty}^{\infty} \frac{1}{\sqrt{2\pi}} e^{-\frac{y^2}{2}} \cosh^{\frac{1}{2}}\left(2\sqrt{2\lambda}y\right) dy \\
&= \int_{-\infty}^{\infty} \frac{1}{\sqrt{2\pi}} e^{-\frac{y^2}{2}} \lim_{\lambda \to 0^+} \cosh^{\frac{1}{2}}\left(2\sqrt{2\lambda}y\right) dy \\
&= 1.
\end{aligned}
\tag{B.3}
$$

Hence we have $\lim\limits_{\lambda\to 0^+} e^{-2\lambda}g(\lambda) = 1$. Since $e^{-2\lambda}g(\lambda) = 2^{1-\nu} - 1$ from (B.2), we also have $\lim\limits_{\nu\to 0^+} e^{-2\lambda}g(\lambda) = 1$. Note that $0 < e^{-2\lambda}g(\lambda) < 1 \ \forall \lambda > 0$. Therefore $\nu \to 0^+$ implies $\lambda \to 0^+$. Then we have

$$
\begin{aligned}
\lim_{\nu\to 0^+} \mu &= \lim_{\nu\to 0^+} \frac{\lambda}{\nu} \\
&= \lim_{\nu\to 0^+} \frac{\lambda}{1 - \log_2\left(1 + e^{-2\lambda}g(\lambda)\right)} \\
&= \lim_{\lambda\to 0^+} \frac{\lambda}{1 - \log_2\left(1 + e^{-2\lambda}g(\lambda)\right)}
\end{aligned}
\tag{B.4}
$$

using L'Hôpital's rule,

$$
\begin{aligned}
&= \lim_{\lambda\to 0^+} \frac{\ln 2 \left(1 + e^{-2\lambda}g(\lambda)\right)}{2e^{-2\lambda}g(\lambda) - e^{-2\lambda}g'(\lambda)} \\
&= \lim_{\lambda\to 0^+} \frac{2\ln 2}{2 - e^{-2\lambda}g'(\lambda)},
\end{aligned}
\tag{B.5}
$$

where

$$
\begin{aligned}
g'(\lambda) &= \frac{d}{d\lambda}g(\lambda) \\
&= \frac{d}{d\lambda} \int_{-\infty}^{\infty} \frac{1}{\sqrt{2\pi}} e^{-\frac{y^2}{2}} \cosh^{\frac{1}{2}}\left(2\sqrt{2\lambda}y\right) dy \\
&= \int_{-\infty}^{\infty} \frac{1}{2\sqrt{\pi}} e^{-\frac{y^2}{2}} \frac{\sinh\left(2\sqrt{2\lambda}y\right)}{\cosh^{\frac{1}{2}}\left(2\sqrt{2\lambda}y\right)} \frac{y}{\sqrt{\lambda}} dy, \\
&= \int_{0}^{\infty} \frac{1}{\sqrt{\pi}} e^{-\frac{y^2}{2}} \frac{\sinh\left(2\sqrt{2\lambda}y\right)}{\cosh^{\frac{1}{2}}\left(2\sqrt{2\lambda}y\right)} \frac{y}{\sqrt{\lambda}} dy.
\end{aligned}
\tag{B.6}
$$

Now we need to compute

$$
\begin{aligned}
&\lim_{\lambda\to 0^+} e^{-2\lambda}g'(\lambda) \\
&= \lim_{\lambda\to 0^+} \int_{0}^{\infty} \frac{1}{\sqrt{\pi}} e^{-\frac{y^2}{2}-2\lambda} \frac{\sinh\left(2\sqrt{2\lambda}y\right)}{\cosh^{\frac{1}{2}}\left(2\sqrt{2\lambda}y\right)} \frac{y}{\sqrt{\lambda}} dy.
\end{aligned}
\tag{B.7}
$$

By letting $n = \frac{1}{\sqrt{\lambda}}$ in the integrand of (B.7), we define a sequence of real valued functions, $f_n(y) \ \forall n \in \mathbb{N}, \quad \forall y \in (0, \infty)$, as

$$f_n(y) = \frac{1}{\sqrt{\pi}} e^{\left(-\frac{y^2}{2} - \frac{2}{n^2}\right)} \frac{\sinh\left(\frac{2\sqrt{2}y}{n}\right)}{\cosh^{\frac{1}{2}}\left(\frac{2\sqrt{2}y}{n}\right)} yn, \tag{B.8}$$

where $\mathbb{N}$ denotes the set of natural numbers. Notice that for a fixed y, as $n \to \infty$, the sequence $\{f_n(y)\}_{n=1}^{\infty}$ converges almost everywhere to a limit function $f(y)$ which is given by

$$f(y) = \sqrt{\frac{8}{\pi}} e^{-\frac{y^2}{2}} y^2. \tag{B.9}$$

Note also that $f_n(y)$ is upper bounded by

$$\begin{aligned} f_n(y) &< \frac{1}{\sqrt{\pi}} e^{\left(-\frac{y^2}{2} + \sqrt{2}\left(1 - \frac{1}{n}\right)y\right)} \frac{\sinh\left(\frac{2\sqrt{2}y}{n}\right)}{\cosh^{\frac{1}{2}}\left(\frac{2\sqrt{2}y}{n}\right)} yn \\ &= \sqrt{\frac{8}{\pi}} e^{\left(-\frac{y^2}{2} + \sqrt{2}y\right)} h\left(\frac{2\sqrt{2}y}{n}\right) y^2, \end{aligned} \tag{B.10}$$

where

$$h(x) \triangleq \frac{e^{-\frac{x}{2}} \sinh(x)}{x \cosh^{\frac{1}{2}}(x)}.$$

Since $h(x) < 1 \ \forall x > 0$, we have

$$f_n(y) < \sqrt{\frac{8}{\pi}} e^{\left(-\frac{y^2}{2} + \sqrt{2}y\right)} y^2. \tag{B.11}$$

It can be easily seen that the right-hand side of (B.11) is integrable over $(0, \infty)$, i.e.,

$$\int_0^{\infty} \sqrt{\frac{8}{\pi}} e^{\left(-\frac{y^2}{2} + \sqrt{2}y\right)} y^2 dy < \infty. \tag{B.12}$$

Then by the dominated convergence theorem,

$$
\begin{aligned}
& \lim_{\lambda \to 0^+} e^{-2\lambda} g^{'}(\lambda) \\
=\ & \lim_{n \to \infty} \int_0^\infty f_n(y)dy \\
=\ & \int_0^\infty f(y)dy \\
=\ & 2.
\end{aligned}
\tag{B.13}
$$

Hence from (B.5) and (B.13), we obtain $\lim_{\nu \to 0^+} \mu = \infty$.

■

APPENDIX C

Proof Of Lemma 2.4

Let $\mu = \left(\frac{E_b}{N_0}\right)^*$, $\nu = R$ and $\lambda = \mu\nu$. From (2.49), we obtain

$$\nu = \frac{3}{2} - \frac{1}{2}\log_2\left(3 + 4e^{-\lambda} + e^{-4\lambda}\right). \tag{C.1}$$

It can be easily shown that $\lambda \to 0^+$ as $\nu \to 0^+$. Then we have

$$
\begin{aligned}
&\lim_{\nu \to 0^+} \mu \\
&= \lim_{\nu \to 0^+} \frac{\lambda}{\nu} \\
&= \lim_{\nu \to 0^+} \frac{\lambda}{\frac{3}{2} - \frac{1}{2}\log_2\left(3 + 4e^{-\lambda} + e^{-4\lambda}\right)}
\end{aligned}
\tag{C.2}
$$

using L'Hôpital's rule,

$$
\begin{aligned}
&= \lim_{\nu \to 0^+} \left(\frac{3 + 4e^{-\lambda} + e^{-4\lambda}}{2e^{-\lambda} + 2e^{-4\lambda}}\right)\ln 2 \\
&= 2\ln 2.
\end{aligned}
\tag{C.3}
$$

■

APPENDIX D

Proof Of Lemma 2.5

Let $\mu = \left(\frac{E_b}{N_0}\right)^*$, $\nu = R$ and $\lambda = \mu\nu$. Define a function $h(\lambda)$ as

$$h(\lambda) = \int_{-\infty}^{\infty} \frac{1}{2\sqrt{\pi}} e^{-\frac{y^2}{4}} \cosh^{\frac{1}{2}}\left(\sqrt{2\lambda}y\right) dy. \tag{D.1}$$

Then from (2.53) we have

$$\nu = 1 - \log_2\left(1 + e^{-\lambda}h(\lambda)\right). \tag{D.2}$$

It is easy to show that $\lambda \to 0^+$ as $\nu \to 0^+$. Now we lower bound $h(\lambda)$. First, we can express $h(\lambda)$ as

$$\begin{aligned} h(\lambda) &= E_Y\left(\cosh^{\frac{1}{2}}\left(\sqrt{2\lambda}Y\right)\right) \\ &= E_Z\left(\cosh^{\frac{1}{2}}\left(\sqrt{2\lambda Z}\right)\right), \end{aligned} \tag{D.3}$$

where Y is a Gaussian random variable with zero mean and variance of 2, $Z = Y^2$ and $E_Y(\cdot)$ denotes expectation over Y. Since $\cosh^{\frac{1}{2}}\left(2\sqrt{2\lambda Z}\right)$ is a concave function,

by Jensen's inequality,

$$
\begin{aligned}
h(\lambda) \;&\geq\; \cosh^{\frac{1}{2}}\left(\sqrt{2\lambda E_Z(Z)}\right) \\
&=\; \cosh^{\frac{1}{2}}\left(2\sqrt{\lambda}\right) \\
&=\; \left(\sum_{n=0}^{\infty} \frac{\left(2\sqrt{\lambda}\right)^{2n}}{(2n)!}\right)^{\frac{1}{2}} \\
&\geq\; \sqrt{1+2\lambda}.
\end{aligned}
\tag{D.4}
$$

Thus we obtain

$$
\begin{aligned}
\lim_{\nu\to 0^+}\mu \;&=\; \lim_{\nu\to 0^+}\frac{\lambda}{\nu} \\
&=\; \lim_{\lambda\to 0^+}\frac{\lambda}{1-\log_2\left(1+e^{-\lambda}h(\lambda)\right)} \\
&\geq\; \lim_{\lambda\to 0^+}\frac{\lambda}{1-\log_2\left(1+e^{-\lambda}\sqrt{1+2\lambda}\right)}
\end{aligned}
$$

using L'Hôpital's rule,

$$
\begin{aligned}
&=\; \lim_{\lambda\to 0^+}\frac{\ln 2\left(1+e^{-\lambda}\sqrt{1+2\lambda}\right)}{e^{-\lambda}\left(\sqrt{1+2\lambda}-\frac{1}{\sqrt{1+2\lambda}}\right)} \\
&=\; \infty.
\end{aligned}
\tag{D.5}
$$

∎

BIBLIOGRAPHY

BIBLIOGRAPHY

[1] R. Ahlswede, N. Cai, S.-Y. Li and R. Yeung, "Network information flow,", *IEEE Trans. Inf. Theory*, vol. 46, no. 4, pp. 1204-1216, July 2000.

[2] S.-Y. Li, R. Yeung, and N. Cai, "Linear network coding," *IEEE Trans. Inf. Theory*, vol. 49, no. 2, pp. 371-381, Feb. 2003.

[3] R. Koetter and M. Médard, "An algebraic approach to network coding," *IEEE Trans. Netw.*, vol. 11, no. 5, pp. 782-795, Oct. 2003.

[4] S. Zhang, S. Liew and P. Lam, "Physical layer network coding," in *Proc. ACM MobiCom*, pp. 358-365, Sep. 2006.

[5] S. Katti, I. Maric, A. Goldsmith, D. Katabi and M. Médard, "Joint relaying and network coding in wireless networks," in *Proc. IEEE ISIT*, June 2007.

[6] B. Nazer and M. Gastpar, "Computation over multiple-access channels," *IEEE Trans. Inf. Theory*, vol. 53, no. 10, pp. 3498-3516, Oct. 2007.

[7] B. Nazer and M. Gastpar, "Lattice coding increases multicast rates for Gaussian multiple-access networks," in *Proc. 45th Annual Allerton Conference on Communication, Control and Computing*, Sep. 2007.

[8] K.Narayanan, M.P. Wilson and A. Sprintson, "Joint physical layer coding and network coding for bi-directional relaying," in *Proc. 45th Annu. Allerton Conf. Communication, Control and Computing*, Sep. 2007.

[9] T. Cover and J. Thomas, *Elements of Information Theory*, John Wiley & Sons, Inc., 1991.

[10] P. Narayan and D. L. Snyder, "The two-user cutoff rate for an asynchronous and a synchronous multiple-access channel are the same," *IEEE Trans. Inf. Theory*, vol. IT-27, no. 4, pp. 414-419, July 1981.

[11] D. Slepian and J. K. Wolf, "A coding theorem for multiple access channels with correlated sources," *Bell System Tech. J.*, vol. 52, pp. 1037-1076, 1973.

[12] A. G. Dyachkov, "Random constant composition codes for multiple access channels," *Probl. Contr. Inform. Theory*, vol. 13, no. 6, pp. 357-369, 1984.

[13] R.G. Gallager, "A perspective on multiaccess channels," *IEEE Trans. Inf. Theory*, vol. IT-31, no. 2, pp. 124-142, Mar. 1985.

[14] J. Pokorny and H. M. Wallmeier, "Random coding hound and codes produced by permutations for the multiple-access channel," *IEEE Trans. Inf. Theory*, vol. IT-31, no. 6, pp. 124-142, Nov. 1985.

[15] Y. Liu and B. L. Hughes, "Random coding hound and codes produced by permutations for the multiple-access channel," *IEEE Trans. Inf. Theory*, vol. 42, no. 2, pp. 376-386, Mar. 1996.

[16] R.G. Gallager, *Information Theory and Reliable Communication*, John Wiley & Sons, Inc., 1968.

[17] N. Shulman and M. Feder, "Random Coding Techniques for Nonrandom Codes," *IEEE Trans. Inf. Theory*, vol. 45, no. 6, pp. 2101-2104, Sep. 1999.

[18] B. Rankov and A. Wittneben,"Achievable Rate Regions for the Two-way Relay Channel," *IEEE Trans. Inf. Theory*, vol. 53, no. 10, pp. 3498-3516, Oct. 2007

[19] S. Litsyn and V. Shevelev, "On Ensembles of Low-denstiy Parity-check Codes: Asymptotic Distance Distributions," *IEEE Trans. Inf. Theory*, vol. 48, pp. 887-908, April 2003.

[20] A. Valembois and M. Fossorier, "Sphere-packing bounds revisited for moderate block lenghts," *IEEE Trans. Inf. Theory*, vol. 50, no. 12, pp. 2998-3014, Dec. 2004.

[21] P. Billingsley, *Probability and Measure*, 2nd ed. John Wiley & Sons, Inc., 1986.

[22] J.G. Proakis, *Digital Communications*, 4th ed. New York: McGraw-Hill, 2001.

[23] S. Y. Chung, G. D. Forney, Jr., T. J. Richardson, and R. Urbanke, "On the Design of Low-Density Parity-Check Codes within 0.0045 dB of the Shannon Limit," *IEEE Commun. Lett.*, VOL. 5, NO. 2, pp.58-60, FEB. 2001

[24] C. Wang, S. Kulkarni and H. Poor, "On Finite-dimensional Bounds for LDPC-like codes with Iterative Decoding,"in *Proc. IEEE Int. Symposium on Inf. Theory and Its Applications*, Oct. 2004.

[25] C. Wang, S. Kulkarni and H. Poor, "Density Evolution for Asymmetric Memoryless Channels," *IEEE Trans. Inf. Theory*, vol. 51, no. 12, pp. 4216-4236, Dec. 2005.

[26] A. Goldsmith and P. Varaiya,"Capacity of fading channels with channel side information," *IEEE Trans. Inf. Theory*, vol. 43, no. 6, pp. 1986-1992, Sep. 1997

[27] Caire and S. Shamai, "On the capacity of some channels with channel state information," *IEEE Trans. Inf. Theory*, vol. 45, no. 6, pp. 2007-2019, Sep. 1999

[28] M. Medard, "The effect upon channel capacity in wireless communications of perfect and imperfect knowledge of the channel," *IEEE Trans. Inf. Theory*, vol. 46, no.6, pp. 933-946, May 2000.

[29] T. J. Richardson and R. L. Urbanke, "The capacity of low-density parity-check codes under message-passing decoding," *IEEE Trans. Inf. Theory*, vol. 47, no. 2, pp. 599-618, Feb. 2001.

[30] T. J. Richardson, M. A. Shokrollahi and R. L. Urbanke, "Design of capacity-approaching irregular low-density parity-check codes," *IEEE Trans. Inf. Theory*, vol. 47, no. 2, pp. 619-637, Feb. 2001.

[31] J. Hou and P. H. Siegel and L. B. Milstein, "Performance analysis and code optimization of low density parity-check codes on Rayleigh fading channels," *IEEE J. Sel. Areas Commun.*, vol. 16, no. 5, pp. 924 - 934, May 2001.

[32] S. M. Kay, *Fundamentals of statistical signal processing*, Volume I: Estimation Theory, Englewood Cliffs, NJ: Prentice-Hall, 1993.

[33] A. Lapidoth and S. Shamai,"Fading channels: How perfect need "perfect side information" be?," *IEEE Trans. Inf. Theory*, vol. 48, no. 5, pp. 1118-1134, May. 2002.

[34] M.Sipser and D. Spielman, "Expander codes," *IEEE Trans. Info. Theory*, vol. 42, no. 6, pp. 1710 - 1722, Nov. 1996.

[35] D. J. C. MacKay and R. M. Neal,"Near Shannon limit performance of low density parity check codes,"*Electronics Letters 32(18)*, pp. 1645 - 1646, 1996.

[36] M. B. Pursley, "Performance evaluation for phase-coded spread-spectrum multiple-access communication – Part I: System analysis," *IEEE Trans. Commun.*, vol. COM-25, no. 8, pp 795 - 799, Aug. 1997.

[37] H. Sari, G. Karam, and J. Janclaude, "Transmission techniques for digital terrestrial TV broadcasting", *IEEE Commun. Mag.*, vol. 36, pp. 100.109, Feb. 1995.

[38] *Broadband Radio Access Networks* (BRAN), HIPERLAN Type 2 Standard, 2000.

[39] T. Zemen, and C. F. Mecklenbräuker, "Time-variant channel estimation using discrete prolate spheroidal sequences", *IEEE Trans. Signal Process.*, vol. 53, no. 9, pp. 3597-3607, Sep. 2005.

[40] X. Ma, and G. Giannakis, "Maximum-diversity transmissions over doubly selective wireless channels", *IEEE Trans. Inform. Theory*, vol. 49 no. 7, pp. 1832-1840, Jul. 2003.

[41] O. Edfors, M. Sandell, J. J. van de Beek, S. K. Wilson, and P. O. Borjesson, "OFDM channel estimation by singular value decompositio", *IEEE Trans. Commun.*, vol. 46, no. 7, pp. 931-939, Jul. 1998.

[42] Y. Gong, and K. B. Letaief, "Low complexity channel estimation for space-time coded wideband OFDM systems", *IEEE Trans. Wireless Commun.*, vol. 2, no. 5, pp. 876-882, Sep. 2003.

[43] Y. Li, L. J. Climini Jr., and N. R. Sollengerger, "Robust channel estimation for OFDM systems with rapid dispersive fading channels", *IEEE Trans. Commun.*, vol. 46, no. 7, pp. 902-915, Jul. 1998.

[44] Y. Li, "Simplified channel estimation for OFDM systems with multiple transmit antennas", *IEEE Trans. Wireless Commun.*, vol. 1, no. 1, pp. 1317-1430, Jan. 2002.

[45] D. Slepian, "Prolate spheroidal wave functions, Fourier analysis, and uncertainty - V: The discrete case", *Bell Syst. Technical Journal*, vol. 57, no. 5, pp. 1371-1430, May-Jun. 1978.

[46] IEEE 802.11a-1999: *High-Speed Physical Layer in the 5 GHz Band*, 1999.

[47] C. E. Shannon, "A mathematical theory of communication," *Bell Syst. Tech. J.*, vol. 27, pp. 379-423, 623-656, 1948.

[48] J. G. Smith, "The information capacity of amplitude and variance-constrained scalar Gaussian channels," *IEEE Transactions on Information Theory*, vol. 18, pp.203-219, 1971

[49] S. Shamai and I. Bar-David, "The capacity of average and peak-power-limited quadrature Gaussian channels," *IEEE Transactions on Information Theory*, vol. 41, pp. 1060-1071, 1995.

[50] I.C. Abou-Faycal, M.D. Trott and S. Shamai, "The Capacity of Discrete-Time Memoryless Rayleigh-Fading Channels," *IEEE Transactions on Information Theory*, vol. 47, pp. 1290-1301, 2001.

[51] R. Palanki, "On the capacity achieving distributions of some fading channels," *Fortieth Annu. Allerton Conf. Communications, Control, and Computing*, Monticello, IL, Oct. 2-4, 2002.

[52] D. Luenberger, *Optimization by Vector Space Methods*, Wiley, 1971.

[53] R. B. Ash, *Information Theory*, interscience, New York,1965

[54] H. Silverman, *Complex Variables*, Boston, MA: Houghton Mifflin, 1975.

[55] R.C. Gunning and H. Rossi, *Analytic functions of several complex variables*, Prentice-Hall, 1965

[56] M. Loéve, *Probability Theory*, Berlin, Germany: Springer-Verlag, 1977.

[57] P.A. Moran, *Introduction to Probability Theory*, Clarendon, Oxford, 1968.

[58] E. Lukacs, *Stochastic Convergence*, Academic Press, 1975.

[59] K.-L. Chung, *A Course in Probability Theory*, 2nd ed. NewYork: Academic, 1974.

[60] W. Feller, *An Introduction to Probability Theory and its Applications*, Wiley, 1971.